UNIVERSITY OF PALERMO

DEPARTMENT OF BIOLOGICAL CHEMICAL AND
PHARMACEUTICAL SCIENCES AND TECHNOLOGIES (STEBICEF)

PhD in Cell Biology
(Cell Biology and Development)

ROLE OF RNA BINDING PROTEIN IN THE NERVE CELL DIFFERENTIATION

AUTHOR:
Patrizia Saladino

PhD COORDINATOR:
Prof. Gabriella Sconzo

TUTOR:
Carlo Maria Di Liegro, PhD

SCIENTIFIC AREA CODE
BIO 06

XXIV CYCLE
2011-2013

Abstract

Synthesis of H1˚ and H3.3 histone proteins, in the developing rat brain, seems to be regulated mainly at the post-transcriptional level. Since regulation of RNA metabolism depends on a series of RNA-binding proteins (RBPs), we have been searching for RBPs involved in the post-transcriptional regulation of the H1˚ and H3.3 genes. Previously, we reported isolation, from a cDNA expression library, of an insert encoding a novel protein, the C-terminal half of which is identical to that of PEP-19, a brain-specific protein involved in calcium metabolism. The novel protein was called long PEP-19 isoform (LPI). We showed that LPI, as well as PEP-19, can bind H1˚ RNA. Since PEP19 and LPI contain a calmodulin binding domain, we also investigated whether their ability to bind RNA is affected by calmodulin. Our results show that calmodulin interferes with binding of H1˚ RNA to both PEP-19 and LPI, while it is not able to bind RNA on its own. Pep-19/calmodulin high affinity binding has been demonstrated by Biolayer interferometry (BLI). This finding suggests that calcium/calmodulin may have a role in controlling H1˚ mRNA metabolism in the developing brain. Moreover, in order to improve production of functional LPI/PEP-19, we modified the protocol normally adopted for preparing histidine tagged-proteins from bacteria, by adding an additional purification step.

Furthermore, we found that both LPI and PEP-19 can compete for H1˚ RNA binding with PIPPin (also known as CSD-C2), another RBP previously discovered in our laboratory. PIPPin/CSD-C2 binds with high specificity to the mRNAs encoding H1° and H3.3 histone variants, undergoes thyroid hormone-dependent SUMOylation, and has been recently demonstrated to interact with other RBPs. PIPPin belongs to the CSD-containing class of RBPs, also called Y-box proteins, that play a key role in controlling the recruitment of mRNAs to the translational machinery, in response to environmental cues, both in development and in differentiated cells.

Another aspect of this study was to confirm histone mRNAs-PIPPin interactions and to describe binding properties through streptavidin-biotin conjugation method, by BLI.

We report the data obtained in the case of H3.3 and H1° mRNA-PIPPin interactions, and the specific affinity constant for these bindings. In order to identify RNA portions involved in binding, we used different RNA probes for H3.3 and H1°. In summary, we were able to confirm that PIPPin binds H3.3 and H1° mRNA with very high affinity.

Searching for other RBPs, we used in vitro transcribed, biotinylated H1° RNA as bait to isolate, by a chromatographic approach, proteins which interact with this mRNA, in the nuclei of brain cells. Abundant RBPs, such as heterogeneous nuclear ribonucleoprotein (hnRNP) K and hnRNP A1, and molecular chaperones (heat shock cognate 70, Hsc70) were identified by mass spectrometry. Western blot analysis also revealed the presence of CSD-C2. Co-immunoprecipitation assays were performed to investigate the possibility that identified proteins interact with each other and with other nuclear proteins. We found that hnRNP K interacts with both hnRNP A1 and Hsc70, whereas there is no interaction between hnRNP A1 and Hsc70. Moreover, CSD-C2 interacts with hnRNP A1, Y box-binding protein 1 (YB-1), and hnRNP K. We also have indications that CSD-C2 interacts with Hsc70.

Aims of the research

• To confirm that LPI is capable of binding RNA and preferentially histone mRNAs, and also to check whether PEP-19 is a RNA binding protein.

• To identify the level of action of the already cloned PIPPin/CSD-C2, LPI, and PEP-19 as well as of p40, p70 and p110 proteins;

• To identify the extracellular signals that modulate the activity of these factors, regulating the synthesis of histone proteins. In the case of PIPPin/CSD-C2, for example, it has been already shown that a fraction of it is bound to chromatin and is stably sumoylated in response to treatment with thyroid hormones (Bono, et al., 2007).

• To highlight post-translational modifications of the studied proteins associated with the extracellular signal transduction events.

• To identify other proteins that interact with the RNA-binding factors under focus in the current study, starting from the assumption that RNA metabolism is regulated in complex structures, containing several different regulatory proteins and RNAs.

• To shed more light on the specific function of these proteins.

Introduction

1. Nucleosomes remodelling

The mammalian brain depends on numerous complex and highly regulated mechanisms to appropriately activate or silence gene programs in response to environmental input and developmental cues. At the molecular level, these events are controlled by signaling pathways that mediate gene expression by modifying the activity, localization, and/or expression of enzymes which regulate transcription, in combination with alterations in chromatin structure in the nucleus (McClung, et al., 2008) .

An epigenetic program is crucial during development, and its stability is essential to maintain all functions of each specific cell type during the organism's life (Li, 2002). Gene expression can be epigenetically regulated at several levels, including the position of the gene in the nuclear matrix and the conformation of chromatin at the genetic locus. The first level of chromatin organization is represented by a basic unit called nucleosome. The core is composed by an octamer of H2A, H2B, H3 and H4 core histones present each in two copies. 145-147 base pairs of DNA are wrapped around the histone octamer that constrains DNA in 1.65 superhelical left-handed turns around its perimeter copies (Luger, et al., 1997). In dividing metazoan cells, transcription and translation of core histones is mainly replication/cell cycle-dependent. Replication-dependent histones are encoded by multi-copy, intronless gene clusters and their inclusion in chromatin is coupled to replication to allow for appropriate packaging of genomic DNA (Albig, et al., 1997).

Chromatin conformation can be modulated in several ways. One way is the addition of methyl groups to DNA, mostly at CpG sites, to convert cytosine to 5-methylcytosine. Some areas of the genome are methylated heavier than others and highly methylated areas tend to be transcriptionally less active. A second way is to post-translationally modify the histones by acetylation, methylation, phosphorylation or ubiquitination (Bhaumik, et al., 2007) (Strah, et al., 2000). Since epigenetic modifications can be correlated with several transcriptional conditions, a "histone code" has been proposed. Following this hypothesis, each combination of histone modifications leads to a specific identity of each nucleosome which can be read as a "molecular bar code" (Henikoff, et al., 2005) (De la Cruz, et al., 2005).

In addition to nucleosomal remodelling and covalent histone modifications, eukaryotic cells can generate variation in chromatin structure through the introduction of variant histone proteins. All core histone proteins in mammals, with the exception of H4, have several sequence variants. Histone variants (Allis, et al., 1980) provide a means for introducing

primary sequence differences that might function, at least in part, by altering the covalent modification status of these variants independently of canonical histones to expand the regulatory repertoire of chromatin (Rando, et al., 2007) (Henikoff, 2008). Histone variants often contain minor sequence variations (eg, H3.1 vs H3.2 vs H3.3) or exhibit significantly dissimilar structures (eg, macroH2A, CENP-A) from their canonical counterparts (Rogakou, et al., 1999). Furthermore, histone variants have been suggested to exhibit cell type-specific expression patterns, which, given the heterogeneous nature of the brain, may prove to be important for their respective functions in the nervous system.

In mammals, major histone variants inclusion in chromatin is replication-independent, taking place during times in which newly synthesized canonical histones are not available. For example, in terminally differentiated post-mitotic neurons, which are no longer undergoing DNA replication, it can be assumed that these cells continue to have access to replication-independent histone variants, often encoded by one or two genes that are synthesized throughout the cell cycle. This process not only provides pools of histones for nucleosome replacement outside of the S phase, but also allows the generation of biochemically distinct nucleosomes that promote different patterns of chromatin regulation in cell type-specific and temporally precise modes.

.1.1 Histone variants (H1°-H3.3)

As mentioned, in most eukaryotes, histone genes are divided into two major classes:

i. Replication-dependent, whose expression is restricted to the S phase of the cell cycle;
ii. Replication-independent, which encode the so called "replacement variants", expressed at low but constant levels throughout the cell cycle;

Genes in the first class are repeated tens of times in the genome, do not contain introns, and encode short transcripts that are not modified by polyadenylation. In contrast, genes in the other classes are mainly single genes that can contain introns and encode longer and polyadenylated transcripts (Castiglia, et al., 1994). Among post-transcriptionally regulated genes, those encoding histone variants, such as H1˚ (Gjerset, et al., 1982), (Ponte, et al., 1994) and H3.3 (Pina, et al., 1987), (Castiglia, et al., 1994) are of particular interest for the possible involvement of histone variants in the replication-independent chromatin remodelling induced by extracellular stimuli.

Mammalian cells express multiple distinct genetically encoded variants of histone H3 proteins (H3.1, H3.2, and H3.3/primate-specific H3.X and H3.Y) (Wiedemann, et al., 2010). H3.3 is constitutively expressed in non-dividing cells, it is encoded by two isolated genes (H3F3A,

H3F3B), and its mRNA is polyadenylated (Wellman, et al., 1987). H3.3 differs from canonical H3 species at one amino-acid residue in the histone tail (serine 31) and at a cluster of three residues in the core histone fold (alanine 87, isoleucine 89, and glycine 90). The three amino-acid variations in the histone fold have been shown to be necessary for H3.3 replication-independent incorporation in chromatin (Ahmad, et al., 2002). H3.3 is specifically enriched at transcriptionally active genes, within gene promoters, at specific genomic repeats, such as telomeres, and at regulatory elements in mammalian embryonic stem cells and in neuronal precursors (Goldberg, et al., 2010).

Inclusion of canonical H3 in chromatin by the CAF 1 complex is a replication-dependent mechanism, whereas positioning of H3.3 histones by the HIRA complex is a replication-independent mechanism (Tagami, et al., 2004). Histone variants differ from each other not only in their chromatin location, but also in their post-translational modifications (Loyola, et al., 2007). For example, compared with the canonical H3, H3.3 histones are enriched in post-translational modifications that correlate with gene expression (Yuan, et al., 2012).

H1˚ is a linker histone subtype whose expression has been mostly correlated with terminal differentiation (Zlatanova, et al., 1994) (Gabrilovich, et al., 2002).

In developing rat brain, the concentration of H1˚ and H3.3 mRNAs decreases between the embryonic day 18 and the postnatal day 10, with inverse correlation to protein accumulation (Castiglia, et al., 1994). The levels of both H1° and H3.3 mRNAs decrease in isolated neurons between the 2^{nd} and 5^{th} day of culture to the same extent as *in vivo*. At the same time, an active synthesis of the corresponding proteins is evidenced, suggesting that H1° and H3.3 expression is regulated mainly at the post-transcriptional level (Scaturro, et al., 1995).

Since post-transcriptional control processes are mediated by several classes of RNA-binding proteins (Burd, et al., 1994) (Hentze, 1995) (Siomi, et al., 1997) (Derrigo, et al., 2000), it was likely that developing rat brain contained mRNA-binding factors involved in H1˚ and H3.3 mRNAs regulation. In the past, various researches led indeed to the identification of RBPs able to bind H1° and/or H3.3 mRNAs, and probably involved in their metabolism. In particular, were identified three H1° mRNA RBPs (p40, p70 and p110; (Scaturro, et al., 2003) and two proteins called PIPPin (Nastasi, et al., 1999), currently also known as Cold-Shock-Domain-C2 (CSD-C2), and Long-Pep19-Isoform (LPI) (Sala, et al., 2007).

2. mRNA metabolism and localization

Transcription transfers the genetic information from a gene to a primary transcript, a precursor-mRNA (pre-mRNA), which undergoes a series of post-transcriptional modifications

in the nucleus. These processing steps include capping at the 5' end, removal of introns by splicing, endonucleolytical cleavage and polyadenylation of the 3' end, and editing. At the end of the processing, mRNAs are constituted by a central coding region, which is translated to the corresponding polypeptide, and by untranslated regions (UTRs) at 5' and 3' ends.

During the last decade, UTRs were shown to harbour different sequence motifs (cis-acting elements, cis-elements) that, in cooperation with specific binding proteins or RNAs (trans-acting factors, trans-factors), regulate post-transcriptional modifications of the messenger and, in turn, its translation, stability and localization. Any alteration in the processing steps can influence the final structure and functional properties of the mRNA 3' end, for instance, and these modifications can lead to a variety of disorders in humans, including cancer (Michalova, et al., 2013).

.2.1 Maturation of pre-mRNA

During all processing steps, RNA is assembled into ribonucleoprotein (RNP) complexes. The RNA-associated proteins in these complexes ensure that each RNA transcript is properly spliced, processed, transported from the nucleus to the cytoplasm and translated by the protein synthesis machinery. The stages of this intricate process are complex and incompletely understood, although much has been learned over the past decade about the major pathways involved.

RNA processing begins while RNA polymerase II is still transcribing a gene. The first step is the addition of a guanosine to the 5’ end, by an unusual 5′ to 5′ triphosphate linkage, and its methylation to create a ‘cap’ that marks the beginning of the mRNA. Proteins binding to the cap structure coordinate subsequent steps in pre-mRNA processing, export, translation, and decay. In pre-mRNA, the protein-coding sequences (exons) are interrupted by numerous non-coding sequences (introns) that are removed in the nucleus by pre-mRNA splicing. More than a hundred proteins and some non coding RNAs participate in the overall splicing reaction. Moreover, the inclusion or exclusion of selected exonic sequences in specific cells at specific developmental stages and in response to specific extracellular stimuli generates multiple mRNA transcripts from the same pre-mRNA sequence via alternative splicing pathways. Perhaps, nowhere is this more prevalent than in neurons, and this accounts for much of the remarkable variability in gene expression seen in the nervous system (Gallo, et al., 2005) (Licatalosi, et al., 2006). The pre-mRNA splicing process is essential for eukaryotic gene expression and is carried out by the spliceosome. The major components of the spliceosome are the U1, U2, U5, and U4/U6 small nuclear ribonucleoproteins (snRNPs), each of which is

composed of one small nuclear RNA (snRNA) molecule, a set of seven common proteins, and several proteins that are specific to individual snRNAs (Luhrmann, et al., 1990) (Will, et al., 2001). snRNP biogenesis is highly regulated and requires ATP hydrolysis (Pellizzoni, et al., 2002) (Meister, et al., 2001). With the exception of U6, which never leaves the nucleus, the newly transcribed U snRNAs are initially exported to the cytoplasm, where the major assembly process of the snRNPs occurs. The common proteins, called Sm proteins, B/B', D1, D2, D3, E, F, and G are arranged into a stable heptameric ring, the Sm core, on a highly conserved, uridine-rich sequence motif, the Sm site, of the snRNAs (Kambach, et al., 1999) (Achsel, et al., 2001) (Stark, et al., 2001). The 5' ends of snRNAs begin with the same 7-methyl guanosine cap which characterizes mRNA structure; however, once assembled, it undergoes additional methylation to a 2,2,7-trimethyl guanosine cap, which signals the re-import of the properly assembled and modified snRNPs into the nucleus, where additional snRNP-specific proteins associate to form fully functional snRNPs (Mattaj, 1986) (Fischer, et al., 1990) (Hamm et al., 1990) (Fischer, et al., 1993) (Mattaj, et al., 1993).

Mature snRNPs then carry out the process of pre-mRNA splicing. Spliceosomal U snRNPs biogenesis occurs in the cytoplasm and is mediated by the SMN (survival motor neuron) complex. The SMN complex directly recognizes and binds to both proteins and RNA of the RNP and facilitates their interaction, thereby ensuring specificity of the snRNP assembly process (Yong, et al., 2004) (Kolb, et al., 2007).

Transcribing RNA polymerase continues past the end of the gene, and downstream sequences are removed by a precise processing event that involves assembly of a large protein complex guided by the conserved AAUAAA sequence and GU-rich sequences downstream of the processing site. This multiprotein complex contains an endonuclease that cleaves the pre-mRNA to create the 3' end and poly(A) polymerase, which adds the poly(A) tail, a homopolymer of ~250 adenosine residues. These latter steps are coordinated by interaction between a splicing factor bound to the last intron of the pre-mRNA and poly (A) polymerase. Afterward, the capped, spliced and polyadenylated mRNA is assembled into an mRNP complex that is competent for export from the nucleus to the cytoplasm. As with snRNP assembly, the export process is a highly coordinated event involving the formation and disruption of specific RNA-protein complexes and intermediaries. The mRNPs move to the cytoplasm through nuclear pore complexes (NPCs), large protein assemblies forming channels that offer the only way to leave the nucleus (Moore, 2005) (Cole, et al., 2006) (Stewart, 2007). The export requires another protein complex, the Mex67:Mtr2 heterodimer, which binds to the mRNP prior to transport. When the mRNP reaches the cytoplasmic side of

the NPC, Mex67:Mtr2 complex is removed by the DEAD-box RNA helicase Dbp5, avoiding retrograde transport back into the nucleus. Dbp5 shuttles between nucleus and cytoplasm, but it binds to, and is activated by, Gle1 on the cytoplasmic side of the NPC. The concurrent loss of Mex67:Mtr2 from the mRNP allows the mRNP to complete transit through the NPC. DEAD-box helicases use the energy of ATP to unwind RNP complexes, and maximum ATPase activity of Dbp5 is achieved when it associates with InsP6, a molecule which facilitates and regulates the interaction between Gle1 and Dbp5 (York, et al., 1999).

Asymmetric subcellular distribution of RNA is critical for proper embryo development, for establishing differences in cell fate, and for neuronal function. mRNA localization is commonly employed to target protein products to specific regions within a cell. Some mRNAs are localized to appropriate sub-cellular structures at the same time they are being translated, and it is the emerging nascent peptide that directs the localization of both the ribosome and the transcript. For example, transcripts encoding secreted proteins are localized to the endoplasmic reticulum (ER) by recruitment of the nascent signal peptide (Nicchitta, 2002). In other cases, such as the localization of some transcripts to mitochondria in yeast, transport is driven by sequences in the RNA itself (Corral-Debrinski, et al., 2000).

mRNA faces different fates after it arrives in the cytoplasm. It is currently thought that coincident with export, the mRNP undergoes a surveillance process where it is scanned by a 'pioneer round' of translation that determines whether the transcript will encode a full-length protein. This is an important, evolutionarily conserved process that protects the cell from the accumulation of C-terminally truncated proteins with potential dominant negative function that may arise from alternative splicing, processing errors or certain inherited mutations, all of which generate mRNAs with a termination codon upstream of the correct position. Splicing deposits a complex of proteins at each exon junction (the exon junction complex, EJC) that accompany the newly processed mRNP into the cytoplasm, and these provide positional information for the location of a stop codon. On a correct mRNA, ribosomes will scan through these. The ribosomes remove each of the complexes in the process until they reach the normal stop codon and are released. However, if the mRNA carries a termination codon that is upstream of an EJC, the ribosome will pause at that position, and this activates the degradation of that mRNA through a process termed 'nonsense-mediated mRNA decay' or NMD. NMD is ultimately responsible for the loss of protein product in many genetic disorders that result from the inheritance of one or more genes that carry a premature termination codon.

After the surveillance process, the mRNA can be bound by initiation factors and translated, silenced (for example by binding of microRNAs), stored or degraded. Each of these processes in itself is highly regulated, and the fate of each mRNA is determined by cis-acting sequence elements within the mRNA and by proteins (and non coding RNAs) that bind to these elements. A case in point is the large family of mRNAs that carry adenosine plus uridine-rich sequence elements (AU-rich elements, or AREs) in their 3' untranslated regions. There are over 3000 mRNAs with AREs, and their differential binding by a number of ARE-binding proteins (including HSPB1) determine their overall accumulation, translation and decay (Kolb, et al., 2010). The role of mRNA stability in neurons is increasingly recognized and seems to be especially important in neuronal development and regeneration (Bolognani, et al., 2008).

Translation of an mRNA is mediated by the ribosome and is conventionally divided into the initiation, elongation and termination stages. During initiation, the ribosome and the tRNA for the first amino acid residue, methionine, recognize and bind to the first codon, AUG, of the mRNA transcript. The polypeptide encoded by the mRNA is assembled during the elongation phase, and termination occurs when the ribosome encounters a 'stop' codon that results in the release of the polypeptide and dissociation of the ribosomal subunits. The entire process is, once again, mediated by the complex association of a host of specific RNP complexes, non-coding RNAs, and proteins.

If one considers the ribosome as a protein-synthesizing machine, the raw materials are the mRNA template and the individual aminoacyl-tRNAs. Aminoacyl-tRNAs are covalently linked RNA-protein complexes that are produced by a number of aminoacyl-tRNA synthetases (ARSs) that catalyze the esterification of specific amino acids to their respective tRNAs. A number of additional functions for particular ARSs have come to light, including roles in transcription, splicing, apoptosis, inflammation and angiogenesis (Ko, et al., 2002) (Park, et al., 2008).

Finally, all mRNAs are degraded and their rate of decay is a controlling factor in the timing, quantity and perhaps even location of their encoded proteins. In general, mRNA decay begins with shortening of the poly (A) tail, followed by removal of the 5' cap and degradation by exonucleases from both the 5' and 3' ends of the mRNA. This is a highly regulated process that involves the interplay between cis-acting sequences and the proteins that bind to them. Both translation and decay are targets of numerous signal transduction pathways, and we are just beginning to understand how they are controlled.

.2.2 mRNA localization in neurons

Eukaryotic cells need to temporally and spatially regulate gene expression in response to a variety of cues. While temporal regulation of gene expression can be achieved through transcriptional regulation, the ability of a cell to spatially restrict synthesis of a specific protein within the cytoplasm requires post-transcriptional control.

Eukaryotic organisms ranging from fungi to mammals and also within different cell types of a given organism, including neurons (St Johnston, 2005), localize mRNAs to spatially restrict synthesis of specific proteins to distinct regions of the cytoplasm. mRNA encoding the protein is localized to the site where the protein functions. Once the mRNA reaches the proper destination, the mRNA is translated, resulting in the spatial restriction of the corresponding protein. There are at least three mechanisms by which an mRNA can be localized: (A) local protection from degradation, (B) diffusion and entrapment by a localized anchor and (C) direct transport by motor proteins on cytoskeletal filaments (Fig.1).

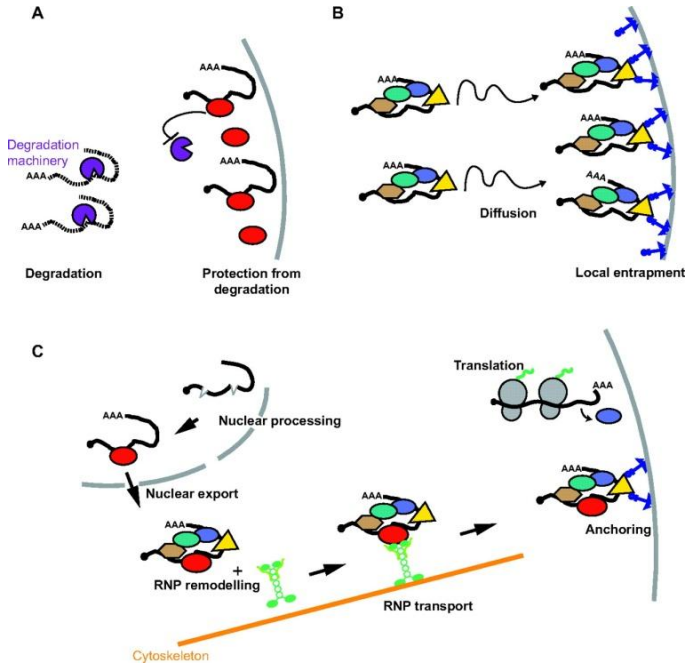

Figure 1

Mechanisms by which an mRNA can be localized

In *Drosophila*, Hsp83 mRNA localizes to the posterior pole plasma of the egg using the "protection from degradation" pathway (Ding, et al., 1993). In this RNA localization pathway, the RNAs are protected from degradation at the site of localization and are highly susceptible to degradation in other areas of the cell. In contrast, the Xcat-2 mRNA in *Xenopus* utilizes the "diffusion and entrapment" mechanism (Chang, et al., 2004). RNA localization substrates that

utilize this pathway randomly diffuse throughout the cytoplasm, and, when the RNA reaches the site of localization, it is captured and retained. In "direct transport" the RNA contains a *cis*-acting localization element, also referred to as a "zip code". The *cis*-acting element directs the RNA to the proper intracellular location. RBPs recognize a nucleotide sequence and/or structure in the *cis*-acting localization element. Some RBPs identify the RNA localization substrate in the nucleus and escort the RNA to the cytoplasm. Subsequently, the RNA-protein complex interfaces with a molecular motor (myosin, kinesin or dynein), which directly transports the RNA on cytoskeletal components. During transport of the RNA to the site of localization, translation of the RNA is repressed. Once the RNA arrives to its destination, it is hypothesized that the RNA is anchored at the site of localization, and translational repression is relieved (Gonsalvez, et al., 2012).

The localization of mRNA critically contributes to many important cellular processes in an organism, such as the establishment of polarity, asymmetric division and migration during development.

Moreover, in the central nervous system, the local translation of mRNAs is thought to induce plastic changes that occur at synapses triggering learning and memory processes. Neuronal function is highly dependent on spatially precise signalling. Increasing evidence indicates that the complex morphology of neurons has created biological compartments that subdivide the neuron into spatially distinct signalling domains important for neuronal function (Hanus, et al., 2013)**.**

Mature neurons are highly polarized and generally consist of a cell body, a single long axon and several shorter branching dendrites. mRNA localization also occurs during development in axonal growth cones of immature neurons as well as in dendrites of fully mature and polarized neurons. In the brain, mRNA localization is not only restricted to neurons, but also occurs in another type of nerve cells, the oligodendrocytes. (Doyle, et al., 2011)

There are a lot of advantages of mRNA localization as a key regulatory mechanism to fine-tune gene expression. First, the localization of mRNA rather than its corresponding protein serves a dual function: it targets the protein directly to the correct intracellular compartment while preventing its expression elsewhere. This is particularly important for those proteins that might be harmful to other parts of the cell, for example myelin basic protein (MBP) in oligodendrocytes, or Tau and microtubule-associated protein 2 (MAP2) that could bind to all microtubules in the cell. Second, it provides a synapse with the unique opportunity to spatially restrict gene expression with high temporal resolution. Therefore, an activated synapse could initiate local protein synthesis that in turn alters its function and morphology in its own

microenvironment that is independent of the distant cell body. Third, it is more economic to reuse a given transcript several times for multiple rounds of translation instead of transporting each protein or transcript individually to a distinct synapse.

.2.2.1 mRNA localization in dendrites

Dendritic protein synthesis appears not to produce general housekeeping proteins, but rather to produce proteins with specialized synaptic functions, for example Ca^{2+} /calmodulin-dependent protein kinase II (CaMKIIα), cytoskeletal proteins (Arc, MAP2) and neurotransmitter receptors of the AMPA (GluR1 and 2) and NMDA (NR1) families. (Doyle, et al., 2011)

Maturation of neuronal circuits involves remodelling of dendritic trees and refinement of synapse number and strength, two processes controlled by local translation of dendritically targeted mRNAs. The complexity of dendritic trees is a key parameter underlying neuronal activity and connectivity. Strikingly, recent studies have revealed that the transport of specific mRNAs to dendrites is crucial for dendritic branching during development. Targeting of *nanos* mRNA to dendrites, for example, is required for proper branching of peripheral sensory neurons in Drosophila larvae. In young mouse hippocampal neurons, inactivation of the RNA-binding protein Staufen1 impairs the transport of β-actin mRNA to dendrites and reduces dendritic length and branching. Similarly, hippocampal neurons lacking the RNA-binding protein Zbp1/Vg1RBP exhibit reduced accumulation of β-actin mRNA and protein in distal dendrites, with a concomitant decrease in dendritic branching. Interestingly, the function of Zbp1/Vg1RBP is developmentally regulated, as it is required for intensive dendritogenesis in young neurons, but not for dendrite maintenance in mature neurons. In rat hippocampal neurons, differential localization of Brain-derived-neurotrophic-factor **(**BDNF) splice variants along dendrites has been shown to lead to spatially restricted effects on dendritic architecture. Whereas BDNF transcripts restricted to the cell soma and proximal dendrites selectively affect proximal dendritic branching, transcripts with a distal dendritic localization affect peripheral dendrites. These results have led to a ‘spatial code hypothesis’, in which selective targeting of BDNF to distinct dendritic regions through differential mRNA localization allows both a precise shaping of dendritic compartments during development and spatially restricted control of dendritic plasticity in mature neurons (Medioni, et al., 2012).

.2.2.2 Synapse formation and plasticity

Formation of new synapses is crucial during early development of the nervous system, and is a multistep process involving initial assembly, maturation and stabilization. As shown in cultured Aplysia neurons, recruitment of the neuropeptide-encoding sensorin mRNA to nascent synapses is induced upon recognition of pre- and postsynaptic partners, and is required for further synaptic development and maturation (Lyles, et al., 2006). These results illustrate that synaptogenesis not only involves recruitment of proteins or organelles, such as synaptic vesicles, but also requires mRNA targeting.

In more mature neurons, local translation of dendritically localized mRNAs encoding proteins such as neurotransmitter receptors, ion channels and signal transduction enzymes is essential for the regulation of synaptic activity. Interestingly, specific populations of mRNAs are recruited to dendrites upon synaptic activity, and their translation can be regulated in a synapse- and stimulus-specific manner, providing a means of individually tagging activated synapses (Fig. 2) (Medioni, et al., 2012).

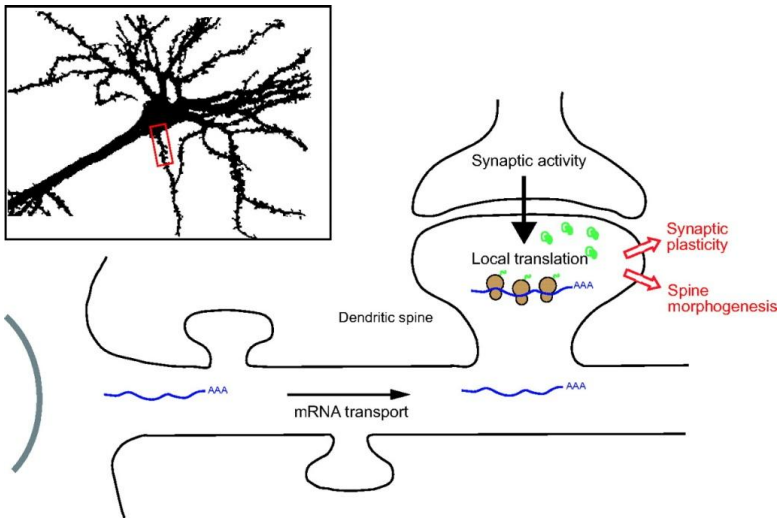

Figure 2

Upper left box: representation of the somatodendritic compartment of a mammalian neuron. Lower panel: schematic of the proximal part of a dendrite that roughly corresponds to the region boxed in the upper panel (red rectangle). Proteins synthesized locally in dendritic spines are represented in green.

Translation of dendritically targeted mRNAs is activated in response to synaptic activity and is essential for modulation of synaptic activity and dendritic spine morphogenesis. Strikingly, translation can be regulated at the synapse level, and thus represents an efficient way to individually tag activated synapses. Mutations in genes involved in dendritic mRNA targeting or translation have been linked to several human neurological disorders, including the most

common cause of inherited mental retardation Fragile X syndrome, consistent with a role for dendritically localized protein synthesis in the regulation of synaptic morphogenesis and plasticity (Liu-Yesucevitz1, et al., 2011).

.2.2.3 mRNA localization in axons

The first evidence for protein synthesis in axons was reported more than 40 years ago using metabolic labeling techniques (Koenig, 1967) (Giuditta, et al., 1968). These initial findings were criticized at the time because the small amount of axonal labeling (only a small percentage of the cellular total) was thought to be due to low-level contamination by cell body material. Ultrastructural studies in the 1970s, however, reported the presence of ribosomes in cultured growth cones and young axons (Tennyson, 1970) (Zelená, 1970) (Bunge, 1973) and, in the last 15 years, biochemical and immunocytochemical approaches have confirmed the presence of axonal ribosomes (Bassell, et al., 1998) along with other components of the translation machinery, including translation initiation factors, mRNA, tRNA, aminoacyl-tRNA synthetases, elongation factors, Golgi, and endoplasmic reticulum proteins (Merianda, et al., 2009) (Shigeoka, et al., 2013)

As revealed by studies performed on cultured Xenopus retinal neurons, axonal growth cone steering decisions require local translation of mRNAs targeted to growing axon tips (Campbell, et al., 2001). Strikingly, two recent microarray analyses have shown that hundreds of mRNAs (6-10% of the transcriptome) are present in the axons of cultured vertebrate sensory neurons, suggesting that a large panoply of proteins might be locally translated (Zivraj, et al., 2010) (Gumy, et al., 2011). Consistent with this, axonal translation of proteins as diverse as polarity proteins involved in axon outgrowth, actin cytoskeleton regulators involved in axon guidance and transcription factors signalling back to the nucleus has been demonstrated to be important for polarized axon growth, maintenance or regeneration (Medioni, et al., 2012). A strong link between axonal mRNA localization, local translation, and axon steering has been provided through studies performed in growing *Xenopus* and murine axons. Asymmetric gradients of attractive cues trigger an asymmetric recruitment of β-actin mRNA and a polarized increase in β-actin translation on the near side of the axon growth cone, both being essential for the turning response (Leung, et al., 2006) (Yao, et al., 2006) (Welshhans, et al., 2011). Interestingly, the nature of locally translated proteins depends on the type of applied stimuli, and the repertoire of axonally localized mRNAs is regulated in response to external signals and developmental cues (Medioni, et al., 2012). In rat sensory

neurons, for instance, mRNAs encoding cytoskeletal regulators and transport-related proteins are found in embryonic, but not adult axons (Gumy, et al., 2011).

In addition to the *ex vivo* results described above, *in vivo* studies have shown that mRNA translation in axons is regulated during nervous system development. For example, translation of EphA2 guidance receptor mRNA reporter constructs is activated in chick spinal cord axons only once commissural growth cones have crossed the midline (Brittis, et al., 2002). Also consistent with developmental regulation of axonal protein synthesis *in vivo*, local translation of mouse odorant receptor mRNAs is higher in immature than in adult olfactory bulbs (Dubacq, et al., 2009).

The best-studied RNA-binding protein involved in axon guidance is zip-code binding protein 1 (ZBP1; Vg1RBP in *Xenopus*, IMP1 in human), which binds the "zip-code", a *cis* element in the 3′ UTR of β-actin mRNA. When the β-actin mRNA–ZBP1 interaction is disrupted either by an antisense oligonucleotide targeting the zip-code sequence (Yao, et al., 2006) or by the knock-out of the ZBP1 gene (Welshhans, et al., 2011), the cue-induced localization of β-actin mRNA in growth cones is significantly reduced, and the translation-dependent growth cone turning response is in turn abolished. These results suggest that ZBP1 interacts with the zip-code element to transport β-actin mRNA, and the interaction is important for growth cone turning. *In vivo* studies of Vg1RBP (ZBP1 homologue) and another RBP, Hermes (RBPMS), in *Xenopus* and zebrafish retinal ganglion cells, respectively, show that loss of function of these genes causes severe defects in axon terminal arborization without affecting the long-range guidance from the eye to the tectum. These studies indicate that the translational regulation mediated by these RBPs has a key role in the axon–target guided cell-specific interactions that lead to axon branching and selective synapse formation (Hörnberg, et al., 2013) (Kalous, et al., 2013).

Tau, a neuronal cytoskeletal protein, is a MT-associated protein (MAP) that stabilizes MTs and promotes their assembly. In neuronal cells, tau is found primarily in the cell body and axon. Axonal localization of tau mRNA to the proximal segment of the axon is dependent on 3′ UTR *cis*-acting signals, neuronal proteins and assembled MTs. The minimal tau axonal localization signal (ALS) sufficient for axonal localization includes the stabilization sequence of tau mRNA, which binds to the HuD stabilization protein.

Tau mRNA was non-randomly distributed in the cells; instead it was localized as discrete granules along the axon and in the growth cone and it co-localized on the MTs with ribosomal proteins, which indicated the presence of protein synthesis machinery in the axon. RNA granules have been observed in fibroblasts, oligodendrocytes and primary neuronal cell

cultures, suggesting that they may consist of RNA-protein complexes that contribute to the formation of cellular microdomains (Aronov, et al., 2002).

3. Post-transcriptional regulation of mRNA metabolism

In eukaryotes, the majority of genes are regulated both at the transcriptional and post-transcriptional level. Post-transcriptional control of gene expression is essential for cell differentiation and cell function and, in complex organisms, is provided by a highly sophisticated regulatory network where the steps of mRNA metabolism (mRNA capping, poly-adenylation, splicing, degradation, etc.) and mRNA localisation are coordinated to modulate local protein concentration.

The coordination between the different processes relies on the assembly of large mRNA-protein complexes that migrate between the sites of processing, storage and translation. Post-transcriptional regulation is also important for expression of mitochondrial proteins (Lithgow, et al., 1997).

RNP particles have been grouped in classes reflecting their protein composition and their association with specific cellular states, and a general regulatory model has been proposed where functionally related genes are co-regulated based on the association of the corresponding mRNAs within the same RNP particles (Keene, et al., 2002) (Mansfield, et al., 2009). In this so-called 'ribonome' model, RNP particles represent the functional equivalent of bacterial operons.

The composition of each RNP particle varies depending on its functional status, and the multi-functional multi-domain protein components can associate with different RNA molecules in a timely and localised fashion. These protein-RNA interactions control the efficiency of mRNA synthesis, processing, nuclear export and degradation as well as the mRNA translation rate and cellular localisation (Keene, et al., 2002) (Mansfield, et al., 2009).

Post-transcriptional regulation critically contributes to the ability of cells to adjust gene expression in the face of a changing external or internal environment (Glisovic, et al., 2008). A combination of biochemical and cell biological research, recently complemented by genome-wide studies, has led to the current notion that each mRNA is bound by multiple RBPs and that individual RBPs have hundreds to thousands of mRNA targets. Furthermore, RBPs are often components of multi-protein complexes and bring additional proteins into mRNPs through protein-protein interactions. It is generally accepted that, during their journey from transcription in the nucleus to translation in the cytoplasm, mRNPs continuously change their composition (Muller-McNicoll, et al., 2013). RBPs assemble on nascent and processed

mRNAs, governing gene regulation at post-transcriptional level in health and disease (Willers, et al., 2011). Indeed, mutations affecting the function of RBPs cause several diseases (Cooper, et al., 2009). RBPs are the primary regulatory factors of the various post-transcriptional stages, including alternative splicing, polyadenylation, mRNA localization, translation and degradation (Fig. 3) (Salas, et al., 2013).

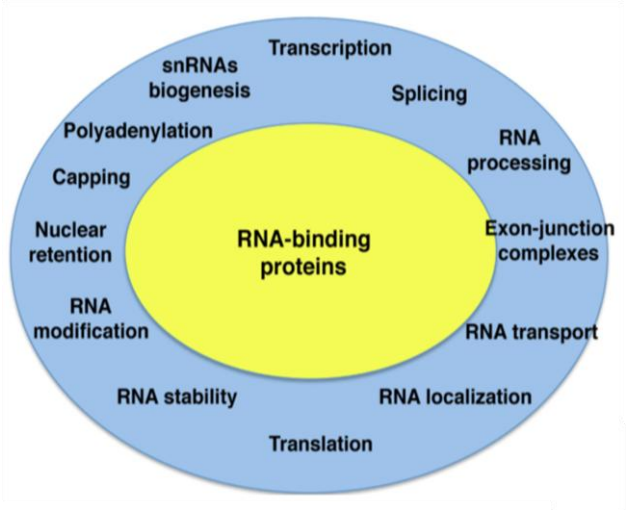

Figure 3
Gene expression control in eukaryotic cells. Each step of gene expression is controlled by RNA-binding proteins (yellow), such that altering one step affects the rest (blue ring), impacting on translation efficiency of mRNAs.

These steps in the RNA lifespan are closely connected to each other, such that altering one of them will affect the others. RBPs interacting with certain UTR structural elements or specific primary sequences play a pivotal role in the response of the cell to different environmental stresses, such as virus infections, heat or osmotic stress, nutrient deprivation and other stimuli that trigger apoptosis, inflammatory response, antiviral response, etc. (Fig. 4) (Walsh, et al., 2011) (Spriggs, et al., 2010) (Liwak, et al., 2012).

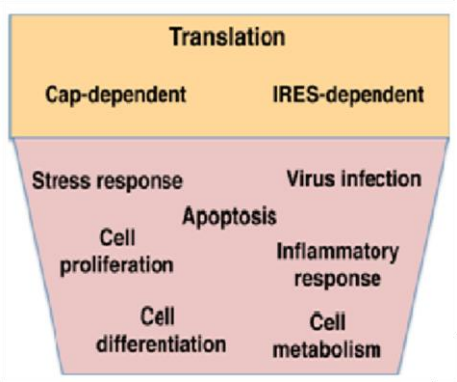

Figure 4

RNA-binding proteins control translation efficiency of mRNAs initiating protein synthesis by the conventional cap-dependent, or the alternative internal ribosome entry site (IRES)-dependent, mechanisms (orange box), impacting on cellular processes in cells undergoing normal growth as well as in response to environmental stresses (pink box).

On the other hand, processes such as cell proliferation, cell death or cell differentiation occurring in healthy organisms also depends on RNA-protein interactions (Komar, et al., 2011).

In response to distinct stresses, cells trigger a differential response that can displace the equilibrium towards cell survival or cell death. Key factors mediating this response are post-translational modification, relocalization, proteolysis or degradation of RBPs.

.3.1 ‘‘Zipcodes’’ are cis-acting motifs

‘‘Zipcodes’’ are *cis*-acting motifs that direct mRNAs for transport to appropriate locations within a cell or organism (Kislauskis, et al., 1992). Zipcodes range in length from a few nucleotides to over 1 kb; however, it is possible that some of the longer zipcodes have not been reduced to their minimally sufficient lengths, making it difficult to identify key RNA determinants of transport. It is believed that zipcodes serve as binding sites for proteins that form complexes with molecular motors, thereby linking the RNA to the cellular transport machinery (Mowry, 1996). Additional RNA sequences may be required to promote the assembly of a localization-competent RNP (Czaplinski, et al., 2006).

An essential feature of zipcodes is that they can direct localization independently of the adjacent RNA sequence: fusing a zipcode to a reporter RNA results in a subcellular distribution of the reporter similar to that observed for the native mRNA. Although zipcodes are usually located in 3’-UTR of transported messages, in some instances they can mediate localization when placed at the 5’ end or even in the middle of a reporter RNA (Jambhekar, et al., 2007). An attractive model for zipcode recognition is that trans-acting factors recognize a

specific secondary structure in the RNA, often a hairpin stem-loop structure, along with a small number of specific nucleotides (Chartrand, et al., 1999). This model has largely proven to be correct in the case of the stem-loop RNA sequence element (TLS) (Cohen, et al., 2005), a zipcode present in both the orb and K10 transcripts of *Drosophila* (Serano, et al., 1995). The native zipcode is predicted to fold in a stem-loop consisting of a 17 base pair stem interrupted by two single-base bulges and an 8 base loop. Fine-mapping studies showed that increasing loop size or decreasing the length of the stem interfered with transport/localization. (Cohen, et al., 2005).

.3.2 Trans-acting factors

.3.2.1 RNA-Binding-Domains (RBDs)

RBDs are evolutionarily conserved protein domains that recognize specific sequence or structural elements in their target RNAs. More than 40 annotated RBDs exist in the databases, but only some of the most frequently occurring, such as the RNA recognition motif (RRM), have been characterized in detail (Fig. 5).

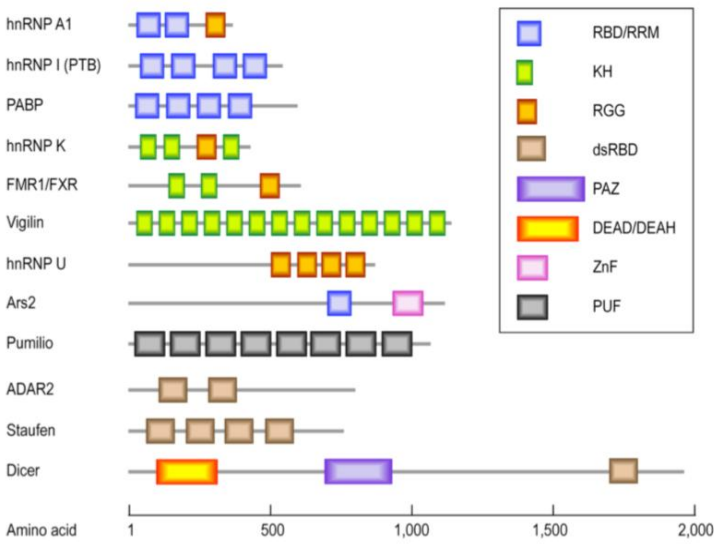

Figure 5

RNA-binding domains of RBPs. Often, several RNA-binding domains are found within one RBP. Different RNA-binding domains include the RNA-binding domain (RBD), K-homology (KH) domain, RGG (Arg-Gly-Gly) box, double stranded RNA-binding domain (dsRBD), Piwi/Argonaute/Zwille (PAZ) domain, RNA helicase DEAD/DEAH box, RNA-binding zinc finger (ZnF) and Puf RNA-binding repeats (PUF). All are presented as colored boxes.

They often bind to short, degenerate 4-6 nucleotide (nt) segments with a weak affinity in a sequence- and/or structure-specific manner (Muller-McNicoll, et al., 2013).

However, many RBPs require multiple RBDs for their *in vivo* functions, and the interplay between these domains is poorly understood. RBPs with multiple RBDs can recognize longer stretches of RNA, can combine multiple weak interactions to achieve high affinity and specificity or can create new or extended binding surfaces for RNAs.

Several non-canonical RBDs were discovered, some of the RBPs contained globular and/or disordered regions enriched in short repetitive amino acid motifs with unusual RBDs. One example is the K patch, which is an unstructured lysine-rich region. This novel RBD occurs in the abundant endoplasmic-reticulum-membrane-bound protein p180, which was recently shown to act as an mRNA receptor that promotes the association of mRNA with the endoplasmic reticulum surface. The K patch in p180 was confirmed to bind RNA directly *in vitro* and *in vivo*, probably through non specific interactions with the RNA backbone and was required for the efficient anchoring of certain transcripts to the endoplasmic reticulum membrane (Muller-McNicoll, et al., 2013).

The ribonucleoprotein (RNP) domain is one of the most common eukaryotic protein folds. Proteins containing RNP domains function in important steps of post-transcriptional regulation of gene expression by directing the assembly of multiprotein complexes on primary transcripts, mature mRNAs, and stable ribonucleoprotein components of the RNA processing machinery. The diverse functions performed by these proteins depend on their dual ability to recognize RNA and to interact with other proteins, often utilizing specialized auxiliary domains (Varani et al., 1998).

Proteins present in Heterogeneous nuclear ribonucleoproteins (hnRNPs) can also contain a variable number of the RGG (Arg-Gly-Gly) box and heterogeneous nuclear ribonucleoprotein K-homology domains (KH).

Cold shock proteins (CSPs) are among the most conserved proteins in evolution, sharing a cold shock domain (CSD) from prokaryotes to eukaryotes (Wolffe, 1994). Numerous functions have been unravelled for members of this protein family. In bacteria, CSPs are co-ordinately up-regulated following a decrease in temperature to rescue bacterial growth (Jones, et al., 1987). In eukaryotic cells, CSPs are involved in the transcriptional regulation of genes related to cell proliferation [e.g. DNA polymerase-α (En-Nia, et al., 2005), cyclins A and B1 (Jurchott, et al., 2003), FAS receptor (Homer, et al., 2005)]. Other target genes coordinate matrix synthesis and degradation (Higashi, et al., 2003), inflammatory responses [e.g. IL-2; (Chen, et al., 2000)], granulocyte macrophage-colony stimulating factor (GM-CSF)

(Diamond, et al., 2001), and antigen presentation [major human leukocyte antigen (Didier, et al., 1988)], ABC transporters (Bargou, et al., 1997).

Y-box protein (YB)-1 is the prototypic member of the cold shock protein family in humans. YB-1 acts in a cell-context specific fashion on gene transcription, for example, of the matrix-metalloproteinase (MMP)-2 and GM-CSF genes. Furthermore, YB-1 has been isolated as a major component of messenger ribonucleoprotein particles (mRNPs) that guide mRNA storage, for instance GM-CSF and renin mRNAs, and is involved in translation processes. The specific association of YB-1 with mRNA evidenced its regulatory role in mRNA processing in concert with splicing factors, such as SRp30c (Roeyen, et al., 2013).

Zinc-finger (ZNF)-containing proteins can be classified into evolutionary and functionally divergent protein families that share one or more domains in which a zinc ion is tetrahedrally coordinated by cysteines and histidines. The ZNF domain defines one of the largest protein superfamilies in mammalian genomes. ZNF-containing proteins can bind to DNA, RNA, other proteins, or lipids as a modular domain in combination with other conserved structures. Owing to this combinatorial diversity, different members of ZNF superfamilies contribute to many distinct cellular processes, including transcriptional regulation, mRNA stability and processing, and protein turnover. The first ZNF domain to be identified in *Xenopus laevis*, basal transcription factor TFIIIA, is the archetype for the most common form of ZNF domain, the C2H2 domain (Ravasi, et al., 2003).

A set of proteins that bind to structured RNA contain double-stranded RNA-binding domains (dsRBD). This ~70-amino-acid sequence motif forms a tertiary structure that interacts with dsRNA, with partially duplexed RNA and, in some cases, with RNA-DNA hybrids, generally without obvious RNA sequence specificity. Among the first to be recognized were Staufen, responsible for mRNA localization in *Drosophila*, and PKR, a dsRNA-activated protein kinase in mammals (Fierro-Monti, et al., 2000).

Other well known RNA-binding domains are Piwi/Argonaute/Zwile (PAZ) domain, DEAD/DEAH box, Sm domain and Pumilio/FBF (PUF or Pum-HD) domain (Glisovic, et al., 2008).

.3.2.1.1 Combinatorial protein-RNA interactions

The use of a modular domain-based approach to RNA recognition allows regulatory proteins to establish reversible interactions with the RNA targets within large RNA-protein particles. This modularity is observed in the bimolecular recognition of an RNA molecule by a multi-domain protein (Fig. 6), or when several RNA molecules or proteins are involved. Protein-

protein interactions can also bring together different parts of the RNA or different RNAs (Fig. 6).

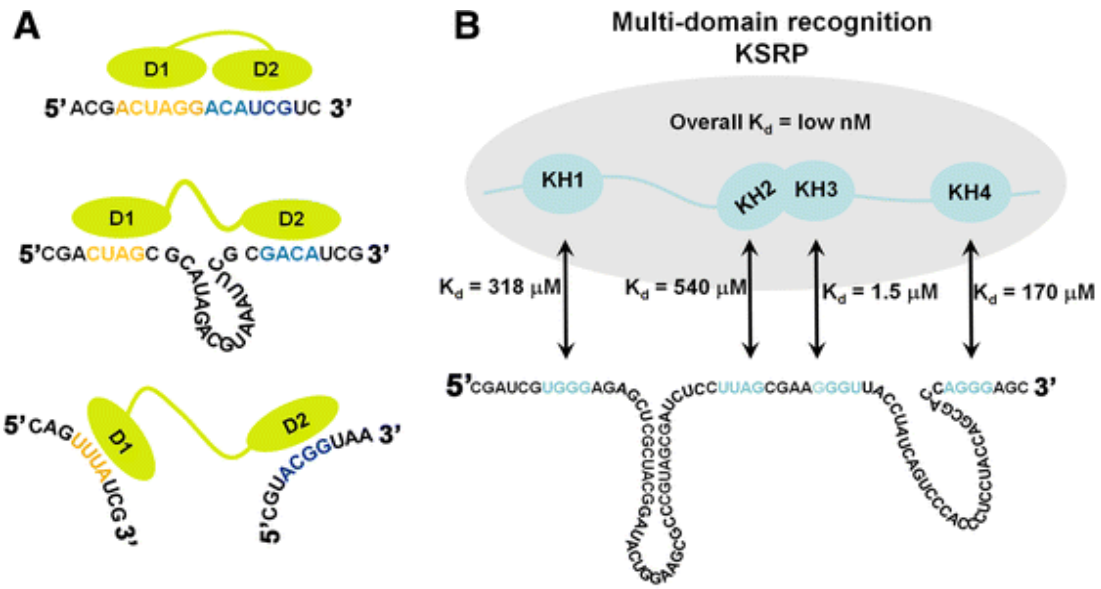

Figure 6

Modular recognition of the RNA. A: Two RNA-binding domains can interact with adjacent RNA sequences (*top*) or distantly located sequences within one RNA molecule (*middle*) or two different RNA molecules (*bottom*), creating an array of possible structural combinations. B: The different RNA-binding affinities of the four KH domains of KSRP for RNA (best binding sequence) underscore their different role and the potential to create a high-affinity interaction in multiple domains recognition.

.3.2.2 RBPs

Among the best characterized RBPs are hnRNPs, a large family of nuclear proteins (hnRNP A1 to hnRNP U) with RNA-binding domains and protein-protein binding motifs, that shuttle with the RNA from the nucleus to the cytoplasm and regulate transcription, splicing, RNA turnover and translation (Lunde, et al., 2007).

HnRNP K, PCBP1 (hnRNP E1) and PCBP2 (hnRNP E2) recognize poly(C) regions and share the KH RNA-binding domain (Makeyev, et al., 2002).

Multi-functional proteins may be crucial for the building of the highly complex networks that maintain the function and structure in the eukaryotic cell possessing a relatively low number of protein-encoding genes. One facet of this phenomenon is the interaction of metabolic enzymes with RNA. The list of such enzymes known to be associated with RNA is constantly expanding (Table 1) (Cieśla, 2006).

Enzyme	Catalyzed reaction	Binds
Glyceraldehyde-3-phosphate dehydrogenase (GAPDH)	3-phosphoglyceraldehyde + NAD+ + Pi → 1,3-diphosphoglycerate + NADH + H+	tRNA IFN-α, c-myc, GM-CSF and IL-2 mRNA 3'UTR (ARE) GLUT1 mRNA 3'UTR (ARE) ribosomal RNA TNF-α hammerhead ribozyme HAV RNA 5'UTR (IRES) HAV RNA 3'UTR (ARE) and 3'coding HCV RNA 3'UTR HBV HPIV RNA 3'UTR (U-rich) HDV antigenomic RNA MyHC mRNA 3'UTR
Aldolase	fructose-1,6-bisphosphate ↔ glyceraldehyde-3-phosphate + dihydroxyacetone phosphate	MyHC mRNA 3'UTR
Lactate dehydrogenase (LDH)	lactate + NAD+ ↔ pyruvate + NADH + H+	GM-CSF mRNA 3'UTR (ARE)
Glucose 6-phosphate dehydrogenase (G6PDH)	glucose-6- phosphate+NADP+ → 6-phosphogluconolacton + NADPH	GLUT1 mRNA 3'UTR (ARE)
Glutamate dehydrogenase (GDH)	l-glutamate + NAD(P)+ + H2O ↔ 2-oxoglutarate + NH4+ + NAD(P)H	cytochrome c oxidase mRNA gRNA 3'oligo(U)
Thymidylate synthase (TS)	Deoxyuridine monophosphate + N5,10-methylene- tetrahydrofolate → deoxythymidine monophosphate + dihydrofolate	TS mRNA p53 mRNA c-myc mRNA various RNAs
Creatine kinase brain form B (CKBB)	creatine + ATP → phosphocreatine + ADP	αMyHC mRNA 3'UTR

Table 1

List of enzymes known to be associated with RNA

Given the many layers of post-transcriptional control operating in the cell, the number of factors involved in various steps of RNA metabolism is much larger than anticipated. Indeed, the recent development of methodologies aimed at searching for new RBPs has produced a

catalogue of factors with RNA binding capacity (Castello, et al., 2012), such as enzymes of intermediary metabolism among others. In the near future, in depth characterization will indicate whether these factors are passengers of RNP complexes or will provide evidences for the functional role of these factors in RNA-dependent pathways.

A great variety of post-translational modifications affecting RBPs have been discovered, such as serine/threonine phosphorylation, proline hydroxylation, arginine/lysine methylation, lysine ubiquitination or SUMOylation, lipidation and so on. All of these chemical modifications can influence affinity and/or specificity of protein-protein and/or RNA-protein interactions, and are consequently critical for rapid remodelling of ribonucleoprotein complexes and for stability and localization of mRNAs (Thapar, et al., 2013) (Lee, et al., 2013).

.3.2.3 miRNAs

Beside RBPs, regulation of mRNA metabolism also involves non coding RNAs (ncRNAs). A very high proportion of complex genomes give indeed rise to ncRNAs, among which the most widely studied class is that of miRNAs. MiRNAs are a novel class of small (21-25 nucleotides), non-coding RNA molecules predicted to post-transcriptionally regulate at least half of the human transcriptome (Friedman, et al., 2009). The discovery, and subsequent characterization, of miRNAs has revealed an intriguing additional level of gene regulation that is fundamental in a diverse range of pathways including development, differentiation and pathological processes. Each miRNA is estimated to regulate around 200 targets, and mRNA transcripts may be regulated by multiple miRNAs.

miRNA genes are transcribed by RNA polymerase II (pol II) to generate long primary transcripts (pri-miRNAs), which can be several kilobases long. The pri-miRNAs are capped, spliced and polyadenylated. Drosha digests pri-miRNAs to release hairpin structures called precursor miRNAs (pre-miRNAs), which are 60-70 nucleotides in length. Exportin-5 interacts directly with the pre-miRNAs to mediate their export into the cytoplasm, where a second RNase III enzyme named Dicer cleaves the pre-miRNA to generate a double-stranded miRNA duplex of ∼22 nucleotides. Following Dicer processing, the miRNA duplex is rapidly unwound as it associates with Argonaute (Ago) proteins, and one strand is retained to become the mature miRNA and is loaded into RNA-induced silencing complexes (RISCs) to participate in mRNA regulation. The complementary strand, which is found at lower concentrations within the cell, is believed to be non-functional and it is rapidly degraded. Altered expression of miRNAs is increasingly recognized as a feature of many diseases,

including neurodegeneration like Alzheimer's disease, Parkinson's disease, amyotrophic lateral sclerosis (ALS) and Huntington's disease (Goodall, et al., 2013).

.3.3 Local control of mRNA translation modulates neuronal development, synaptic plasticity, and memory formation

The complex interplay of post-transcriptional regulatory mechanisms mediated by RBPs at different steps of RNA metabolism is pivotal for the development of the nervous system and the maintenance of adult brain activities.

For example, Hu proteins are human homologues of *Drosophila* ELAV, an RBP whose deletion results in an embryonic lethal abnormal vision phenotype in flies. There are four mammalian ELAV/Hu proteins, HuA, HuB, HuC, and HuD. These proteins are encoded by separate genes and are present in the cell in multiple splice variants. In mammals, birds, and *Xenopus*, three of the members (HuB, HuC, and HuD) are neuronal-specific, while the fourth member, HuA, is expressed in other tissues. Hu proteins are thought to be one of the earliest markers of neuronal differentiation (Marusich, et al., 1994). In the evolution from *Drosophila* to man, ELAV proteins seem to have changed their biological functions in relation to their different subcellular localization. While in *Drosophila* they are localized in the nuclear compartment of neuronal cells and regulate splicing and polyadenylation, in mammals, the neuronal ELAV proteins are mainly present in the cytoplasm where they participate in regulating mRNA target stability, translation and transport into neurites. However, recent data indicate that the mammalian ELAV RBPs also have nuclear activities, similarly to their fly counterpart, being them able to continuously shuttle between the cytoplasm and the nucleus (Colombrita, et al., 2013).

They enhance gene expression increasing mRNA half-life and promoting protein synthesis by a still-unknown molecular mechanism. Developmentally, nELAV proteins have been shown to act as inducers of the transition between neural stem/progenitor cells and differentiation-committed cells, also assisting these neuroblasts in the completion of their maturation program. In brain physiology, they are also the first RBPs demonstrated to have a pivotal role in memory, where they probably control mRNA availability for translation in subcellular domains, thereby providing a biochemical means for selective increase in synaptic strength (Pascale, et al., 2008).

Neural ELAV proteins are key inducers of neuronal differentiation through the stabilization and/or translational enhancement of target transcripts bearing the AU-rich elements (AREs),

whereas Musashi-1 maintains the stem cell proliferation state by acting as a translational repressor. Colocalization of nELAV proteins with Musashi-1 clearly shows that ELAV proteins are expressed at early stages of neural commitment, whereas interaction studies demonstrate that neural ELAV proteins exert an ARE-dependent binding activity on the Msi1 mRNA. This binding activity has functional effects, since the ELAV protein family member HuD is able to stabilize the Msi1 ARE-containing mRNA in a sequence-dependent way in a deadenylation/degradation assay (Ratti, et al., 2006).

One target of ELAV-like proteins is the mRNA of the GAP-43 gene, known to be a determinant of neural development, regeneration of neural connections, and synaptic plasticity in mature synapses. Whereas GAP-43 neuron-specific expression is controlled by elements in the promoter of this gene, its induction during neuritogenesis has been ascribed essentially to post-transcriptional events involving mRNA stabilization. Experimental data suggested that activation of ELAV-like proteins by spatial learning could result in a downstream up-regulation of GAP-43 expression (Quattrone, et al., 2001).

Interestingly, among the target mRNAs regulated by nELAV proteins some encode, in turn, proteins involved in mRNA metabolism; among these, mRNA encoding the neuro-oncological ventral antigen 1 (Nova1), a neuron-specific splicing factor that controls by alternative maturation several mRNAs important for synaptic function. Nova1 mRNA stability and translation are positively controlled by nELAV proteins. Moreover, PKC-dependent nELAV phosphorylation induces recruitment of Nova1 mRNA to polysomes (Ratti, et al., 2008). These findings suggest that, as in the case of transcription factors, a hierarchy of RNA-binding proteins exists whose members are expressed as part of a regulatory cascade.

.3.4 RBPs involved in the study

.3.4.1 PIPPin

PIPPin cDNA was cloned using an experimental approach based on the screening of an expression library, via a binding assay with an *in vitro* transcribed and labeled RNA encoding H1°. PIPPin is highly enriched in the rat brain, it binds specifically both H1° and H3.3 histone mRNAs at the very end of their 3'-UTR, around the putative polyadenylation signals, and contains two putative double-stranded RNA-binding motifs (PIP1 and PIP2), each on one side of a central CSD (Fig. 7A) (Nastasi, et al., 1999). The presence of additional RNA-binding domains, besides the CSD, is not unusual in Y-box proteins, where they enhance RNA-

specific binding mediated by CSD (Graumann, et al., 1998). Only the entire PIPPin is able to bind RNA (Raimondi, et al., 2003).

PIPPin is specifically enriched in some pyramidal neurons of the cerebral cortex and in the Purkinje cells of the cerebellum (Castiglia, et al., 1996), it is present in both the cytoplasm and the nucleus of nerve cells and inhibits translation of H1° and H3.3 mRNA in a cell-free system.

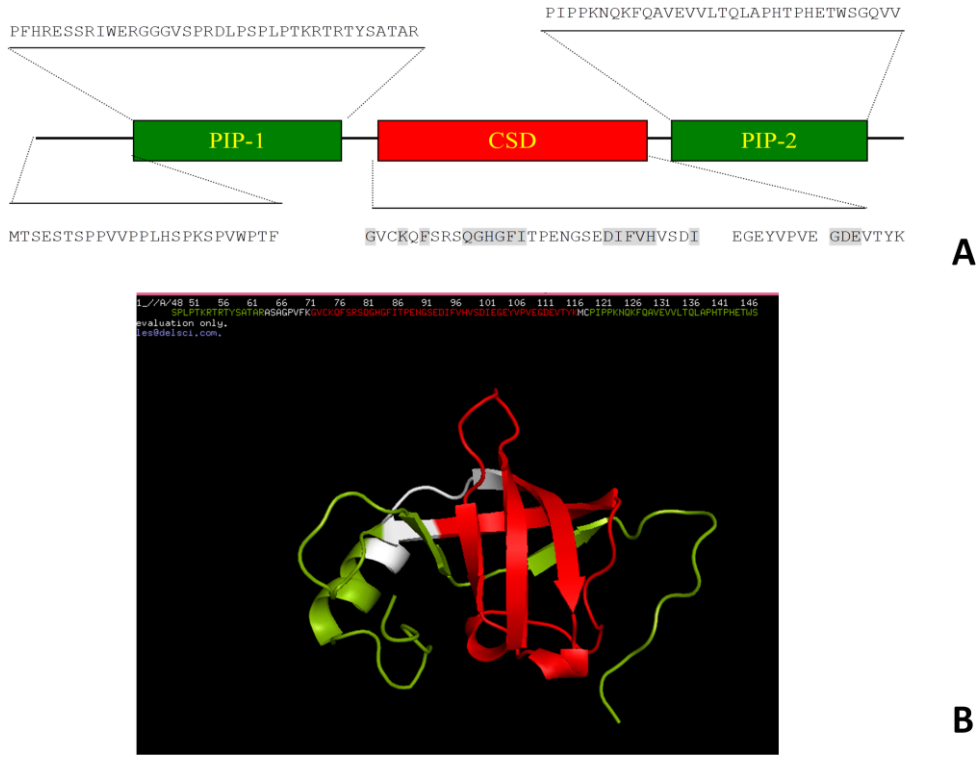

Figure 7

A: Schematic representation of PIPPin protein; B: Tridimensional PIPPin protein.

To better understand which RNA sequence bind to PIPPin, different fragments of the H1° and H3.3 inserts were amplified and cloned (Fig. 8A) and these new plasmids were used as templates to synthesize a set of unlabeled competitor RNAs. As shown in Fig.8 B, all the unlabeled RNAs that contain the very end of the 3'-UTR of both H1° (Fig. 8B, lane H1°, d) and H3.3 RNAs (Fig. 8B, all the lanes marked as H3.3) are able to abolish binding (Nastasi, et al., 1999).

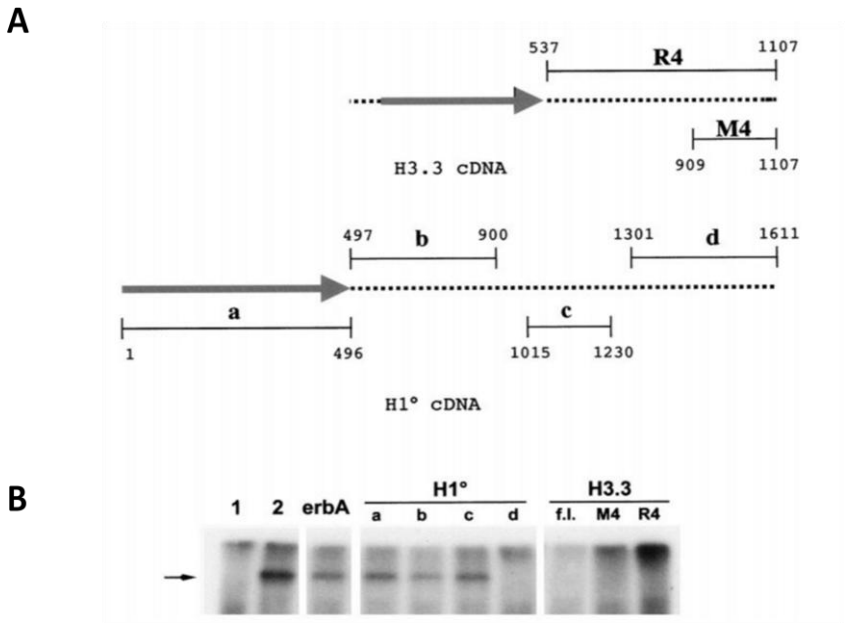

Figura 8

A: Schematic maps of the rat H3.3 and H1° cDNAs; B: subclones corresponding to the four different portions (a to d) of H1° RNA and to the three H3.3 sequences of decreasing sizes (full-length, f.l., R4, and M4), shown in A, and the plasmid pA1.3K were used as templates for the synthesis of unlabeled H1°, H3.3, and erbA transcripts, respectively. The unlabeled RNAs were included, as competitors. The covalent complexes obtained, in the absence of competitors, after incubation of the same amount of radioactive RNA with MBP (lane 1) or MBP/PIPPin fusion protein (lane 2) are shown as internal controls. (Nastasi, et al., 1999)

PIPPin is found both in the nucleus and in the cytoplasm, but immunoprecipitation assays identified RNA-PIPPin complex mainly in nuclear extracts, suggesting that the nuclear form is modified to become able to bind RNA. In fact, in the amino acid sequence several potential phosphorylation sites are present. Moreover, two-dimensional electrophoretic analysis showed that nuclear PIPPin is present in two forms, one more acidic (sparsely present in the cytoplasm) and one more basic (identical to that present in the cytoplasm). It was therefore hypothesized that the nuclear acidic form is phosphorylated and that phosphorylation can promote binding of H1° and H3.3 mRNAs to PIPPin and that, in turn, this interaction could have an effect on their transport to the cytoplasm.

.3.4.2 PEP-19/LPI

LPI (long PEP-19 isoform) was also cloned previously in the laboratory where I carried on my project. LPI is a rat-specific protein of 94 amino acids, with a molecular mass of 10.7 kDa. It is derived from alternative splicing of the gene PCP4, which encodes PEP19, a small brain-specific and calmodulin-binding protein probably involved in the homeostasis of calcium in the brain. PEP-19 is mainly expressed in the central nervous system (in Purkinje

cells of the cerebellum and in the olfactory bulbs), but is present also in the peripheral nervous system. LPI cDNA contains an internal sequence of 127 nucleotides (nt 111-237, indicated as ΔLPI in figure 9) that is not present in the PEP19 cDNA. (Fig.9) (Sala, et al., 2007)

Figure 9

Schematic representation of LPI cDNA.

.3.4.3 hsc70

The Heat shock cognate RNA-binding protein 70 is a constitutively expressed member of the family of 70 kDa chaperones and it is regulated by cycles of ATP/ADP binding. Thanks to its ability to bind AU-rich sequences, hsc 70 is important for the stabilization of mRNAs (Matsui, et al., 2007).

.3.4.4 YB -1

The Y-box binding protein-1 (YB-1) belongs to a large family of proteins that harbor a conserved nucleic acids binding domain, known as CSD. This protein regulates gene expression both at the level of transcription and translation, and it is also implicated in the stabilization of cytoplasmic mRNAs. YB-1 is widely expressed during development and its expression level is closely correlated with cell proliferation. High levels of YB-1 were detected *in vivo* in actively proliferating adult tissues (Lu, et al., 2005).

.3.4.5 hnRNP A1

The Heterogeneous nuclear RNP (hnRNP) A1 is one of the most important pre-mRNA binding proteins. It belongs to the A/B subfamily of hnRNPs, expressed ubiquitously and present both in the nucleus and in the cytoplasm. A1 sequence has been determined and it contains two RNA-binding domains near the amino-terminal end, and a glycine-rich domain near the carboxy-terminal (Good, et al., 1993). hnRNP A1 participates in the maturation of pre-mRNAs and in other aspects of mRNA metabolism, and it has been demonstrated to be involved in the transport of mRNA from nucleus to cytoplasm.

.3.5 RBPs dysfunction in neurological disease

Alterations in neuronal RNA processing are characteristic of many if not all neurodegenerative disease conditions. In many cases, the contribution of RNA alterations to disease is not clear; however, it is increasingly recognized that RNA metabolic abnormalities are capable of directly initiating the neurodegenerative disease process and/or accelerating its progression. In these diseases, inherited mutations lead to disrupted function of RBPs and subsequent deleterious changes in RNA metabolism.

Inherited mutations leading to neurodegenerative disease can be in genes coding for RBPs and directly affect RBP function; alternatively, expansion of trinucleotide repeats in non-RBP genes leads to the production of abnormal RNA that can then affect RBP function. Loss-of-function of RBPs is found in both types of disease, and the resulting global changes in RNA processing are thought to underlie disease pathogenesis.

.3.5.1 Spinal Muscular Atrophy

Spinal Muscular Atrophy (SMA) is an autosomal recessive disease characterized by the degeneration of motor neurons in the spinal cord, leading to weakness, muscle atrophy and, in severe cases, death. SMA is caused by deletion or mutation of the survival of motor neuron (SMN1) gene, which encodes a protein that is critical for the assembly of snRNP particles. In combination with other factors, snRNPs form the core of the spliceosome complex that processes immature mRNA. SMN1 binds to both snRNAs and heptameric Sm proteins and mediates their assembly into snRNPs. SMN1 also facilitates transport of the complex into the nucleus where the mature spliceosome operates (Gubitz, et al., 2004) (Yong, et al., 2004). Human genome contains a second SMN gene, SMN2, that harbors a single nucleotide mutation that leads to skipping of exon 7 and production of only small quantities of functional SMN2 protein (Hastings, et al., 2009). Copy number variations in the SMN2 gene modulate the severity of SMA in SMN1 mutant individuals, and enhancing SMN2 expression is being explored as a therapeutic option in SMA (Hanson, et al., 2012).

.3.5.2 Mutations in FMR1

Repeat expansions in the gene FMR1 can lead to disrupted RBP function by two distinct mechanisms, leading to different conditions.

.3.5.2.1 Fragile X Syndrome

Fragile X Syndrome (FXS) is an X-linked disease caused by CGG repeat expansions in the 5′-UTR of the FMR1 gene (Heulens, et al., 2011). FXS is the most common genetic cause of mental retardation, with an incidence of ~1:2500. Unlike other repeat-expansions diseases, in which the expanded RNA or protein is pathogenic, expanded CGG repeats in the 5′ region of FMR1 lead to its transcriptional silencing and loss of the FMRP protein.

FMRP is an RBP that associates with RNA in polyribosomes found in dendrites, and is thought to regulate the local translation required for synaptic plasticity. In support of this idea, one primary feature of patients with FXS is the presence of immature dendritic spines (Lukong, et al., 2008) (Bassell, et al., 2008). FMRP also localizes to RNPs on microtubules and may play a role in the transport of RNA to the synapse (Antar, et al., 2005).

.3.5.2.2 Fragile X Tremor Ataxia Syndrome

In normal individuals, the FMR1 gene contains 5-50 CGG repeats, whereas those with the full disease have >200. Interestingly, individuals with an intermediate number of repeats, termed an FMR1 premutation, do not develop FXS. Males with an FMR1 premutation, however, develop FXTAS, a late-onset disorder characterized by dementia, gait abnormality, and tremor (Li, et al., 2010). In contrast to FXS, in which the FMR1 gene is silenced, individuals with FXTAS do produce FMRP protein (Tassone, et al., 2000). However, the expanded RNA forms nuclear foci similar to those observed in myotonic dystrophy; these foci also contain RBPs, specifically Pur-α and hnRNPA2/B1 (Jin, et al., 2007) (Sofola, et al., 2007).

Sequestration and loss of function of these RBPs seems to be important for disease pathogenesis, as overexpression of either protein rescues disease phenotypes in FXTAS animal models. Similarly, another study found that CGG-expanded RNA can sequentially recruit distinct RBPs, including MBNL, to nuclear foci, leading to changes in alternative splicing in FXTAS patients (Sellier, et al., 2010).

.3.5.3 ALS

ALS is a neurodegenerative disease that targets the spinal motor neurons controlling voluntary movement, and is characterized by rapidly progressive weakness and paralysis. ALS carries a cumulative lifetime risk of 1 in 1,000 and is fatal, leading to respiratory failure within 3-5 years. Approximately 90% of ALS cases are sporadic (sALS) and of unknown etiology, whereas ~10% of cases are classified as familial (fALS) and have a clear genetic cause. Dominant mutations in superoxide dismutase 1 (SOD1) account for up to 20% of

fALS cases, which are pathologically and clinically similar to sALS (Rosen, et al., 1993). Mutation in SOD1 is thought to cause an abnormal gain-of-function that is toxic to neurons (Boillée, et al., 2006).

Recently, Neumann and colleagues sought to identify novel disease-related proteins in patients with ALS and ubiquitin-positive frontotemporal lobar degeneration (FTLD-U), a pathologically similar disease affecting the cortex. They identified the 43-kDa TAR DNA-binding protein (TDP-43) as a common constituent of cytoplasmic inclusions in both ALS and FTLD-U patients. Predominantly nuclear in normal tissues, in disease TDP-43 is mislocalized to the cytoplasm, ubiquitinated, and hyperphosphorylated. Additionally, inherited mutations in TDP-43 and a related RBP, FUS/TLS (fused in sarcoma/translated in liposarcoma, referred to as FUS), were found to cause familial ALS (Hanson, et al., 2012). Since these discoveries, it has been hypothesized that alterations in RNA processing due to TDP-43 and FUS proteinopathy may underlie disease pathogenesis.

4. Techniques for studying RNA-protein interactions

.4.1 Analysis of RNA-PIPPin (and -Pep-19) interactions by T1 assay

In vitro transcribed, radiolabeled RNA is incubated with the lysate or with purified recombinant protein to allow the formation of RNA-protein complexes, and the mixture is exposed to ultraviolet radiation to convert non-covalent interactions in covalent bonds. Samples are then treated with RNase T1, which digest the RNA with the exception of the sequences protected by bound proteins (Fig.10) and analyzed by SDS-PAGE. After exposure to autoradiographic film, only RNA-protein complexes will be visible as dark bands (Fig.8).

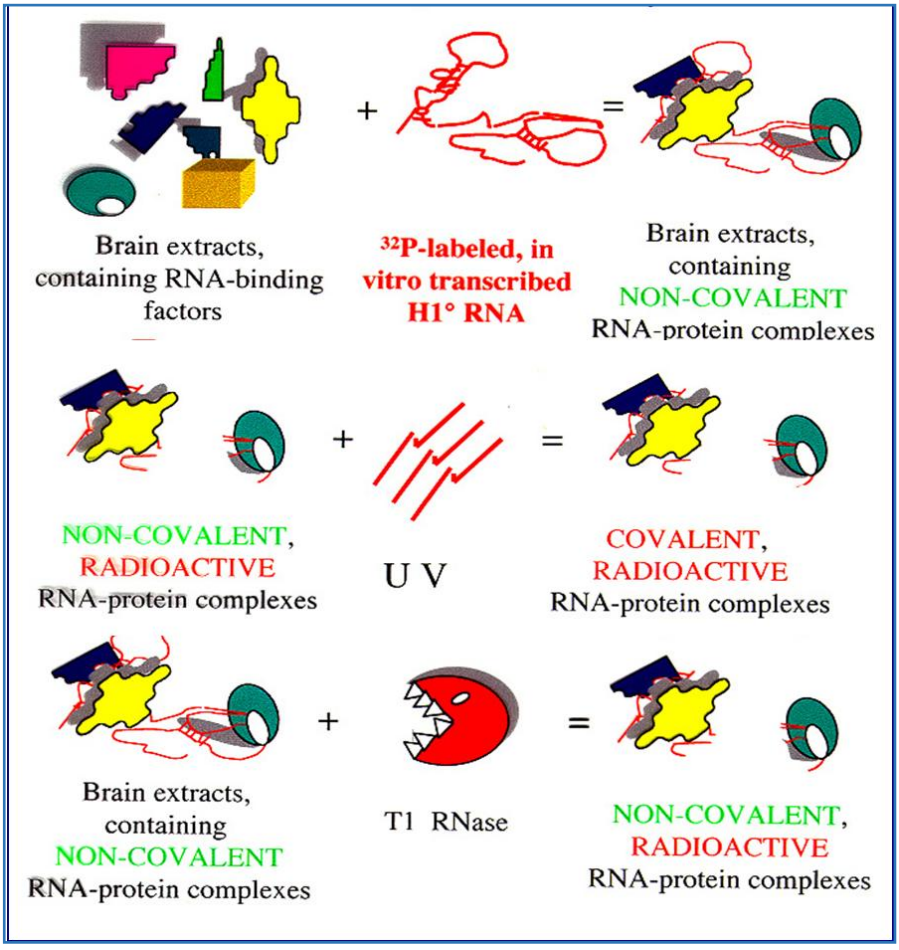

Figure 10

T1 RNase protection assay

.4.2 Analysis of RNA-proteins interactions by BLI

Label-free biosensor methods provide information on binding, kinetics, concentration, and affinity of an interaction. These techniques provide real-time monitoring of interactions between an immobilized ligand (such as a receptor) to an analyte in solution without the use of labels. Advances in biosensor design and detection using BioLayer Interferometry (BLI) provide a simple platform that enables label-free monitoring of biomolecular interactions without the use of flow cells.

Specific RNA-PIPPin binding was demonstrated using a biotinylated RNA via the streptavidin-biotin conjugation method, which makes possible a simple analysis of RNA-protein interactions. The design of the sensor used for detection of RNA-PIPPin interactions by the streptavidin-biotin conjugation method is illustrated in Fig. 11.

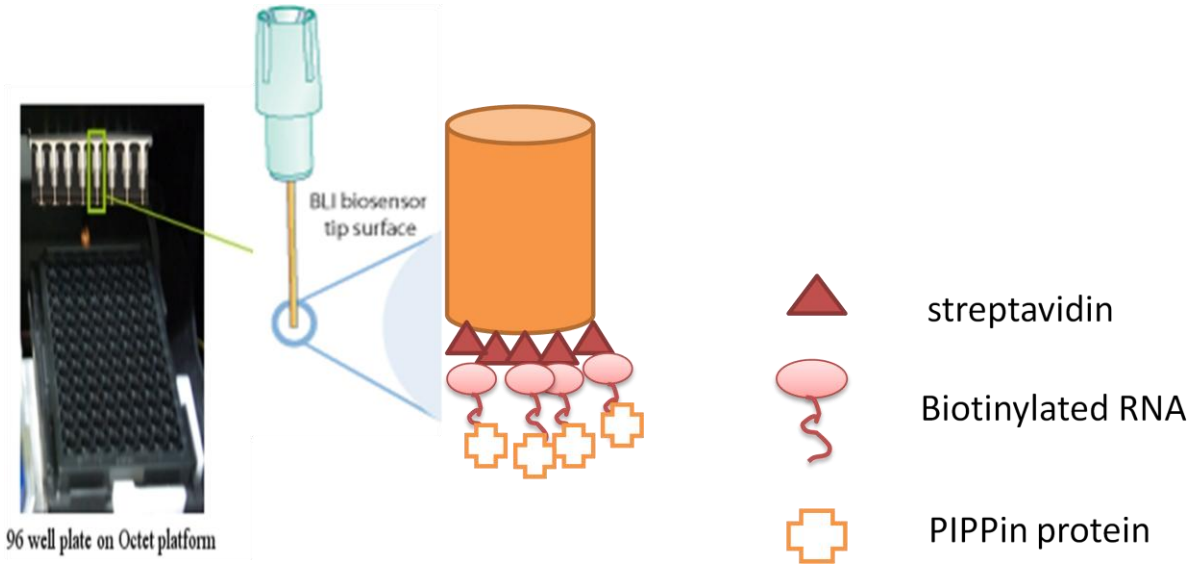

Figure 11

A representative scheme for detection of RNA-PIPPin interaction using streptavidin-biotin conjugation method on the Octet platform.

.4.2.1 Principles of the Octet Platform

BioLayer Interferometry (BLI) technology was invented by Lotze (Lotze, 2009), and it is a label-free, fluidics-free, real-time detection method based on an optically-coated streptavidin biosensor (Farkas, et al., 2007). Interferometry is a technique based on the measurement of light intensity produced by the interference of two or more light beams. This technique can be used for detecting optical properties, such as a refraction index, and physical properties, such as the thickness of a thin film when a difference between the light beams is due to the light passing through it. The principle of BLI method applied to the Octet optical biosensor is illustrated in Fig. 12.

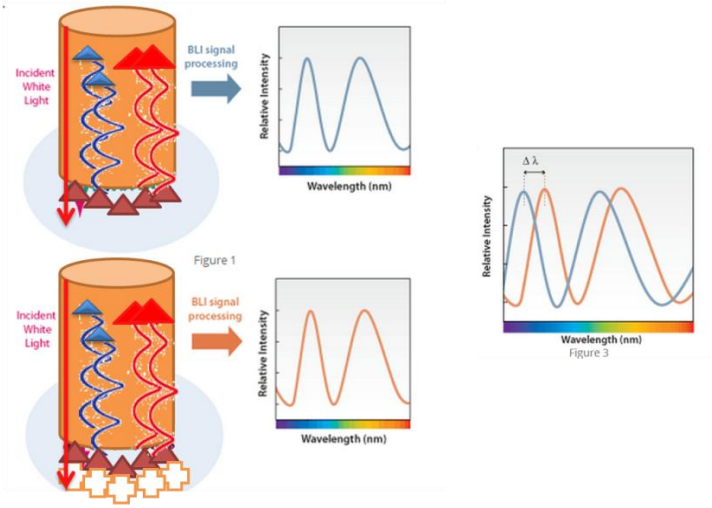

Figure 12

A layer of molecules attached to the tip of an optic fiber creates an interference pattern at the detector with optically coated streptavidin biosensor in solution. Any change in the number of bound molecules causes a measured shift in the pattern. Relationship of distance between reflecting surfaces and reflected intensity would be investigated. As molecules bind, the spectrum of signal changes as a function of the layer increasing on the sensor.

In Figure 11, the biotinylated RNA is attached to a tip coated with a streptavidin optical layer. The tip is dipped into a sample containing the target molecule. The target molecule binds to the captured molecule and the two forms a molecular layer. A white light is directed into the fiber. Two beams will be reflected to the back end. The first beam comes from the tip as a reference. The second light comes from the molecular layer. The difference in the two beams will cause a spectrum pattern as shown in figure 12. The phase is a function of the molecular layer thickness and corresponds to the number of molecules on the tip surface. When the molecules bind to the sensor, the reflections on the internal reference layer will remain constant, while those on the interface between the molecular layer on the fiber and the solution will change with the addition of bound molecules. Bio-layer interferometry within the sensor will monitor this change. For a thin film based on an optically-coated streptavidin biosensor placed on a molecule, that is, the biotinylated RNA, the two interfering beams in reflection mode can be as follows: a beam passing through the thin film and reflected from the interface between the substrate and the film or, alternatively, a beam reflecting from the interface between the thin film and the air. If the biotinylated RNA is optically transparent, interference can also be measured in transmission mode. Interferometry can be used for detecting a change in thickness of an organic film, comprised of an RNA-protein molecules binding, consequent to exposure to a biological sample, and thereby determining the amount of RNA-protein conjugates in the sample by detecting change in thickness. As RNA binds to

PIPPin, the spectrum of the signal will change as a function of the signal increasing on the sensor. The Octet will monitor changes in wavelength over time.

The protein-ligand interaction is generally governed by the following chemical equilibrium:

P + L↔ PL that can be quantitatively described by the equations

Ka = [PL] / [P] [L] association constant

and

Kd = [P] [L] / [PL] dissociation constant

The affinity constant **KD** is the ratio between Kd and Ka, so that a low value of Kd corresponds to a high affinity of the protein for the ligand, and vice versa.

Results and discussion

1 RNA-binding activity of the rat calmodulin-binding PEP-19 protein and of the long PEP-19 isoform

.1.1 RNA-binding activity of PEP-19 and LPI and specificity of RNA-binding

Post-transcriptional regulation of RNA fate depends on the association with different sets of RBPs, which often contain different RNA-binding domains as well as additional domains involved in protein-protein interactions (Burd, et al., 1994).

The RNA-RBP association can be modulated by environmental cues, both during development and in differentiated cells (Derrigo, et al., 2000) (Hall, 2002). During mammalian brain maturation, several classes of neurons accumulate both H3.3, a core histone (Cestelli, et al., 1992), and H1˚, a linker histone (Castiglia, et al., 1994). The concentration of the corresponding mRNAs decreases between embryonic day 18 (E18) and postnatal day 10 (P10), with an inverse correlation to the accumulation of the corresponding proteins. The observed differences are not due to modifications of gene transcription (Scaturro, et al., 1995), and should depend on post-transcriptional regulation. The search of RBPs able to bind H1˚- and/or H3.3-mRNA, and possibly involved in their metabolism, led in the past to the identification of three H1˚ RNA-binding proteins (p40, p70 and p110) (Scaturro, et al., 1998) and to cloning of an H3.3/H1˚ RNA-binding protein (PIPPin/CSD-C2), which contains a cold-shock domain (Nastasi, et al., 1999). More recently, a second protein has been cloned: the experimental approach used was based on the screening of an expression cDNA library with a labeled, in vitro transcribed histone RNA (Sala, et al., 2007). The novel cDNA corresponds to a splicing variant of the mRNA encoding PEP-19, an already known peptide which contains, in its C-terminal half, IQ motifs, able to bind calmodulin. The new protein, that has been called LPI, shares with PEP-19 the calmodulin-binding C-terminal half. The first aim of the present study was therefore to investigate whether PEP-19 and/or LPI interact with H1˚ RNA. The analysis required preparation of recombinant PEP-19 and LPI, but, when produced in bacteria in the form of 6 histidine-tagged recombinant proteins, most of these were found in the inclusion bodies. It was therefore necessary to set an experimental procedure that, moving from the standard denaturation/refold protocols, could allow a high

yield of functional protein. In particular, according to standard protocols, proteins are finally dialyzed. During this step, however, most of the protein aggregated and precipitated. We found that replacement of the final dialysis with a filtration through an equal volume of G-100 Sephadex could restore solubility of the proteins. Moreover, solubility is maintained even after repeated freeze-thaw cycles (Patent N° PA2009A000029).

To confirm that LPI can bind H1° RNA, as suggested by the approach used to identify it, and to investigate PEP-19 binding properties, T1 RNase assays were performed, using in vitro transcribed H1° RNA and 50 ng of each protein. Both LPI (Fig. 13A) and PEP-19 (Fig. 13B) were able to bind rat H1° RNA, each forming a major complex which migrates with an apparent molecular weight of 14 and 12 kDa, respectively.

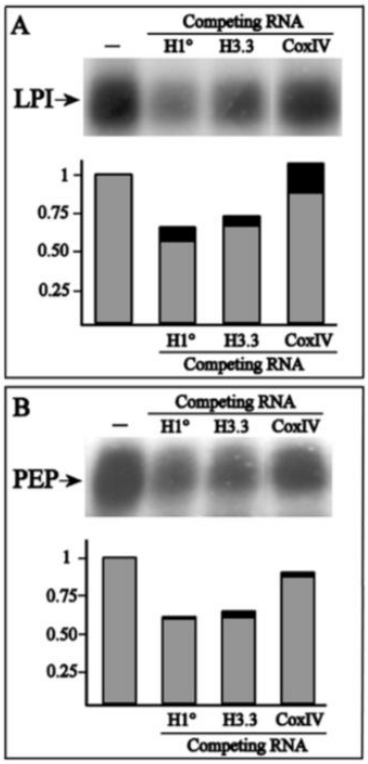

Figure 13

LPI and PEP-19 bind H1° RNA. (A) 6His-tagged LPI or (B) PEP-19 (50 ng each) were incubated with $0.5x10^6$ cpm of radiolabeled H1°RNA. Competition experiments were performed in the presence of excess unlabeled H1° RNA (2:1), H3.3 RNA (2:1) or Cox IV RNA (5:1). At the end of the T1 RNase protection assay, RNA-protein covalent complexes were analyzed by SDS-PAGE and the gels were exposed to X-ray films for 16 h. Representative films showing the RNA-protein complexes obtained in the absence (-) or in the presence of competing RNA are shown in the upper part of A and B. The lower parts of A and B are graphical representations of the statistical analysis of at least three independent experiments. Grey bars indicate mean values for each condition. SDs are also indicated (black bars) (Saladino, et al., 2012).

In addition, to ascertain that the binding of LPI and PEP-19 to H1° RNA was specific, T1 RNase protection assays were performed in the presence of excess unlabeled RNAs. Unlabeled H1° RNA competed with his labeled counterpart in the binding reactions with both

LPI (Fig. 13A) and PEP-19 (Fig. 13B). Unlabeled H3.3 RNA (Fig. 13) also competed with H1˚ RNA binding, suggesting an interaction of both proteins with both RNAs. In contrast, the 3'UTR of Cox IV RNA (Fig. 13) was unable to compete. Fig. 13 also shows a graphical representation of the statistical analysis of at least three independent experiments, for both proteins. The ability of LPI and PEP-19 to bind H3.3 RNA was confirmed by direct T1 RNase protection assay (Fig. 14).

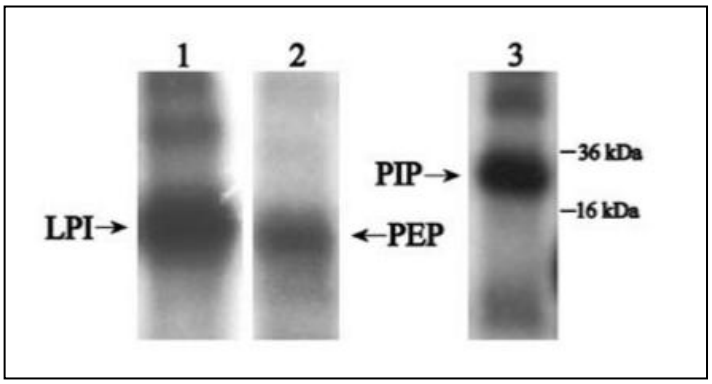

Figure 14

LPI and PEP-19 bind H3.3 RNA. LPI (lane 1), PEP-19 (lane 2) or PIPPin/CSD-C2 (lane 3, PIP) (50 ng each) was incubated with $0.5x10^6$ cpm radiolabeled H3.3 RNA. At the end of the T1 RNase protection assay, the RNA-protein covalent complexes were analyzed as described in Materials and Methods and in Fig. 11 legend (Saladino, et al., 2012)**.**

Both LPI (Fig.14 lane 1) and PEP-19 (Fig.14 lane 2) strongly bound H3.3 RNA, suggesting an interaction of these proteins with both H1˚ and H3.3 RNAs. Fig. 14 also shows H3.3 RNA binding to PIPPin/CSD-C2, the RNA-binding activity of which has been previously reported (Castiglia, et al., 1996) (Nastasi, et al., 1999).

.1.2 PEP-19 and LPI compete with PIPPin/CSD-C2 for H1˚ RNA-binding.

Since both LPI and PEP-19 are able to bind the H1˚ RNA, we assessed their ability to compete with PIPPin/CSD-C2 for binding. Fig. 15 shows the results of these analyses: when used in equimolar amounts, LPI and PIPPin/CSD-C2 form roughly similar amounts of complexes.

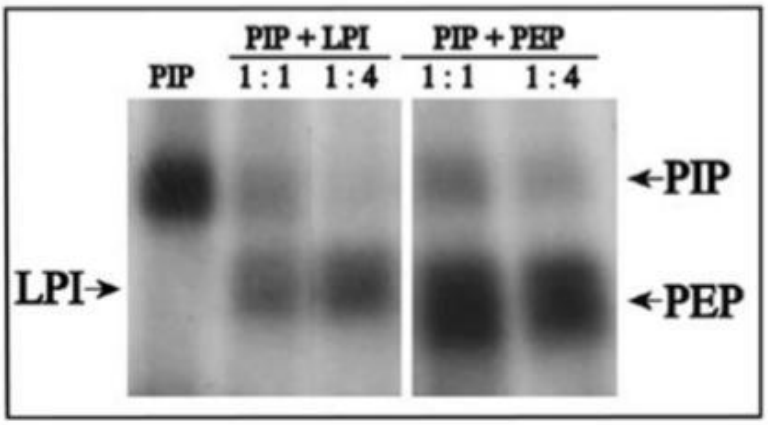

Figure 15

PEP-19 and LPI compete with PIPPin/CSD-C2 for H1˚ RNA binding. PIPPin/CSD-C2 (PIP) (50 ng) were incubated with $0.5x10^6$ cpm of radiolabeled H1˚RNA. Competition experiments were performed in the presence of a 1:1 or 1:4 excess of LPI or PEP-19 (PEP) (Saladino, et al., 2012)**.**

On the other hand, PEP-19 seems to bind H1˚ RNA more strongly than PIPPin/CSD-C2.

.1.3 Effect of calmodulin on PEP-19 and LPI binding to H1˚ RNA

Since both LPI and PEP are able to bind H1˚ RNA, we reasoned that the site involved in RNA binding might be in their common C-terminal half. This part of both molecules also contains the calmodulin-binding site. We, therefore, asked whether calmodulin can interfere with RNA binding. And, indeed, calmodulin was able to reduce the binding of both proteins to RNA (Fig.16).

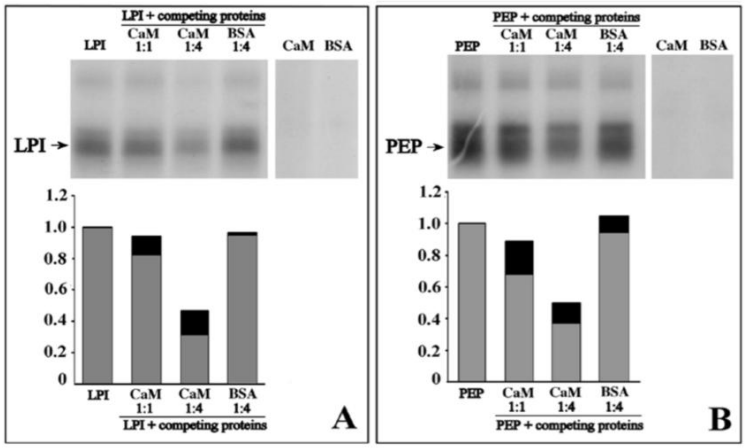

Figure 16

Calmodulin interferes with RNA binding to PEP-19 and LPI but does not bind RNA. (A) LPI or (B) PEP-19 (50 ng each) were incubated with radiolabeled H1˚RNA. Competition experiments were performed in the presence of 1:1 or 4:1 excess of calmodulin (CaM), or 4:1 excess of bovine serum albumin (BSA). At the end of the T1 RNase protection assay, RNA-protein covalent complexes were analyzed as described in the legend to Fig. 13. Representative films are shown in the upper part of A and B. The lower parts of A and B are graphical representations of the statistical analysis of at least three independent experiments. Grey bars indicate mean values for each condition. SDs are also indicated (black bars) (Saladino, et al., 2012)**.**

The interfering effect of calmodulin is specific, since the same amount of BSA did not compete. Graphical representations of the statistical analysis of at least three independent experiments are shown in Fig. 16, for both proteins. The effect of calmodulin is not due to its putative ability to bind RNA: this protein, like BSA, was unable to form complexes with H1˚ RNA on its own (Fig.16)

The specific interaction between calmodulin and Pep-19 protein was also confirmed by the ForteBio's Octet platform, which uses disposable nickel-charged tris-nitriloacetic acid (Tris-NTA) biosensor, and biolayer interferometry to detect and quantify molecular interactions.

In order to calculate the affinity constant of PEP-19-Cam binding, different concentrations of calmodulin were used, from 5ng/µl to 40 ng/µl, while a sample without calmodulin (yellow line) was used as a negative control. The results obtained in this kind of analysis are shown in Fig.17 (See also section 9 in Mat and Met).

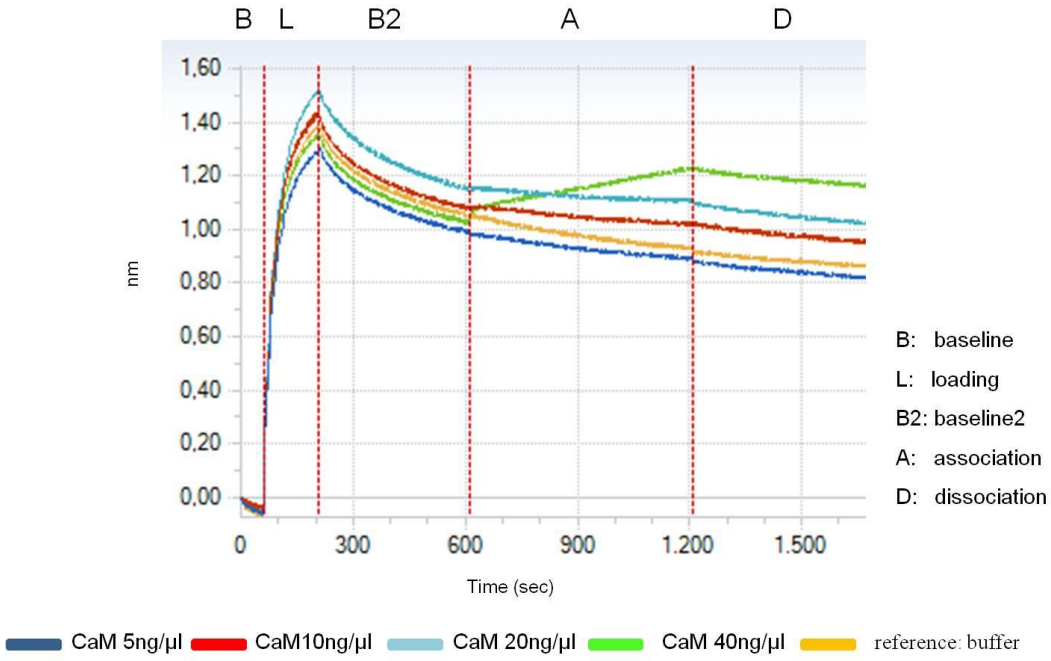

Figure 17

Pep-19/Calmodulin interaction

The binding data obtained were processed to calculate the affinity constants.

The processing procedure includes:

Subtraction Phase: Subtraction of the binding values from reference (Fig.18)

Align Y-Axis: alignment of the curves with Association phase (Fig.18)

Subtraction phase

In the specific experiment shown in Fig. 18, the yellow sensor was used as a reference, i.e. in the absence of calmodulin, to evaluate the signal given by the nonspecific PEP-19 binding to the sensor. Subtracting the values of the yellow sensor (Reference Wells) from the values obtained from the other wells, we obtained the real values for Pep-19/calmodulin interaction.

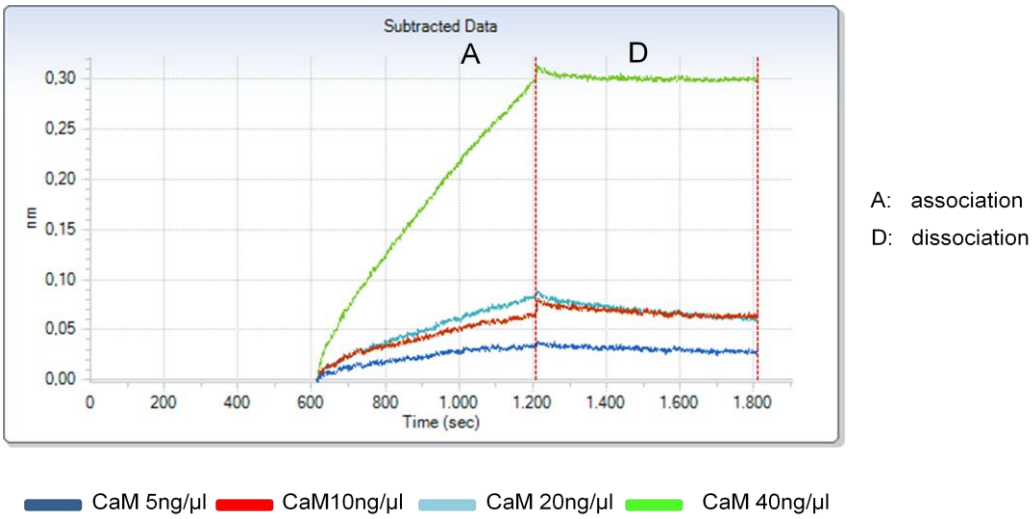

Figure 18

Pep-19/Calmodulin processing

Once completed the processing procedure described above, the kinetic data obtained were analyzed by the Data Analysis 7 Software.

For the analysis, data resulting from the association as well as those from dissociation phase were taken. The chosen “mathematical model of interaction” was the "1:1 model", according to which an analyte in solution binds a single site in the ligand bound to the sensor.

Data analysis made possible the calculation of the affinity constant for the binding between Pep-19 and calmodulin, for each sample.

Graphical representation of the statistical analysis of at least three independent experiments are shown in Fig. 19

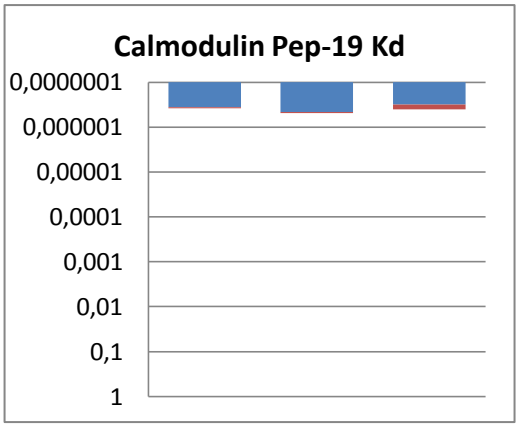

Figure 19

Graphical representation of the statistical analysis of at least three independent experiments. Blue bars indicate mean values for each condition. SDs are also indicated (Red bars).

Here we show that PEP-19 binds calmodulin (in a calcium-independent manner), with an apparent K_d close to 3,70E-^{07}M, which is fairly similar to the value reported by Slemmon and colleagues (Slemmon, et al., 1996).

In conclusion, LPI and PEP-19, like the previously identified PIPPin/CSD-C2 protein, are able to bind both H1˚ and H3.3 RNAs. The fact that all three proteins, which are also able to compete for binding to RNA, recognize both histone variant RNAs suggest the existence of a common regulation of the synthesis of replacement histones. Once we had demonstrated that both LPI and PEP-19 are able to bind H1˚ and H3.3 RNAs, we assessed the possible interfering effect of calmodulin on RNA-binding. The finding that calmodulin actually reduces binding of H1° RNA to both proteins sheds light on the putative signals which could regulate expression of histone variants in the brain. Calcium-dependent signals are indeed of particular importance in the nervous system, and deregulated increases in intracellular ionized calcium can result in neuronal damage and death. Many of the effects of calcium are mediated by calmodulin, and the brain contains tissue-specific peptides (such as PEP-19, neurogranin and neuromodulin) which seem to act as calmodulin antagonists (Slemmon, et al., 1996). Moreover, it has been recently suggested that PEP-19 is a critical determinant of synaptic plasticity (Wei, et al., 2011). Our discovery that PEP-19 and LPI bind H1˚ histone mRNA and that this binding is affected by calmodulin suggests that, in the brain, post-transcriptional regulation of H1˚ histone synthesis may be regulated by calcium signals, and perhaps by neuronal activity.

2. Identification in the rat brain of a set of nuclear proteins interacting with H1° mRNA

.2.1 Chromatographic purification and identification of H1° RNA-interacting proteins

As previously mentioned, the expression of H1° histone is regulated at the post-transcriptional level and is clear that in this regulation numerous RNA binding proteins are involved, some of which are specific for H1° mRNA, while others are universal factors.

It is known that both specific and general RBPs form complexes with RNA, and that, within these complexes, some proteins bind directly to RNA while others may interact in an indirect manner.

Starting from the assumption that RNA metabolism is regulated within complex structures, containing different RNAs and several regulatory proteins, in order to identify other proteins involved in the packaging of H1° mRNA in the nucleus, chromatographic analyses were conducted. We used as bait biotinylated H1° mRNA and, as preys, proteins present in total nuclear cell lysates (Nex) prepared from rat brains at the twentieth day of life. With this approach it is possible to highlight both proteins that interact directly with the H1° mRNA and proteins involved in indirect interactions.

As shown in Fig.20A, affinity chromatography on biotinylated H1° RNA (R) allowed enrichment of nuclear proteins which could not be evidenced in the mock procedure, i.e. in the absence of RNA (C).

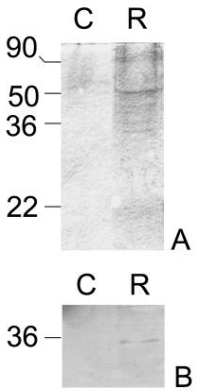

Figure 20

Chromatographic enrichment of H1° mRNA-binding proteins from nuclear extracts of 20 days old rat brains. A: coomassie blue staining of the proteins bound to the streptavidin-conjugated beads in the presence (R) or in the absence (C) of biotinylated H1° mRNA. B: Western blot of proteins shown in A, with anti-PIPPin/CSD-C2 antibodies. Molecular marker sizes are shown on the left (Di Liegro, et al., 2013)**.**

Isolated proteins were analyzed by mass spectrometry. Proteins for which at least 7 peptides were identified are listed in Tab.2.

Protein	**Peptide**	**Principal localization**	**Note**	**Access code**	**kDa**
Tubulin beta-2A	**18**	cytoplasm	Identified in mRNP granule complex	**P85108**	**50**
Glutamate dehydrogenase	**16**	mitochondrial		**P10860.2**	**61**
hnRNP A2/B1	**15**	nucleus	Identified in the spliceosome C complex	**A7VJC2**	**36**
hnRNP K *	**15**	nucleus	Identified in the spliceosome C complex	**P61980**	**60**
hnRNP A1 *	**10**	nucleus, cytoplasm	Identified in the spliceosome C complex	**P04256**	**34**
aldolase a	**10**	cytoplasm		**P05065**	**39**
Tubulin beta-3 chain	**9**	cytoplasm	Neuron-specific	**Q4QRB4**	**50**
aldolase c	**9**	cytoplasm	brain-specific	**P09117**	**39**
glyceraldehyde-3-phosphate dehydrogenase	**8**	cytoplasm		**P04797**	**35**
Heat shock * cognate 71 kDa protein	**8**	cytoplasm, nucleolus, nucleus	Identified in a mRNP granule complex	**P63018**	**70**
Y-box-binding * protein 1	**7**	cytoplasm, nucleus	Identified in histone pre-mRNA complex and cytoplasmic mRNP	**P62961**	**50**

Table 2

List of proteins enriched by chromatography on biotinylated H1° RNA and identified by mass spectrometry. Only proteins for which at least seven peptides were identified were included. Proteins indicated by an asterisk were taken into account in the co-immunoprecipitation analyses. Examples from the literature which describe the identification of listed proteins in RNP complexes as well as their main known localization and molecular mass are reported

Most of these proteins were already known to be involved in RNA metabolism. For example, hnRNP K, originally identified as part of hnRNP particles, has been reported to play a crucial role in axon development (Liu, et al., 2011) and, in general, in development of both central and peripheral nervous systems (Blanchette, et al., 2006), because of its implication in multiple aspects of post-transcriptional gene regulation. Most of hnRNP K roles depend on its ability to interact with a number of partners, some of which were found in unexpected compartments, such as the plasma membrane. Such interactions are also modified by extracellular signals (Mikula, et al., 2006). Other proteins are instead known components of the cytoskeleton and their chromatographic isolation is probably due to indirect interactions with the RBPs.

Interestingly, it has been recently reported that, in embryonic rat brain, Hsc70, YB1 and alfa-/beta-tubulins are present, together with other proteins, in a complex which also contains Staufen-2 (Maher-Laporte, et al., 2010).

By western analysis (Fig.20B), we also found that the RNA-bound fraction (R) of proteins also contains PIPPin/CSD-C2.

.2.2 Co-immunoprecipitation assays

The above results demonstrated that a group of proteins could be isolated through chromatography on biotinylated H1° RNA. To investigate the ability of identified proteins to interact with one another, we then used paired co-immunoprecipitation assays (Fig.21).

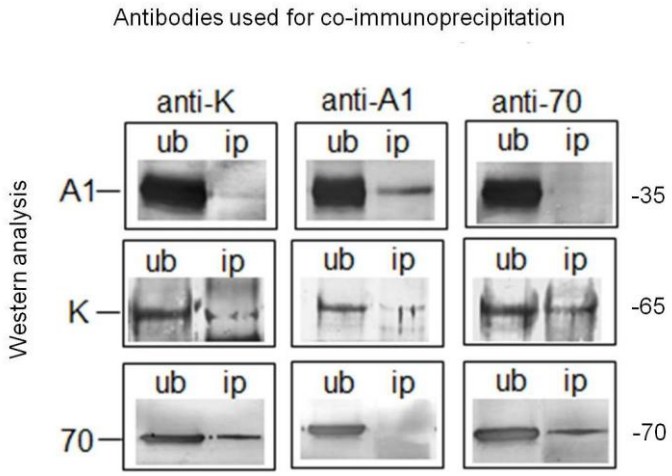

Figure 21
hRNP K, hRNP A1, and Hsc70 co-immunoprecipitation assay.
Proteins were immunoprecipitated from nuclear extracts of 20 days old rat brains with anti-hRNP K (K), anti-hRNP A1 (A1), or anti-Hsc70 (70), and analyzed by western blot. Ub, unbound fraction; Ip, immunoprecipitated proteins. Molecular mass of the proteins is indicated (KDa) (Di Liegro, et al., 2013)**.**

As shown in Fig.21, hnRNP K and Hsc70 were co-immunoprecipitated by both anti-hnRNP K and anti-Hsc70 antibodies. Similarly, hnRNP K and hnRNP A1 were co-immunoprecipitated by both anti-hnRNP K and anti-hnRNP A1 antibodies.

On the other hand, anti-hnRNP A1 antibodies could not immunoprecipitate Hsc70 and *vice versa*. Similarly, anti-A2B1 antibodies used were not able to co-immunoprecipitate other proteins (data not shown).

HnRNP A1 can also interact with PIPPin/CSD-C2 (Fig. 22), which also interacts with YB1, another CSD-containing protein and a 5' cap-dependent mRNA stabilizer (Evdokimova, et al., 2006).

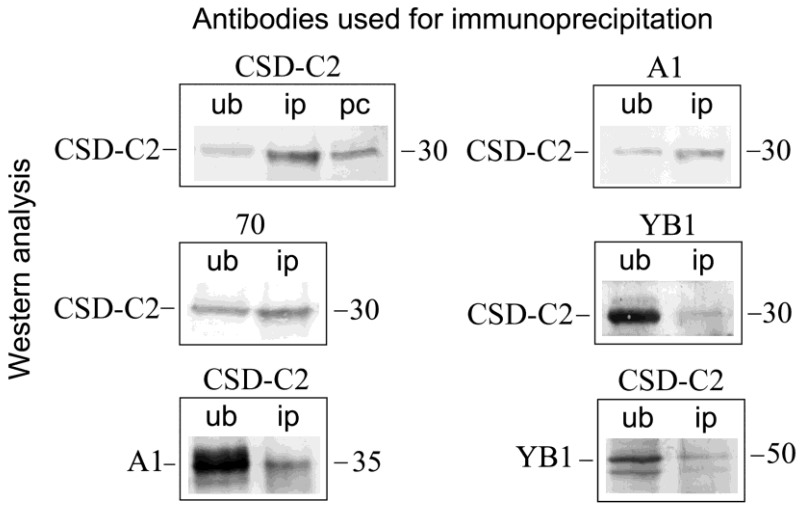

Figure 22

PIPPin/CSD-C2, hRNP A1, YB1, and Hsc70 co-immunoprecipitation assay. Proteins were immunoprecipitated from nuclear extracts of 20-day-old rat brains with anti-hRNP A1 (A1), anti-Hsc70 (70), anti-PIPPin/CSD-C2, or anti-Y-box 1 (YB1), as indicated over each box, and analyzed by Western blot. Ub, unbound fraction; Ip, immunoprecipitated proteins; pc, pre-cleared nuclear extract. Molecular mass of the proteins is indicated (kDa) (Di Liegro, et al., 2013)**.**

YB1 is able to shuttle between the nucleus and cytoplasm, probably contributing to regulation of synthesis, splicing, packaging, and transport of several mRNAs. Like PIPPin/CSD-C2, this protein can be post-translationally modified and the modifications have an effect on its RNA-binding activity (Evdokimova, et al., 2006) (Stratford, et al., 2008). In addition, anti-Hsc70 antibodies were able to co-immunoprecipitate PIPPin/CSD-C2 (Fig.22). However, we were not able to evidence co-immunoprecipitation of Hsc70 and PIPPin/CSD-C2 when anti-PIPPin/CSD-C2 antibodies were used (not shown). Monoclonal PIPPin/CSD-C2 antibodies were also able to co-immunoprecipitate hnRNP K (Fig.23).

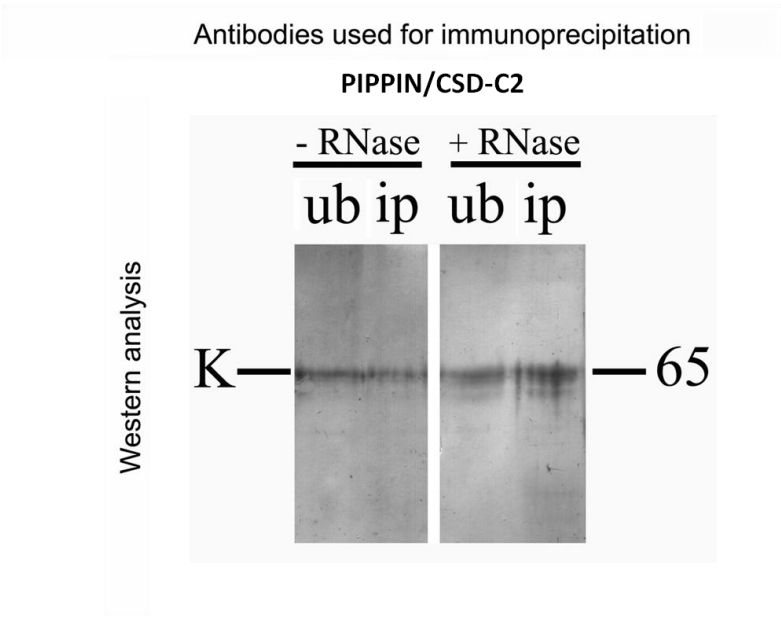

Figure 23

PIPPin/CSD-C2 and hnRNP K co-immunoprecipitation assay. Proteins were immunoprecipitated from nuclear extracts of 20-day-old rat brains with anti-PIPPin/CSD-C2 and analyzed by Western blot with anti-hRNP K (K), in the presence (+) or not (−) of RNase A. Molecular mass is indicated (kDa) (Di Liegro, et al., 2013)**.**

In order to be sure that the observed interactions were not mediated by endogeneous RNA molecules, one half of the extract was incubated with RNase A before each co-immuno-precipitation experiment. We did not find any difference between treated or not treated samples. The results of one of these control experiments are shown in Fig.23.

.2.3 Immunofluorescence

Possible colocalization of Hsc70 and PIPPin/CSD-C2 was further studied by immunofluorescence in cultured astrocytes. As shown in Fig.24 a, yellow spots, indicated by arrows, are clearly visible in the nucleus, thus suggesting the existence of complexes which contain both proteins.

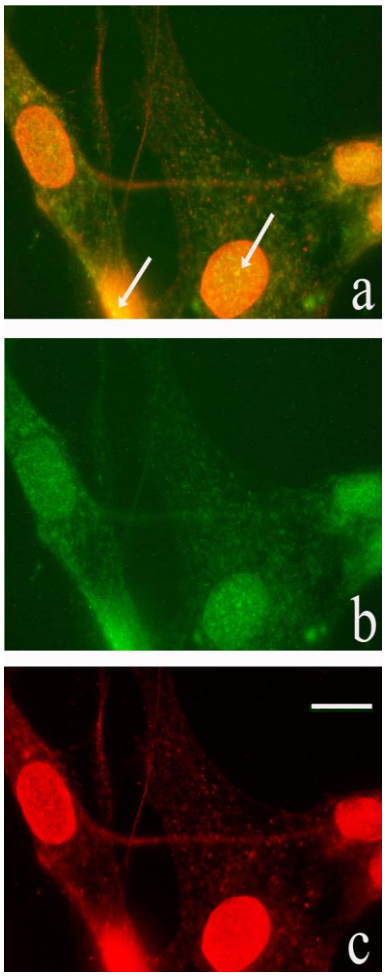

Figure 24

Fluorescence microscopy. Immunofluorescence performed with anti-Hsc70 (b, green fluorescence), and with anti-PIPPin/CSD-C2 (c, red fluorescence) on astrocytes cultured for 5 days in Maat Medium. The overlap of the two fluorescence is shown in (a)

A fluorescent microscopy image, which shows immunostained astrocytes with their peculiar morphology, is shown in fig.25

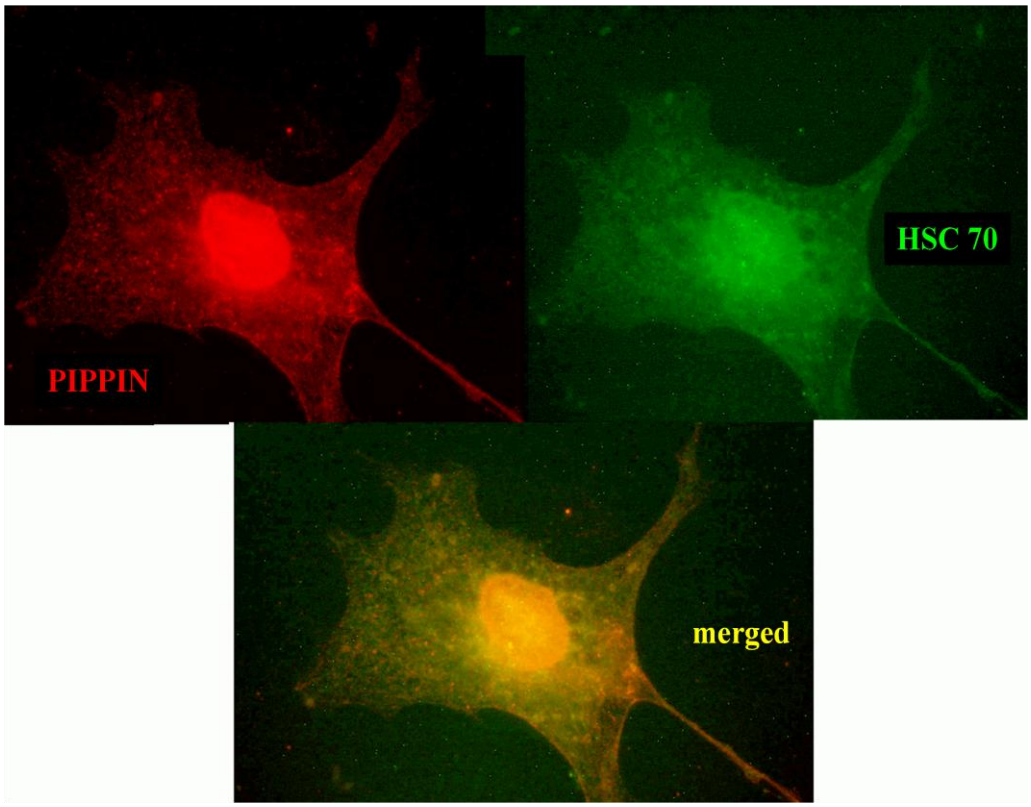

Figure 25

Fluorescence microscopy. Immunofluorescence performed with anti-Hsc70 (green fluorescence), and with anti-PIPPin/CSD-C2 (red fluorescence) on astrocytes cultured for 5 days in Maat Medium. The overlap of the two fluorescences is shown in bottom panel (merged).

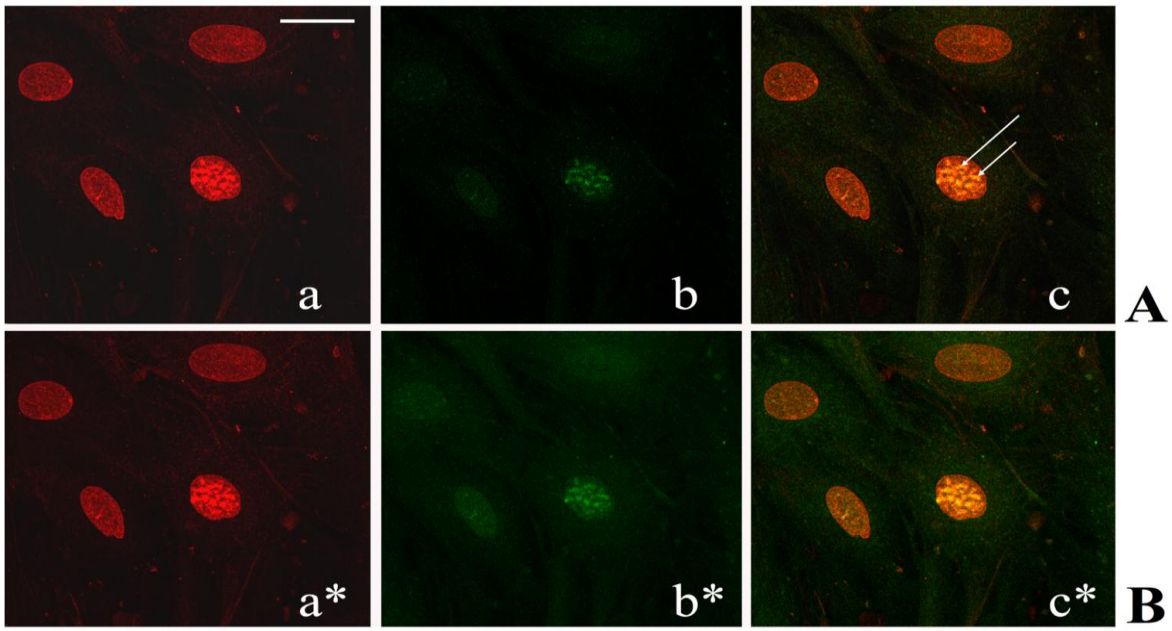

Figure 26

Confocal microscopy of primary astrocytes with anti-Hsc70 and anti-PIPPin/CSD-C2 antibodies. Astrocytes cultured for 5 days in Maat Medium were immunostained with anti-Hsc70 antibodies (b and b*, green fluorescence) or with anti-PIPPin/CSD-C2 antibodies (a and a*, red fluorescence). Merge of the two fluorescences is shown in c and c*. A single optical section is shown in A, while a whole merged view is shown in B. Sites of colocalization, which appear as yellow bodies, are indicated by arrows. Bar = 10 µm (Di Liegro, et al., 2013).

We repeated the experiments by using confocal microscopy (Fig. 26), which allowed us to confirm co-localization of the two proteins.

In conclusion, our data suggest the existence of ribonucleoprotein particles, including PIPPin/CSD-C2 and YB1, as well as hnRNP K and A1, and the molecular chaperone Hsc70. Adding up specific regulatory proteins to general packaging factors can be a key element for the regulation of export and translation of H1° mRNA in response to differentiation cues.

Experiments are currently underway to draw a detailed model of the RNA-protein interactions and protein-protein involved in the regulation of H1° mRNA metabolism.

3. Analysis of interaction between messenger RNAs encoding H3.3 and H1° histone variants and PIPPin/CSD-C2 protein by biolayer interferometry

The aim of the final part of our study was to confirm, by an independent technique, histone mRNA-PIPPin/CSD-C2 interaction and to describe its binding properties through the streptavidin-biotin conjugation method. This method is based on the RNA aptamer sensor system that uses a biotinylated RNA oligonucleotide bound to an Octet optical biosensor. Biolayer interferometry (BLI) measures changes in an interference pattern, generated from visible light when reflected by an optical layer (control sensor), and a biolayer containing the proteins of interest. BLI uses disposable sensors immersed in 96-well plates. The technique has been validated for small molecule detection and for fragment screening with model systems and well-characterized targets, where affinity constants and binding profiles are generally similar to those obtained with surface plasmon resonance (SPR).

Here we report the data obtained in the case of H3.3/H1° mRNA-PIPPin/CSD-C2 interactions, and the specific affinity constant for these bindings.

The following experiments were carried out in the laboratory of prof. Daniel Gygax (University of Applied Sciences and Arts Northwestern Switzerland FHNW), under the supervision of Mr. Peter Spies.

.3.1 Calculation through BLI of the binding affinity for the interaction between PIPPin/CSD-C2 and H3.3 RNA

In order to identify H3.3 RNA portions involved in binding, we used two RNA probes (Fig.27):

R4: which corresponds to the whole 3'-untranslated region (3'-UTR) of the H3.3 mRNA (R4RNA 2 x 10^5 Daltons);

M4: which corresponds to the last 198 nucleotides of the 3'-UTR of the same mRNA (M4RNA 0.6 x 10^5 Daltons);

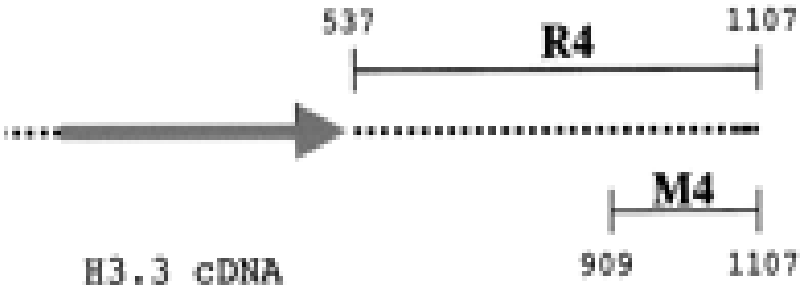

Figure 27

Schematic map of the rat H3.3 cDNA. R4RNA, complete 3'-UTR; M4RNA, 3'-UTR, from nt 909 to nt 1107
From: Nastasi, et al., 1999

As shown in Fig. 28, the biotinylated RNA clearly binds to the streptavidin (SA) biosensor (loading). Moreover, R4RNA-PIPPin/CSD-C2 binding is protein concentration-dependent (signal intensity was found to increase gradually from 5 µg to at least 40 µg mL^{-1} of protein). It was observed that the signal intensity of the conjugated R4RNA could be detected even at the lowest RNA concentration (0,00001pm/l). These results confirm that this RNA specifically drives PIPPin/CSD-C2 binding to the Octet platform.

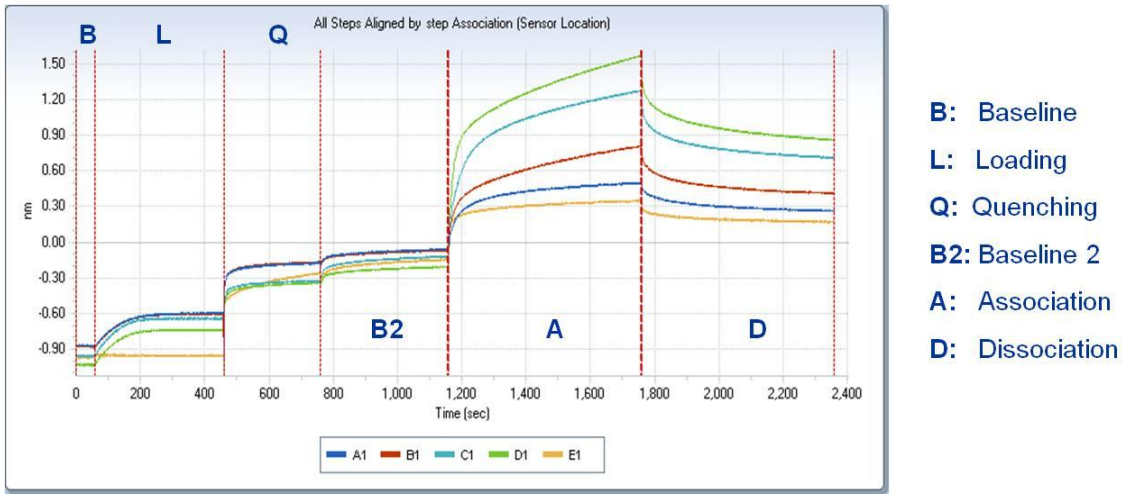

Figure 28

R4RNA-PIPPin/CSD-C2
A1 R4RNA/pip 5 ng/ul; B1 R4RNA/pip10 ng/ul; C1 R4RNA/pip 20 ng/ul; D1 R4RNA/pip 40 ng/ul; E1 reference: buffer/pip.

The binding data obtained were then processed to calculate the affinity constants.

The processing includes:

Subtraction-Phase: Subtraction of the values from the wells used as reference (E1) (Fig. 29 A*). To confirm specific binding, we used as a reference the sensor E1, in which we did not

add RNA, to evaluate the signal given by unspecific binding of the protein to the sensor. By subtracting from the samples the values obtained for the controls (E1 reference in fig. 28), the real binding values of R4RNA-PIPPin/CSD-C2 were obtained (Figure 29 A*).

Y-Axis Align: alignment of the curves with association phases (Fig.29 B*).

To compare the different curves obtained for RNA-protein interaction at different PIPPin/CSD-C2 concentrations, they were aligned to the association phase, in order to obtain the same starting point for all the curves (Fig.29B*).

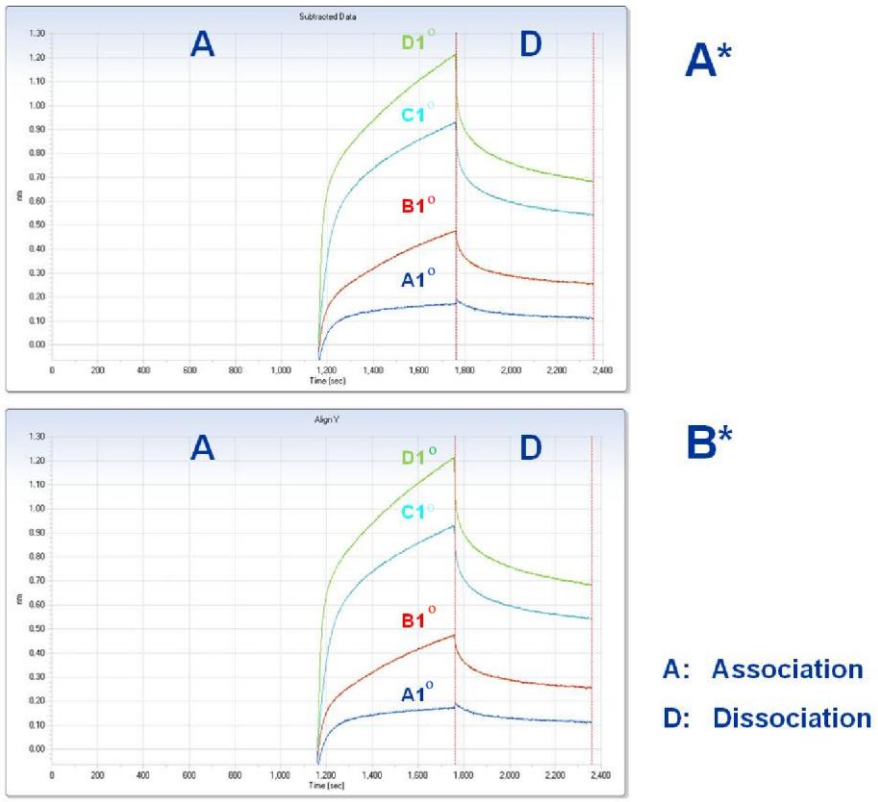

Figure 29

R4-RNA/PIPPin/CSD-C2 processing.
A1°= A1(Fig.28)-E1; B1°= B1(Fig.28)-E1; C1°= C1(Fig.28)-E1; D1°= D1(Fig.28)-E1.

The real-time binding data shown in Fig. 29 for R4RNA-PIPPin/CSD-C2 interaction suggest that both the association and dissociation phases are biphasic processes: an initial short and steep increase in signal intensity is followed by a long flat increase in signal intensity. At the highest analyte concentrations, steady-state was reached. Binding curve fitting was done using the 2:1 heterogeneous ligand (hl) equations; these equations assume that biphasic association arises from: i) two populations of immobilized ligands, that differ in their ability to bind the analyte and/or ii) heterogeneity of the ligand itself, and/or iii) the existence of two

independent ligand-binding sites. As a consequence, the binding curves are described by two reactions with different rates, KD and KD2 (Fig.30).

Figure 30

KD of R4RNA-PIPPin/CSD-C2 interaction
Graphical representation of the statistical analysis of at least three independent experiments. Blue bar indicates the mean of the values obtained for each condition. SD is also indicated (red bar).

Factors that can cause deviations from pseudo-first order approximation of binding data include: mass transfer effects, immobilized ligand density, lack of homogeneity of immobilized ligand or soluble analyte, immobilization chemistry, and rebinding of dissociated analyte. Residual plots derived from comparison of real curves and the mathematical model (curve fitting: Fig 31B) show very small (less than 10%) and random residuals, supporting the use of the 2:1 hl-fitting model for the data. The values of the coefficient of determination R^2 (i.e. an estimate of the goodness of the curve fit) were above 0.9 (note that values close to 1.0 indicate a good curve fit). Moreover, $\chi 2$ values were close to 0.2 for all the fits (χ^2 is a measure of the goodness of the curve fitting: values close to zero indicate a good curve fit.)

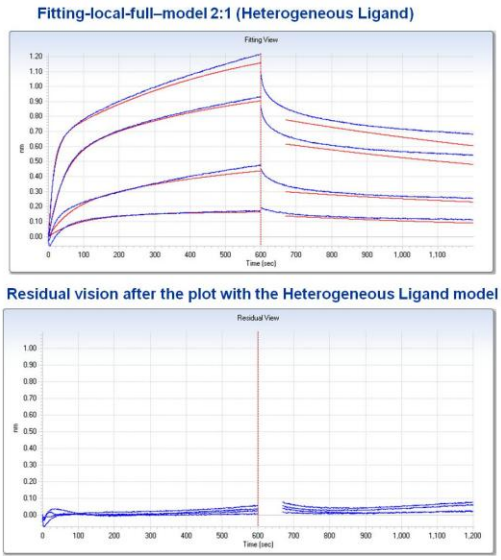

Figura 31

Blue: real curves given by the analysis of interaction data, Red: curves generated by the program based on the mathematical model 2:1 Heterogeneous Ligand.

The above analysis was also carried out for M4RNA. Figure 32 shows the interaction with the protein PIPPin/CSD-C2; also in this case the interaction is concentration-dependent.

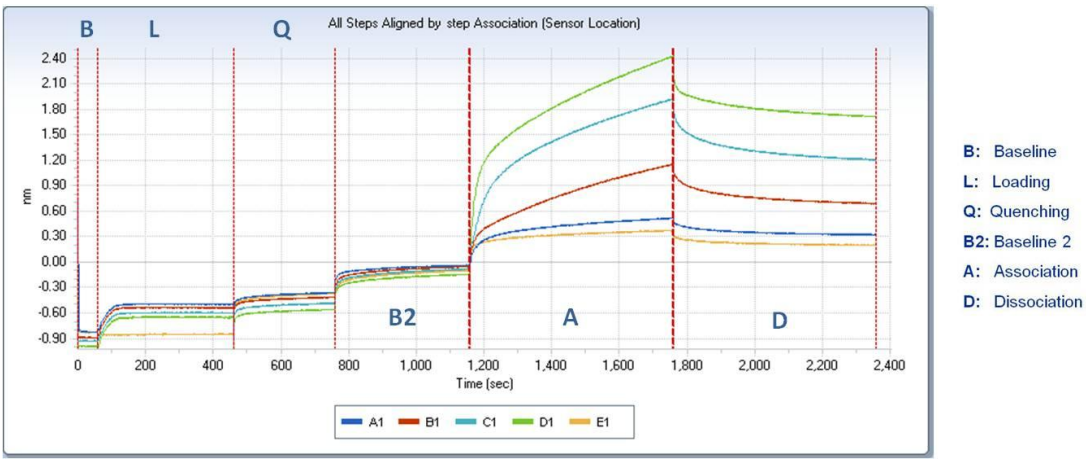

Figure 32

M4RNA-PIPPin/CSD-C2

A1 M4 RNA/pip 5 ng/ul; B1 M4 RNA/pip10 ng/ul; C1 M4 RNA/pip 20 ng/ul; D1 M4 RNA/pip 40 ng/ul; E1 reference: buffer/pip.

As shown in figure 32, it is clear that the interaction is reproducible and concentration-dependent.

Processing: in the subtraction phase (Fig.33A*), sensor E1 (Fig. 32) was used as reference**;** fitting with mathematical model 2:1, and residual view are shown in figure 33B* and 33C*, respectively.

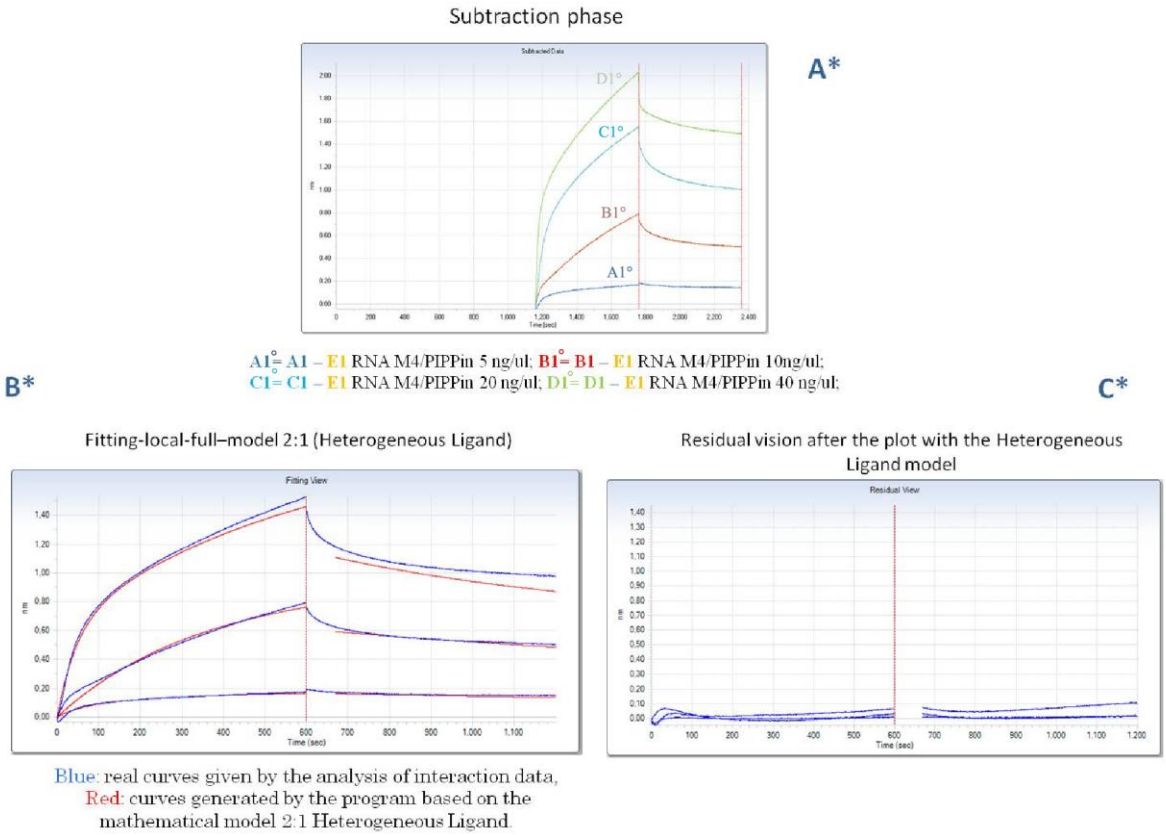

Figure 33

M4RNA-PIPPin/CSD-C2 processing

The binding curves are described by two reactions with different rates, KD and KD_2 (Fig.34)

Figure 34

KD of the M4RNA-PIPPin/CSD-C2 interaction
Graphical representation of the statistical analysis of at least three independent experiments. Blue bar indicates the mean of the values obtained for each condition. SD is also indicated (red bar).

These results confirmed the specific interaction between biotinylated R4 and M4 RNAs and PIPPin/CSD-C2 by biolayer interferometry.

.3.2 Calculation through BLI of the binding affinity for the interaction between PIPPin/CSD-C2 and H1° RNA

In order to identify H1° RNA portions involved in binding, we used four RNA probes (Fig.35):

a: H1° RNA coding region: nt 1–496 (aRNA:1.7 x 10^5 Daltons)

b: H1° RNA 3'-UTR, from nt 497 to nt 900 (bRNA:1.4 x 10^5 Daltons)

c: H1° RNA 3'-UTR of H1°, from nt 1015 to nt 1230 (cRNA: 0.7 x 10^5 Daltons)

d: H1° RNA 3'-UTR, from nt 1301 to nt 1611 (dRNA: 2.4 x 10^5 Daltons)

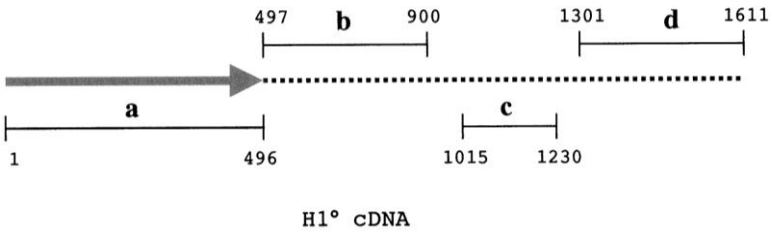

Figure 35

(From: Nastasi, et al., 1999) Schematic map of the rat H1° cDNA.
a, nt 1–496, coding region; b, 3'-UTR from nt 497 to nt 900; c, 3'-UTR, from nt 1015 to nt 1230; d 3'-UTR of H1° insert, from nt 1301 to nt 1611.

In the first analysis, we used all four probes and two negative controls **(E1** and **F1)**, to determine which of them had the greatest affinity for PIPPin/CSD-C2**.**

E1: the experiment was done with control RNA (Pierce Biotechnology, see Mat & Met);

F1: the experiment was done in the absence of RNA, to calculate the signal given by unspecific binding of the protein to the sensor.

As shown in figure 36, probe **d** shows the highest affinity.

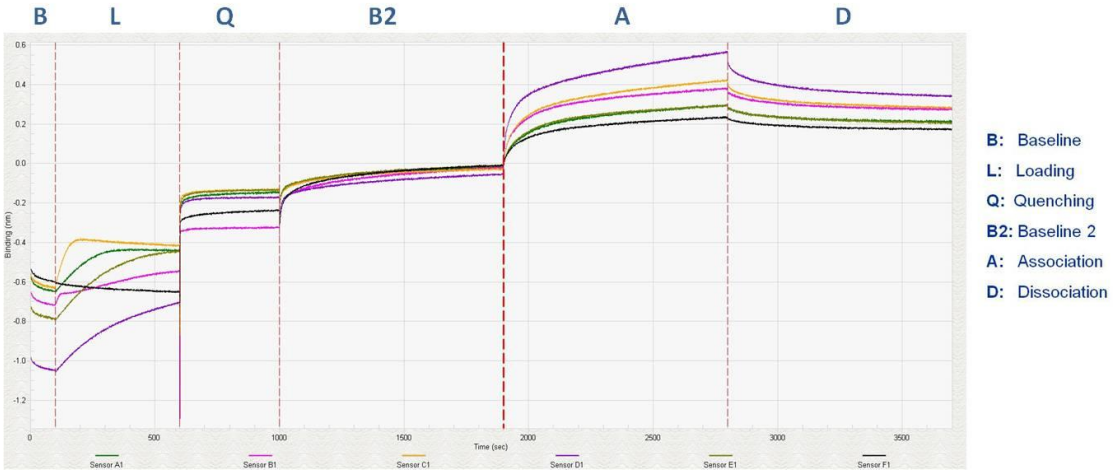

Figura 36

A1-aRNA-PIPPin/CSD-C2 30 ng/ul; B1- bRNA-PIPPin/CSD-C2 30 ng/ul; C1-cRNA-PIPPin/CSD-C2 30 ng/ul; D1- dRNA-PIPPin/CSD-C2 30 ng/ul; E1- control RNA-PIPPin/CSD-C2 30 ng/ul; F1- Negative control (buffer-PIPPin/CSD-C2);

Next, the affinity constant for all the fragments was calculated, and the experiments relative to the calculation of the affinity constant of probe **d** are described in detail below.

As shown in Fig. 37, dRNA-PIPPin/CSD-C2 binding is protein concentration-dependent (signal intensity was found to increase gradually from 5 µg to at least 30 µg mL^{-1} of protein). It was observed that the signal intensity of the conjugated dRNA could be detected even at the lowest RNA concentration (0,00001pm/l). These results confirm that dRNA specifically drives PIPPin/CSD-C2 binding to the Octet platform.

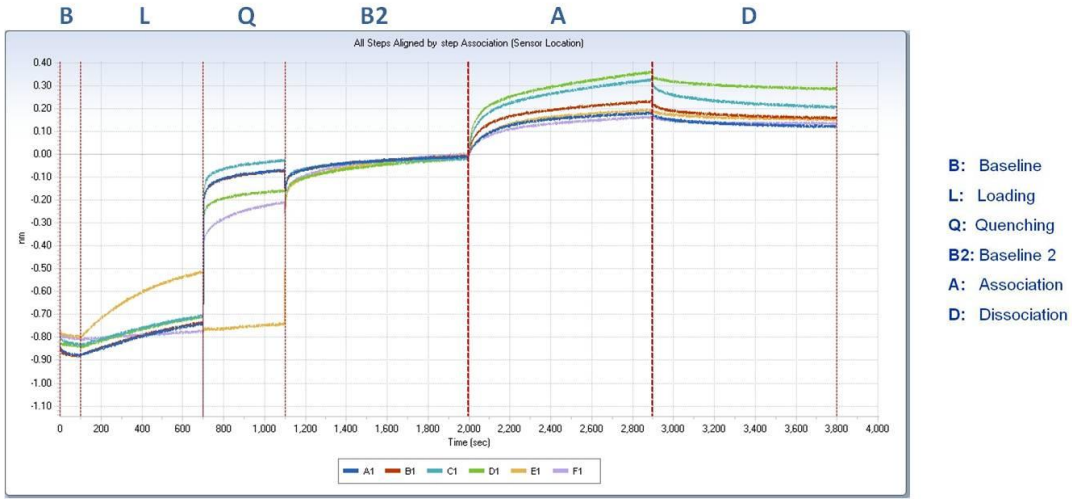

Figure 37

A1- dRNA-PIPPin/CSD-C2 5 ng/ul; B1- dRNA-PIPPin/CSD-C2 10 ng/ul; C1- dRNA-PIPPin/CSD-C2 20 ng/ul; D1- dRNA-PIPPin/CSD-C2 30 ng/ul; E1- control RNA-PIPPin/CSD-C2 30 ng/ul; F1- Negative control (buffer- PIPPin/CSD-C2 30 ng/ul);

The binding data obtained were then processed:

Subtraction-Phase (Fig. 38 A*):

E1: the experiment was done with control RNA (Pierce Biotechnology, see Mat & Met);

F1: the experiment was done in the absence of RNA, to evaluate the signal due to unspecific binding of the protein to the sensor.

The values obtained for the controls (**E1**, **F1**) were then subtracted from the sample values, in order to obtain the actual binding values for the dRNA-PIPPin/CSD-C2 complexes (Figure 38 A*).

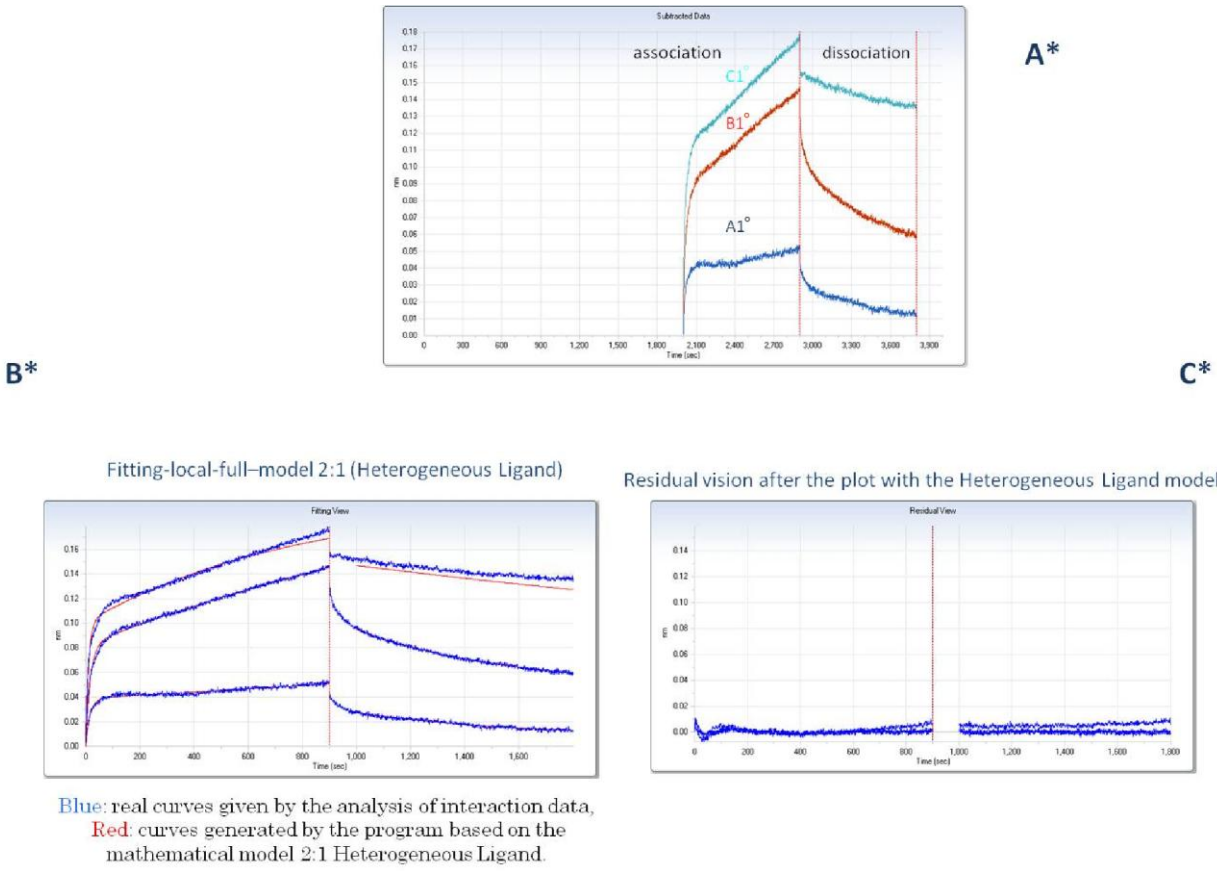

Figura 38

dRNA-PIPPin/CSD-C2 processing.
A1°= A1(Fig.37)-[(E1+F1)/2]; B1°= B1(Fig.37)-[(E1+F1)/2]; C1°= C1(Fig.37)-[(E1+F1)/2].

Binding data, shown in Fig 38 (A*- B*), for dRNA-PIPPin/CSD-C2 interaction suggested that, also in this case, both the association and dissociation phases are biphasic processes. At the highest analyte concentrations, steady-state was reached. Binding curve fitting was done using the 2:1 hl equations. As a consequence, the binding curves are described by two reactions with different rates, KD and KD2 (Fig.39).

Figure 39

KD of the dRNA/PIPPin/CSD-C2 interaction
Graphical representation of the statistical analysis of at least three independent experiments. Blue bar indicates the mean of the values obtained for each condition. SD is also indicated (red bar).

We can conclude that as long as RNA H1° is concerned, data already published (Nastasi, et al., 1999), and based on biochemical analyses, were confirmed; in addition, we could calculate the KD for dRNA-PIPPin/CSD-C2 complex: approximately $3.4E^{-08}$M.
The affinity constant was calculated for all the fragments, as shown in figure 40.

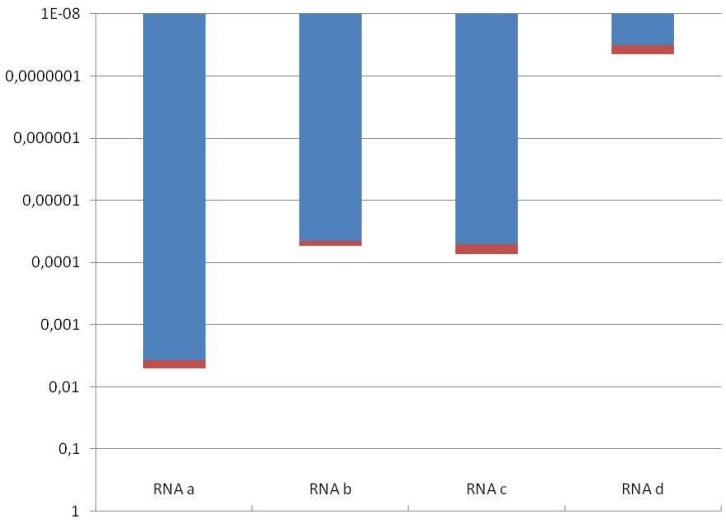

Figure 40

KD of the H1° 3'UTR fragments-PIPPin/CSD-C2 interactions
Graphical representation of the statistical analysis of at least three independent experiments. Blue bars indicate mean values for each RNA. SDs are also indicated (red bars).

.3.2.1 dRNA mutants (dRNA*)

The alignment of H1° and H3.3 cDNAs revealed the presence, downstream to the coding regions of the two inserts, of a number of sites with moderate to high sequence homology. One region, in particular, shows high similarity (Fig. 41); interestingly, this sequence of about 40 nucleotides covers in both messages the terminal portion of the 3'-UTR,

encompassing the polyadenylation signal (underlined in the figure). Moreover, the same region is part of a sequence that was previously suggested to be potentially able to form a stem-loop structure, highly conserved in vertebrate H3.3 mRNAs [Fig. 41 and (Nastasi, et al., 1999)].

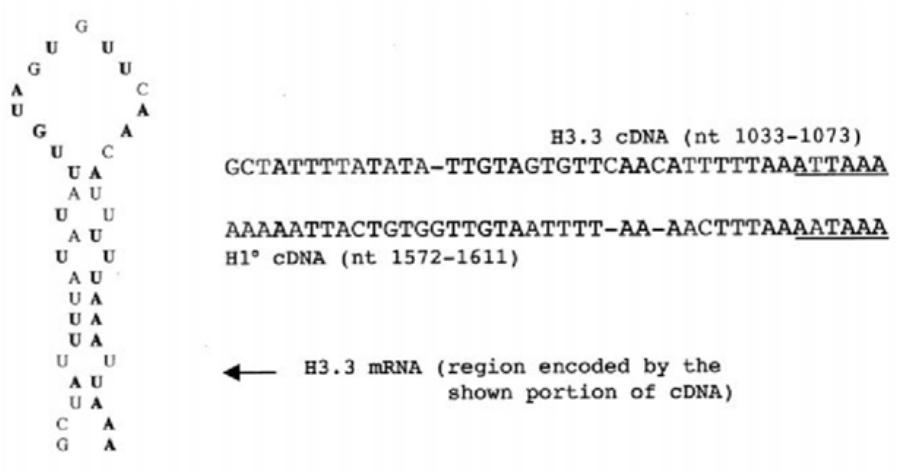

Figure 41

Alignment of the last 41 nt of the H3.3 cDNA with the last 40 nucleotides of the H1° cDNA, done by the Complign Module of the MacMolly Tetra Program (Gene Soft). The corresponding H3.3 RNA sequence has been previously suggested to form the stem-loop structure shown on the left. Nucleotides conserved between H3.3 and H1° inserts are in black. Putative polyadenylation signals are underlined (Nastasi, et al., 1999)

We used two H1° RNA 3'-UTR mutants (both mutated in the region between nucleotides 1572 and 1611 by PCR mutagenesis), a kind gift from Dr. René Prétot (University of Applied Sciences and Arts Northwestern Switzerland FHNW).

The first mutant, clone 37, was created deleting 40 nucleotides which constitute the putative stem-loop structure (fig.42).

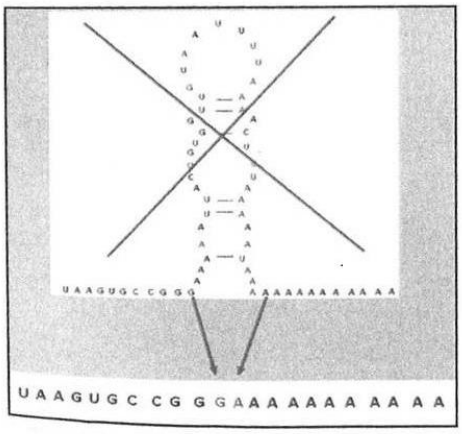

Figure 42

Clone 37
Last 40 nucleotides of H1° 3'UTR were deleted obtaining a construct of 319 bp

The second clone, 4b1, was made substituting a stretch of four nucleotides (UGUG with CAAC), and deleting three nucleotides (UGU), in the putative loop-forming region (fig.43).

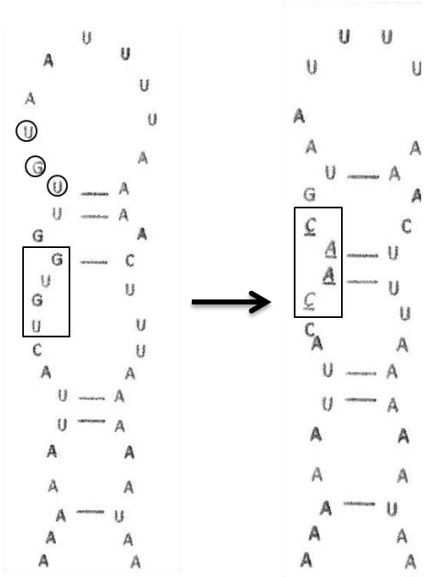

Figura 43

Clone 4b1
Three nucleotides of H1° mRNA 3'UTR were deleted (black circles) and four were substituted (black rectangle)

The PCR products were purified by "Nucleospin Extract II PCR clean-up Gel extraction" (Macherey-Nagel) and directly used as template for *in vitro* transcription and 3'-end biotinylation.

To determine the affinity for PIPPin/CSD-C2, we used the three H1° 3'UTR probes (d, 4b1 and 37) and two negative controls (**G1** and **H1**) (Fig.44). In particular, **G1** refers to the

experiment done with control RNA, and H1 to the experiment done in the absence of RNA, to calculate the values of the signals due to unspecific binding.

As shown in figure 44, probe 37 shows the highest affinity.

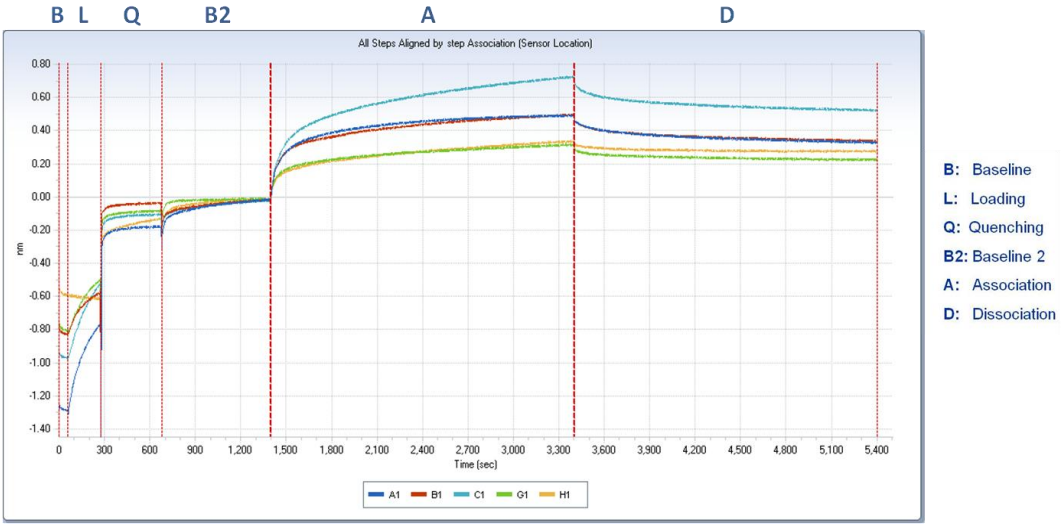

Figura 44

A1-dRNA -PIPPin 20ng/ul; B1- 4b1RNA-PIPPin 20 ng/ul; C1- 37RNA-PIPPin 20 ng/ul; G1- control RNA-PIPPin 20ng/ul; H1- Negative control (buffer-PIPPin 20ng/ul);

The affinity constant was calculated for all the mutants, as shown in figure 45

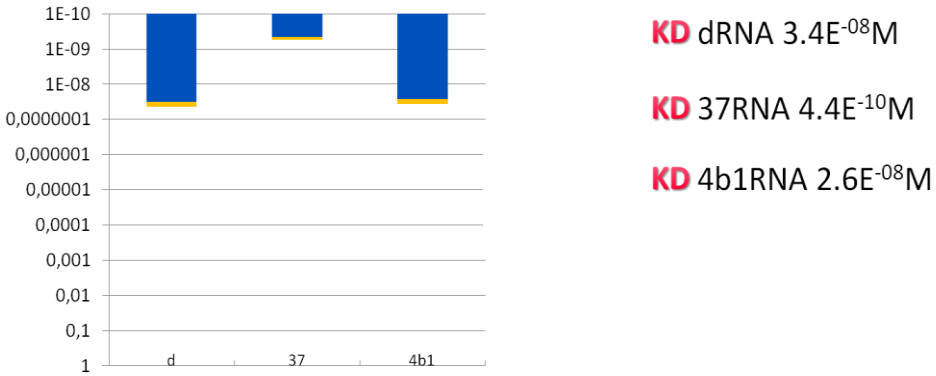

Figura 45

Graphical representation of the statistical analysis of at least three independent experiments. Blue bars indicate mean values for each fragment. SDs are also indicated (orange bars).

One hypothesis is that PIPPin normally binds RNA at two sites and that the elimination of the loop, approaching these two sites, provides a stronger binding site for PIPPin (Fig.46).

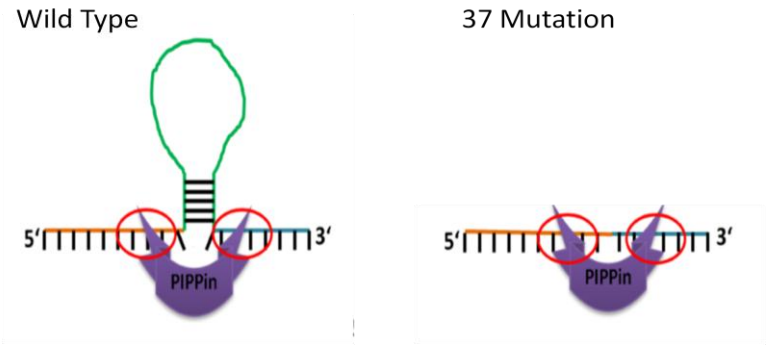

Figura 46

.3.2.2 Mapping of the d region

In order to identify dRNA portions involved in binding, we used three RNA probes, obtained by in vitro transcription and 3'end biotinylation of three regions of the **d** fragment, constructed and kindly provided by Dr. René Prétôt, namely SH1 (nt.1400-1712), SH2 (nt.1515-1712) and SH3 (nt.1566-1712) (Fig.47).

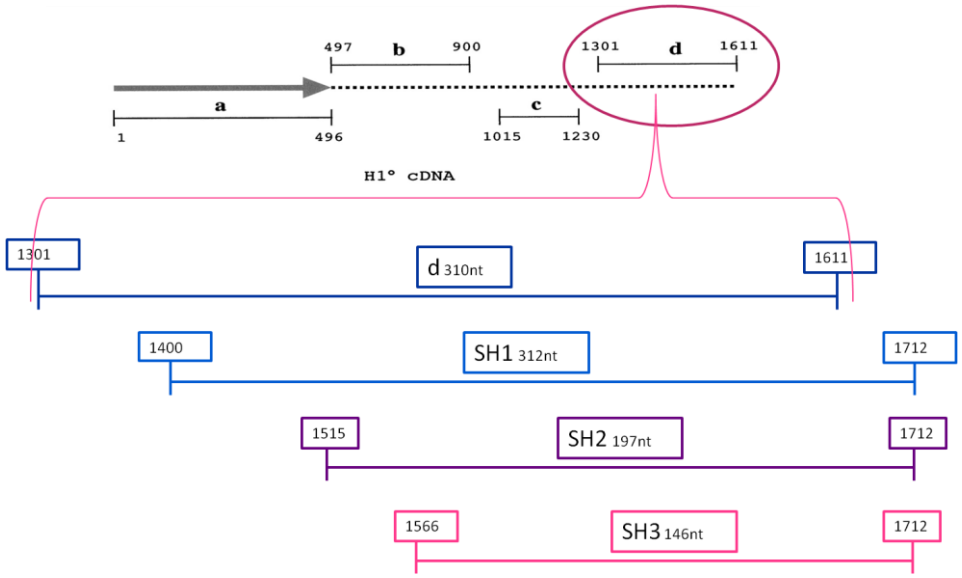

Figura 47

Different portions of d-region

These RNA probes, and two negative controls **(E1** and **F1),** were used to determine the affinity for PIPPin/CSD-C2 (Fig.48).

E1: the experiment was done with control RNA (Pierce Technology, see Mat & Met);

F1: the experiment was done in the absence of RNA, to evaluate the signal given by unspecific binding of the protein to the sensor.

As shown in figure 48, probe **SH1** has the highest affinity.

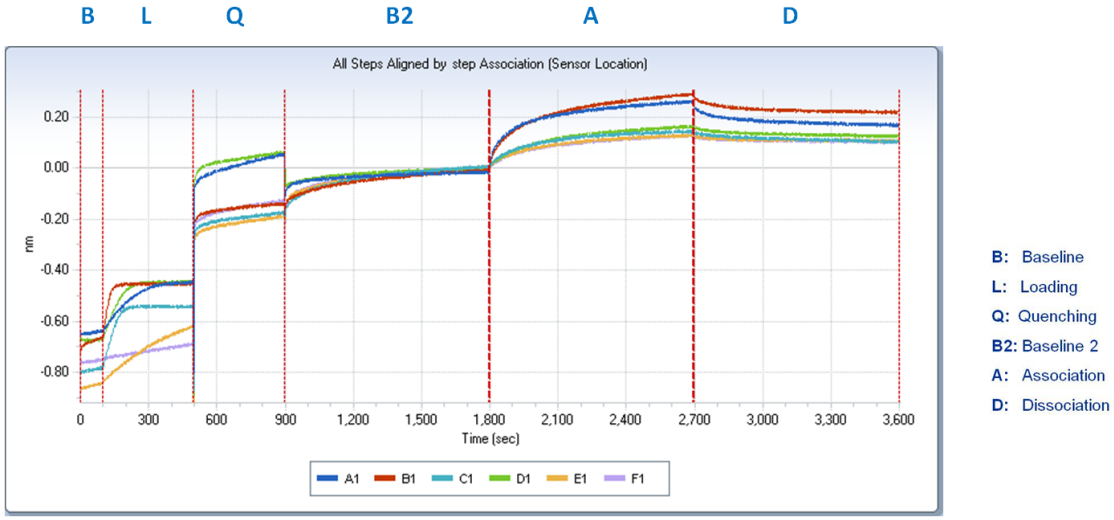

Figura 48

A1-dRNA-PIPPin/CSD 30 ng/ul; B1- SH1RNA-PIPPin/CSD30 ng/ul; C1- SH2RNA-PIPPin/CSD 30 ng/ul; D1- SH3RNA-PIPPin/CSD30 ng/ul; E1- control RNA / PIPPin/CSD 30 ng/ul; F1- Negative control (PIPPin/CSD-buffer);

The affinity constant was calculated for all the fragments, as shown in figure 49.

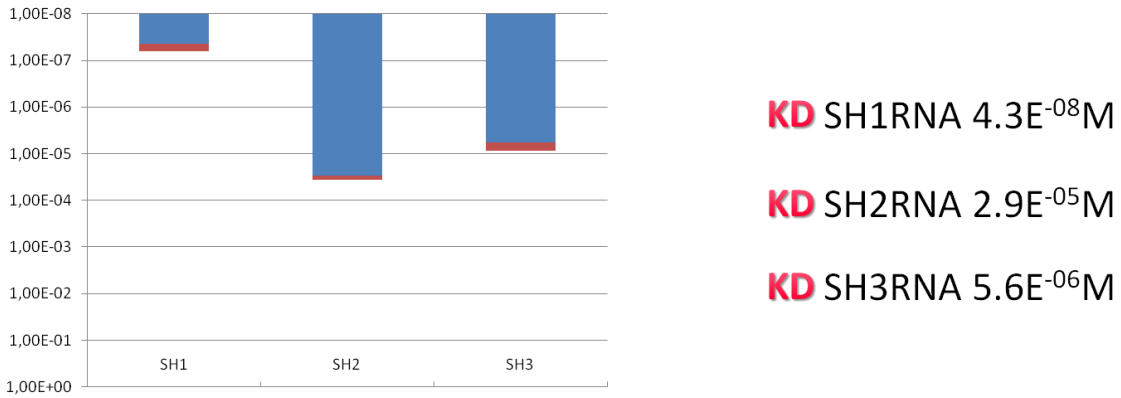

Figura 49

Graphical representation of the statistical analysis of at least three independent experiments. Blue bars indicate mean values for each fragment. SDs are also indicated (red bars).

In order to more precisely identify SH1RNA portions involved in binding with PIPPin, we made by PCR three fragments named SH1-S1 (nt.1400-1536), SH1-S2 (nt.1434-1574) and SH1-S3 (nt.1468-1598) (Fig.50), and we used them to prepare three new 3'end biotinylated RNA probes.

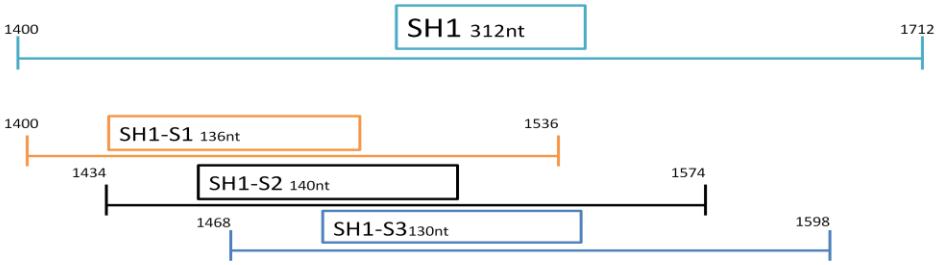

Figure 50

Different portions of SH1

Again, we used these probes (Fig.51) to determine the affinity for PIPPin/CSD-C2, together with two negative controls (**E1** and **F1**):

E1: the experiment was done with control RNA (Pierce Technology, see Mat & Met);

F1: the experiment was done in the absence of RNA, to evaluate the signal due to unspecific binding of the protein to the sensor.

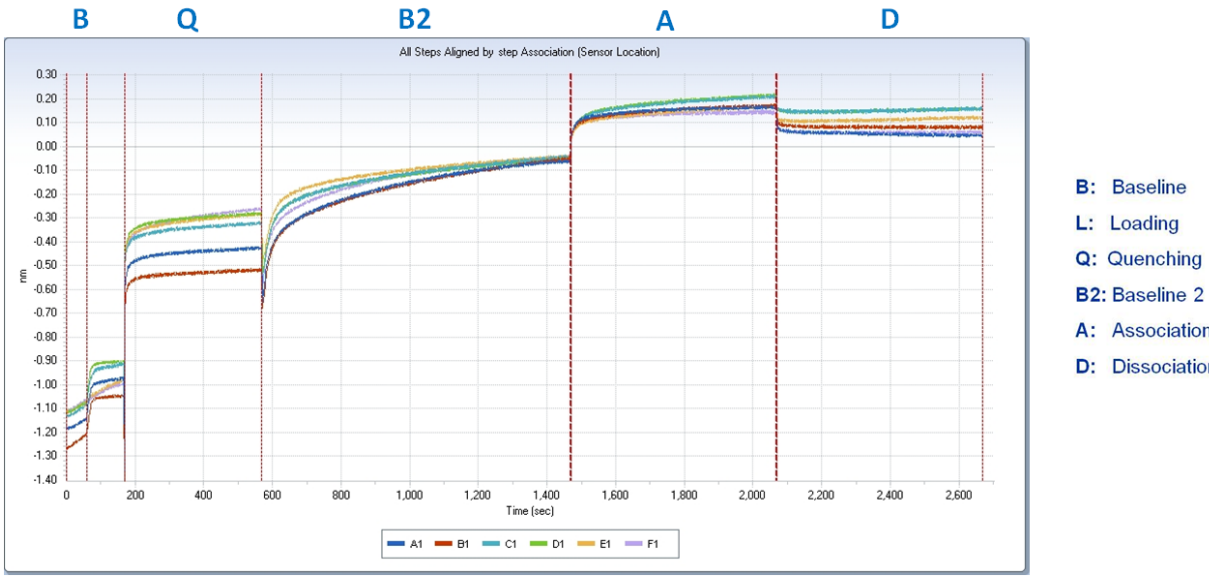

Figure 51

A1-xRNA -PIPPin/CSD 20 ng/ul; B1- RNA SH1-S1-PIPPin/CSD 20 ng/ul; C1- RNA SH1-S2 -PIPPin/CSD 20 ng/ul; D1- RNA SH1-S3 -PIPPin/CSD 20 ng/ul; E1- RNA control -PIPPin/CSD 20 ng/ul; F1- Negative control (PIPPin/CSD-buffer);

As shown in figure 51, the difference between the values obtained from the specific probes and from negative controls is too low.

In conclusion, these results confirmed the specific interaction between H1° RNA and PIPPin/CSD-C2 by biolayer interferometry, indicating that the SH1 region of the **d** fragment of the 3'UTR of H1° mRNA possess the highest affinity (KD $4{,}3E^{-08}$) for this protein. To establish which nucleotides actually participate to the binding, further analyses are needed.

Conclusions

In this work, we confirmed the ability of the PIPPin/CSD-C2 protein to bind both M4 and R4 regions of the H3.3 mRNA, as well as **d** (and in particular SH1) region of H1° mRNA. Thanks to BLI, we were also able to calculate the corresponding KD, all in the range of high affinity:

M4 RNA: KD $6{,}67E^{-09}$

R4 RNA: KD $2{,}03E^{-08}$

dRNA: KD $3{,}79E^{-08}$ (SH1 KD $4{,}3E^{-08}$).

In according with the assumption that RNA metabolism is regulated in the context of complex ribonucleoprotein particle, we evidenced by immunoprecipitation a set of proteins that are able to interact with each other. These proteins were isolated from brain cell nuclei by a chromatographic approach and identified by mass spectrometry; as demonstrated also by western analysis, PIPPin/CSD-C2 is present among them.

The results presented are in agreement with the idea that post-transcriptional regulation of H1° and H3.3 histone expression depends on a group of proteins which are probably part of a specific ribonucleoprotein particle that contain also PIPPin. Such particle should contain, together with specific proteins, also proteins which are known to bind other mRNAs.

Finally, our discovery that PEP-19 and LPI bind H1˚ histone mRNA and that this binding is affected by calmodulin suggests that, in the brain, post-transcriptional regulation of H1˚ histone synthesis may be regulated by calcium signals, and perhaps by neuronal activity.

Materials and methods

1 Preparation of recombinant LPI and PEP-19 proteins, containing N-terminal tags of 6 histidines

In order to synthesize recombinant PEP19, LPI and PIPPin, the entire coding regions of all cDNAs were amplified, by polymerase chain reaction. In all cases, the 5'- and 3'-primers included attB1 and attB2 recombination sequences for cloning the amplification products sequentially into the pDONR201 plasmid vector and into the pDEST™-17 plasmid expression vector (Gateway™ Technology, Invitrogen), according to Gateway Technology (Invitrogen), that is based on the site- specific recombination reactions of bacteriophage λ in E. coli. The expression clones pDEST-17 was finally transferred into E. coli BL21-AI competent cells to obtain expression of the N-terminal histidine fusions with PEP19, LPI and PIPPin respectively.

.1.1 Induction of the protein containing the presequence of six histidines

A single colony is inoculated in 15 ml of LB, in the presence of ampicillin (50μg/ml) and are allowed to grow overnight at 37°C in shaker. The cells were then diluted (1:20) and let grow to a concentration corresponding to 0.4 OD_{600}. After putting aside 1ml of not induced culture for further analysis, L-arabinose is added to the culture to a final concentration of 0.2%, leaving the cells grow for another 2-3 hours at 37°C.

1ml of the induced cultures was saved, and the remaining culture is centrifuged for 20 min at 4000xg at 4°C. The pellet is maintained overnight at -20°C. Aliquots of not induced and induced bacteria are analyzed by Sodium Dodecyl Sulfate-polyacrylamide gel electrophoresis (SDS-PAGE), to confirm protein expression.

.1.2 Protein Purification with 'tags' of 6 histidines

Induced bacteria are thawed and resuspended in Lysis Buffer (50 mM NaH_2PO_4, 50 mM NaCl, 10 mM imidazole, pH 8), and, after the addition of lysozyme (1mg/ml), is incubated on ice for 30 min and sonicated (Vibracell VR6000 for 2min, 60W). After sonication, the sample is centrifuged for 20 min at 12.000xg, at 4°C, to remove cellular debris.

.1.3 Purification of the insoluble fraction of the protein

The pellet, containing also the inclusion bodies, is resuspended in a buffer containing 50 mM Tris -HCl, pH7.2, 50 mM NaCl, 8 M urea, and heated 5 min at 80°C. The insoluble material is removed by centrifugation at 18.000xg for 1min (this step is very important to remove remaining aggregates which could act as nuclei for further aggregation). Meanwhile, nickel-nitrile-triacetic acid agarose (Ni-NTA agarose, Invitrogen) chromatographic column is prepared. The column is washed and equilibrated with 10 volumes of the same buffer in which the pellet was resuspended. The protein suspension is gently layered on the column and proteins are purified by affinity chromatography, based on the fact that histidines bind nickel-NTA by imidazole ring. The renaturation is carried out on the column using urea solutions of decreasing concentrations (up to 0 M). After washing with a solution without urea, the protein is eluted with a solution of 50 mM NaCl, 50 mM Tris HCl pH 7.2, 350 mM imidazole, pH 6. Protein concentration is measured by spectrophotometer and fractions with higher concentration are pooled and used in the following purification. Specific activity of the recombinant protein was highly improved by gel filtration of the imidazole-eluted protein through G-100 Sephadex in 50 mM Tris-HCl (pH 7.2) (patent N° PA2009A000029).

2. Plasmids

pMH1° (EMBL accession number X70685) contains an insert of 1711 nucleotides (nt). To obtain smaller H1° transcripts, we used the subclones described previously (Nastasi et al., 1999). ***a***, nt 1–496, coding region of H1° RNA; ***b***, 3′-UTR of H1° insert, from nt 497 to nt 900; ***c***, 3′-UTR of H1° insert, from nt 1015 to nt 1230; ***d,*** 3′-UTR of H1° insert, from nt 1301 to nt 1611.

In order to obtain different portions of the SH1-region, three different pairs of primers were used in the PCR reactions:

SH1-S1 (1400-1536) 137nt

F: 5’AATTAACCCTCACTAAAGGGAAGCGGGATTGTGTGCATG 3’

R: 5’AGGGTACCCGAGTTTCCTAC3’

SH1-S2 (1434-1574) 141nt

F: 5’AATTAACCCTCACTAAAGGGATCCATATCTAAGACTAGTAC 3’

R: 5’TTTCCCGGCACTAGTTACAC3’

SH1-S3 (1468-1598) 131nt

F: 5’AATTAACCCTCACTAAAGGGGCGGGAGCTGGGAGAAAAACTC 3’

R: 5’TAAAATTACAACCACAGTAA3’

pDH3 (EMBL accession number X73683). To obtain smaller transcripts, corresponding to different portions of the 3′-UTR of the H3.3 mRNA, we used the subclones ***R4***, complete 3′-UTR of H3.3 RNA, and ***M4***, 3′-UTR of H3.3 RNA, from nt 909 to nt 1107, previously described (Nastasi et al., 1999).

3. In Vitro Transcription

.3.1 33P-radiolabeled transcripts

The plasmids were linearized by restriction with BamH1 (pMH1^0) or Hind III (pDH3, *pR4, pM4, pH1°a, pH1°b, pH1°c* and BS-CoxIV-3UTR) and used as templates for *in vitro* transcription. Cold H1^0, H3.3, *pR4, pM4, pH1°a, pH1°b, pH1°c* and CoxIV transcripts and ^{33}P-radiolabeled H1^0 RNA were generated by Riboprobe system (Promega). RNA was extracted once with phenol and twice with chloroform and precipitated with ethanol and sodium acetate (0.3 M final concentration). The transcripts were collected by centrifugation at 10,000 × *g* for 15 min, washed in 75% ethanol, and resuspended in distilled water. Small aliquots were used for analysis on denaturing gels.

.3.2 Biotinylated transcripts

The plasmid pMH1° was used as a template for *in vitro* transcription of biotinylated H1° RNA in the presence of biotin-21-UTP (Ambion-Life Technologies, Paisley, UK).

.3.2.1 3 ' end RNA Biotinylation

The RNAs (a,b,c,d,R4 and M4) produced by in vitro transcription were biotinylated using the "RNA 3' end biotinylation kit" (Pierce Biotechnology), following the manufacturer's instructions (Fig.52).

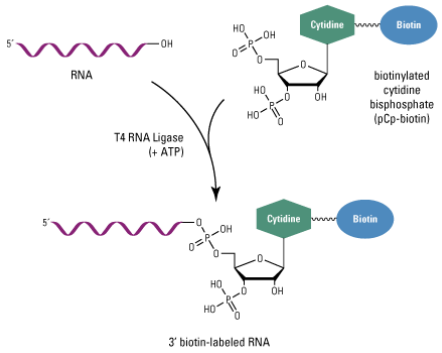

Figure 52 3' end biotinylation of the RNA

4. T1 Nuclease Protection Assay

Recombinant proteins (50 ng) were incubated for 10 min, at room temperature, with 0.5–1.0×10^6 cpm (specific activity: 0.5–2.0×10^7 cpm/pmol of RNA) of radiolabeled, *in vitro* transcribed H1° RNA. The samples were exposed to a Spectroline UV (254 nm) lamp (Aldrich Chemical Co., Inc.) for 40 min, in ice bath, to cross-link RNA to proteins. Samples were then incubated for 45 min at 37 °C, with 100 units of T1 RNase (EC3.1.27.3) to degrade the whole of the RNA except the portions protected by bound proteins; RNA-protein complexes were analyzed by denaturing electrophoresis on SDS-PAGE. At the end of the run, the gel was dried and exposed to X-ray film for autoradiography. The gels were also stained with Coomassie Brilliant Blue R-250 (Sigma), to confirm loading of equal amounts of proteins per lane.

.4.1 Competition experiments

Experiments aimed at analyzing RNA-binding specificity were performed in the presence of 2:1 or 5:1 excess of unlabeled RNA.

Experiments aimed at analyzing interference effects of LPI or PEP-19 on PIPPin (CSD-C2) binding to H1˚ RNA were performed in the presence of 1:1 or 4:1 excess of the competing protein.

Experiments aimed at analyzing interference effects of calmodulin on LPI and PEP19 binding to H1˚ RNA were performed in the presence of 1:1 or 4:1 excess of calmodulin. In these experiments bovine serum albumin at the same concentration as calmodulin was used as a control.

5. Animals and research ethics.

Wistar rats (*Harlan, Udine, Italy*) were housed in the animal care facility of the STEBICEF Department, University of Palermo, Palermo, Italy. Procedures involving animals were conducted according to the European Community Council Directive 2010/63/EU, reducing to a minimum the use and suffering of animals. All experiments were performed under the direction of the licensed veterinary of the University who approved of the protocols.

.5.1 Preparation of nuclear extracts from rat brain

Fresh brains from 20-day-old rats were homogenized in nuclei buffer (NB: 0.32 M sucrose; 50 mM sodium phosphate buffer, pH 6.5; 50 mM KCl, 0.15 mM spermine; 0.15 mM spermidine; 2 mM EDTA and 0.15 mM EGTA), containing protease inhibitors (2 µg/ml aprotinin, 2 µg/ml antipain, 2 µg/ml leupeptin, 2 µg/ml pepstatin A, 1.0 mM benzamidine, and 1.0 mM phenylmethylsulfonyl fluoride, Sigma).

Once homogenized, the samples are centrifuged at 1000 xg for 10 min at 4°C. The obtained fractions are treated as described below:

a) The supernatant can be used as such (post-nuclear fraction, PN) or further centrifuged at 12000 xg for 20 min at 4°C, to obtain a post-mitochondrial fraction and a mitochondrial pellet, which is resuspended in RSB (10 mM NaCl, 10 mM TrisHCl pH 7.4, 1.5 mM $MgCl_2$). All fractions were immediately aliquoted and frozen at -80°C.

b) The pellet (nuclei) is washed in RSB, centrifuged at 1000 xg for 10 min at 4°C, and resuspended in RSB; an equal volume of RSB with high salt concentration (RSB HS: Tris-HCl, pH 7.5, 10 mM MgCl2, 1.5 mM, 1.6 M KCl, 0.5 mM PMSF) was added to solubilize nuclear proteins not strongly bound to DNA: the nuclear suspension was incubated for 30 min on ice and centrifuged for 20 min at 17000 x g. The supernatant (nuclear extracts: NEX) is aliquoted and frozen at -80°C. The pellet (containing DNA and proteins strongly associated to it) is resuspended in RSB and 0.4 M HCl, and maintained at 4°C for at least 4 hours. The suspension is then centrifuged at 10,000 xg for 15 min at 4°C; histones and acid-soluble proteins, present in the supernatant, are recovered by precipitation with 10 volumes of acetone at -20°C and centrifugation at 10000 xg for 20min at 4°C.

.5.2 Chromatographic purification of H1° RNA-binding factors from rat brain nuclear extracts.

Streptavidin-conjugated paramagnetic beads (Magnesphere™, Promega, Madison, WI), treated according to the manufacturer's instructions, were mixed with 300 μg of nuclear salt-extract from the rat brain, in 500 μl (final volume) of binding buffer (BB: 75 mM Tris–HCl, pH 7.5; 50 mM KCl; 5 mM dithiothreitol; (Scaturro et al., 2003), containing protease and phosphatase inhibitors (Sigma–Aldrich, St. Louis, MO). Samples were incubated with an aliquot of beads for 1 h, at 25 °C, under shaking, to absorb to the paramagnetic particles all the proteins which bind them directly (pre-clearing step). After centrifuging for 5 min at 12,000 rpm in an eppendorf microfuge, the pre-cleared extracts were saved for binding experiments with RNA, while the beads were washed three times in BB and then incubated in BB containing 2 M NaCl, for 15 min, at 25 °C. After incubation, samples were centrifuged for 10 min, 12,000 rpm in an eppendorf microfuge, and the supernatants were frozen (control sample: proteins isolated by binding to the magnespheres in the absence of RNA). Pre-cleared extracts were incubated with 5 μg of H1° RNA in BB, for 30 min, at 25°C. After the binding reaction, a fresh aliquot of beads was added further incubating for 1 h, at 25°C, under shaking. Then, the tubes were placed in a magnetic device (Magnesphere™, Promega) and the recovered supernatants, containing unbound proteins, were frozen and saved. Paramagnetic beads were washed four times in BB and then resuspended in BB containing 2 M NaCl, for 15 min, at 25°C. After incubation, samples were centrifuged at 12,000 rpm in an eppendorf microfuge. The obtained supernatants, that contain proteins which bind paramagnetic streptavidin particles in the presence of biotinylated H1° RNA, were frozen and saved for analyses.

Isolated proteins were analyzed by electrophoresis on denaturing SDS–polyacrylamide gels, and identified by mass spectrometry (Taplin mass spectrometry facility, Harvard University, Boston, (Aebersold, et al., 2001).

6. Antibodies

Primary antibodies used in coimmunoprecipitation assays and western analyses were: (i) rabbit polyclonal anti-hnRNP K-, anti-Y box-binding protein 1 (YB-1)-, and anti-CSD-C2 antibodies; (ii) mouse monoclonal anti-hnRNP A1-, anti-heat shock cognate 70 (Hsc70)-, and anti-CSD-C2 antibodies. All the primary antibodies, except for anti-YB1 (Sigma–Aldrich) and the home-made polyclonal anti-CSD-C2, were purchased from Santa Cruz (Santa Cruz,

CA). Goat anti-mouse-, goat anti-rabbit- and bovine anti-goat secondary antibodies were from Promega.

7. Co-immunoprecipitation assay

Co-immunoprecipitation experiments using paramagnetic particles were performed essentially following the manufacturer's instructions (Dynabeads™, Invitrogen, Carlsbad, CA), using a magnetic device (DinaMag™, Invitrogen) for the separation of supernatants from beads. Each reaction step was performed in a volume of 250 µl under rotation. For each sample, 40 µl of beads suspension was used. Nuclear extracts were first incubated with paramagnetic particles, in order to clear the extract from proteins which bind to the beads directly. In some experiments, one half of the nuclear extract was also incubated with 50 µg/ml of RNase A (Promega). Beads coupled with 10 µg of the chosen antibodies were incubated in conjugation buffer (0.15 M NaCl, 20 mM sodium phosphate, pH 7.8), containing 5 mM suberic acid [bis (3-sulfo-N-hydroxysuccinimide ester)] (Sigma–Aldrich), for 30 min, to link covalently the antibodies to protein G, and to minimize contamination with antibodies of the eluted fractions. For each immunoprecipitation reaction, 150 µg of pre-cleared extracts was used, incubating for 1 h, at 25 °C. At the end of the reaction, the supernatants, which contained unbound proteins, were saved, while the beads were washed and resuspended in denaturing sample buffer and finally boiled for 5 min to elute bound proteins.

8. Astrocyte primary cultures and confocal microscopy

Astrocytes were prepared from 2-day-old rats, as previously described (Schiera, et al., 2005), and cultured on a coverslip in DME/Hams F-12 (2/1), supplemented with 10% heat-inactivated fetal calf serum (Sigma–Aldrich), until half confluent. Astrocyte cultures were then progressively adapted to Maat Medium (Cestelli, et al., 1985). After 5 days cells were fixed in 96% ethanol and immunostained with the same antibodies used for co-immunoprecipitation. The secondary antibodies were tetramethylrhodamine isothiocyanate-conjugated anti-rabbit- and fluorescein isothiocyanate-conjugated anti-mouse immunoglobulin (both from Sigma). Cells were finally observed by confocal laser scanning microscopy (Olympus FV-300 equipped with argon, 488 nm and helium/neon, 543 nm, lasers), under a 60× oil immersion lens.

9. BLI on Octet Optical Biosensor

.9.1 Scheme for RNA-PIPPin interaction on Octet Optical Biosensor

The binding assays were performed in 96-well plates at 30°C with the system Octet Red (Forte Bio). The experiment was performed by placing the SA sensors (conjugated with streptavidin) in the wells and measuring the variations in time of the thickness of the layer (in nanometers, nm). Serial dilutions of the protein were performed in 200 microliters of PBS-T (phosphate buffered saline with 0.01% tween).

Typical cycles for analysis include:

Baseline 1: SA sensors are incubated in PBS for 60 s.

Loading: SA sensors are saturated with 200 microliters of RNA (2 picomoles) in PBS buffer for 600 s.

Quenching: SA sensors are transferred to biocytin 1.8mg/ml for 300s (saturation of non specific binding sites on the sensors).

Baseline 2: SA sensors are transferred in PBST and incubated for another 400 s (removal of RNA in excess).

Association: SA sensors are exposed to protein at different concentrations (1 mg/ml to 40 mg/ml). The association was monitored for 600 s.

Dissociation: SA sensors are transferred to PBST for 600 s.

The data were processed automatically using the software version 7 of the Octet.

.9.2 Scheme for detection of Pep-19/Calmodulin interaction on Octet Optical Biosensor

The binding assays were performed in 96-well plates at 30°C with the system Octet Red (Forte Bio).The experiment was performed by placing the NI-NTA sensors in the wells and measuring the variations in time of the thickness of the layer (in nanometers, nm).

Baseline: NI-NTA sensors are incubated in buffer A (25mM Tris-HCl, 150mM NaCl, 2mM $CaCl_2$, 1mM $MgCl_2$, 0,05% Tween-20, pH 7.4), for 60 s

Loading: NI-NTA sensors are saturated with 200 microliters of 5ng/µl Pep-19 protein, in **Buffer A,** for 600 s

Baseline2: NI-NTA sensors are transferred in buffer B **(**25mM Tris-HCl, 150mM NaCl, 50µM EGTA, 1mM $MgCl_2$, 0,05% Tween-20, pH 7.4), to remove unspecific binding, for 400 s

Association: NI-NTA sensors are exposed to calmodulin at different concentrations (10 to 40 mg/ml), in buffer B. The association was monitored for 600 s.

Dissociation: NI-NTA sensors are transferred to buffer B for 600 s.

References

Achsel, T., Stark, H., & Luhrmann, R. (2001). The Sm domain is an ancient RNA-binding motif with oligo(U) specificity. *PNAS, 98*, 3685–3689.

Aebersold, R., & Goodlett, D. (2001). Mass spectrometry in proteomics. *Chem Rev, 10*, 269-95.

Ahmad, K., & Henikoff, S. (2002). Histone H3 variants specify modes of chromatin assembly. *PNAS , 99*, 16477-16484.

Ahmad, K., & Henikoff, S. (2002). The histone variant H3.3 marks active chromatin by replication-independent nucleosome assembly. *Mol Cell.* 9, 1191-200.

Albig, W., & Doenecke, D. (1997). The human histone gene cluster at the D6S105 locus. *Hum Genet, 101*, 284-294.

Allis, C., Glover, C., Bowen, J., & Gorovsky, M. (1980). Histone variants specific to the transcriptionally active, amitotically dividing macronucleus of the unicellular eucaryote, Tetrahymena thermophila. *Cell , 20*, 609–6.

Antar, L., Dictenberg, J., Plociniak, M., Afroz, R., & Bassell, G. (2005). Localization of FMRP-associated mRNA granules and requirement of microtubules for activity-dependent trafficking in hippocampal neurons. *Genes Brain Behav , 4*, 350–359.

Aronov, S., Aranda, G., Behar, L., & Ginzburg, I. (2002). Visualization of translated tau protein in the axons of neuronal P19 cells and characterization of tau RNP granules. *J Cell Sci , 115*, 3817-3827.

Bargou, R., & Jurchott, K. W. (1997). Nuclear localization and increased levels of transcription factor YB-1 in primary human breast cancers are associated with intrinsic MDR1 gene expression. *Nat Med , 11*, 447–450.

Bassell, G., & Warren, S. (2008). Fragile X syndrome: loss of local mRNA regulation alters synaptic development and function. *Neuron , 60*, 201–214.

Bassell, G., Zhang, H., Byrd, A., Femino, A., Singer, R., Taneja, K., et al. (1998). Sorting of beta-actin mRNA and protein to neurites and growth cones in culture. *J. Neurosci , 18*, 251–265.

Bhaumik, S., Smith, E., & Shilatifard, A. (2007). Covalent modifications of histones during development and disease pathogenesis. *Nat Struct Mol Biol , 14*, 1008–1016.

Blanchette, A., Fuentes Medel, Y., & Gardner, P. (2006). Cell-type-specific and developmental regulation of heterogeneous nuclear ribonucleoprotein K mRNA in the rat nervous system. *Gene Expr Patterns , 6*, 596-606.

Boillée, S., Vande Velde, C., & Cleveland, D. (2006). ALS: a disease of motor neurons and their nonneuronal neighbors. *Neuron , 52*, 39–59.

Bolognani, F., & Perrone-Bizzozero, N. (2008). RNA-protein interactions and control of mRNA stability in neurons. *J Neurosci Res , 86*, 481–489.

Bono, E., Compagno, V., Proia, P., Raimondi, L., Schiera, G., Favaloro, V., et al. (2007). Thyroid hormones induce sumoylation of the cold shock domain-containing protein PIPPin in developing rat brain and in cultured neurons. *Endocrinology , 148*, 252-257.

Brittis, P., Lu, Q., & Flanagan, J. (2002). Axonal protein synthesis provides a mechanism for localized regulation at an intermediate target. *Cell , 110*, 223–235.

Bunge, M. (1973). Fine structure of nerve fibers and growth cones of isolated sympathetic neurons in culture. *J. Cell Biol. , 56*, 713–735.

Burd, C., & Dreyfuss, G. (1994). Conserved structures and diversity of functions of RNA-binding proteins. *Science , 265*, 615-621.

Burd, C., & Dreyfuss, G. (1994). Conserved structures and diversity of functions of RNA-binding proteins. *Science , 265*, 615-621.

Campbell, D., & Holt, C. E. (2001). Chemotropic responses of retinal growth cones mediated by rapid local protein synthesis and degradation. *Neuron , 32*, 1013–1026.

Castello, A., Fischer, B., Eichelbaum, K., Horos, R., Beckmann, B., Strein, C., et al. (2012). Insights into RNA biology from an atlas of mammalian mRNA-binding proteins. *Cell , 149*, 1393–1406.

Castiglia, D., Cestelli, A., Scaturro, M., Nastasi, T., & Di Liegro, I. (1994). H1° and H3.3B mRNA levels in Developing Rat Brain. *Neurochemical reserch , 19*, 1531-1537.

Castiglia, D., Scaturro, M., Nastasi, T., Cestelli, A., & Di Liegro, I. (1996). PIPPin, a putative RNA-binding protein specifically expressed in the rat brain. *Biochem Biophys Res Commun , 218*, 390-394.

Cestelli, A., Castiglia, D., Di Liegro, C., & Di Liegro, I. (1992). Qualitative differences in nuclear proteins correlate with neuronal terminal differentiation. *Cell Mol Neurobiol , 12*, 33-43.

Cestelli, A., Savettieri, G., Ferraro, D., & Vitale, F. (1985). Formulation of a novel synthetic medium for selectively culturing rat CNS neurons. *Brain Res , 354*, 219-27.

Chang, P., Torres, J., Lewis, R., Mowry, K., Houliston, E., & King, M. (2004). Localization of RNAs to the mitochondrial cloud in Xenopus oocytes through entrapment and association with endoplasmic reticulum. *Molecular biology of the cell* , 15:4669–81.

Chartrand, P., Meng, X., Singer, R., & Long, R. (1999). Structural elements required for the localization of ASH1 mRNA and of a green fluorescent protein reporter particle in vivo. *Curr. Biol. , 25*, 333–336.

Chartrand, P., Singer, R., & Long, R. (2001). RNP localization and transport in yeast. *Annu. Rev. Cell Dev. Biol. , 17*, 297–310.

Chen, C., Gherz, R., Andersen, J., Gaietta, G., Jurchott, K., Royer, H., et al. (2000). Nucleolin and YB-1 are required for JNK-mediated interleukin-2 mRNA stabilization during T-cell activation. *Genes Dev , 11*, 1236–1248.

Cieśla, J. (2006). Metabolic enzymes that bind RNA: yet another level of cellular regulatory network? *Acta Biochim Pol , 53*, 11–32.

Cohen, R., Zhang, S., & Dollar, G. (2005). The positional, structural, and sequence requirements of the Drosophila TLS RNA localization element. *RNA , 11*, 1017–1029.

Cole, C., & Scarcelli, J. (2006). Unravelling mRNA export. *Nature cell biology , 8*, 645–647.

Colombrita, C., Silani, V., & Ratti, A. (2013). ELAV proteins along evolution: Back to the nucleus? *Mol and Cell Neu , 56*, 447–455.

Cooper, T., Wan, L., & Dreyfuss, G. (2009). RNA and disease. *Cell , 136*, 777–793.

Corral-Debrinski, M., Blugeon, C., & Jacq, C. (2000). In yeast, the 39 untranslated region or the presequence of ATM1 is required for the exclusive localization of its mRNA to the vicinity of mitochondria. *Mol. Cell. Biol. , 20*, 7881–7892.

Czaplinski, K., & Mattaj, I. (2006). 40LoVe interacts with Vg1RBP/ Vera and hnRNP I in binding the Vg1-localization element. *RNA , 12*, 213–222.

De la Cruz, X., Lois, S., & Sanchez-Molina, S. (2005). Do protein motifs read the histone code? *Bioessays , 27*, 164–75.

Derrigo, M., Cestelli, A., Savettieri, G., & Di Liegro, I. (2000). RNA-protein interactions in the control of stability and localization of messenger RNA. *Int J Mol Med , 5*, 111-123.

Di Liegro, C., Schiera, G., Proia, P., Saladino, P., & Di Liegro, I. (2013). Identification in the rat brain of a set of nuclear proteins interacting with H1° mRNA. *Neuroscience , 229*, 71–76.

Diamond, P., Shannon, M., Vadas, M., & Coles, L. (2001). Cold shock domain factors activate the granulocyte-macrophage colony-stimulating factor promoter in stimulated jurkat T cells. *J Biol Chem , 11*, 7943–7951.

Didier, D., Schiffenbauer, J., Woulfe, S., Zacheis, M., & Schwartz, B. (1988). Characterization of the cDNA encoding a protein binding to the major histocompatibility complex class II Y box. *Proc Natl Acad Sci U S A , 11*, 7322–7326.

Ding, D., Parkhurst, S., Halsell, S., & Lipshitz, H. (1993). Dynamic Hsp83 RNA localization during Drosophila oogenesis and embryogenesis. Molecular and cellular biology. *F1000 Biology Reports , 13*, 3773–81.

Doyle, M., & Kiebler, M. (2011). Mechanisms of dendritic mRNA transport and its role in synaptic tagging. *The EMBO Journal , 30*, 3540-52.

Dubacq, C., Jamet, S., & Trembleau, A. (2009). Evidence for developmentally regulated local translation of odorant receptor mRNAs in the axons of olfactory sensory neurons. *J. Neurosci , 29*, 10184–10190.

En-Nia, A., Yilmaz, E., Klinge, U., Lovett, D., Stefanidis, I., & Mertens, P. (2005). Transcription factor YB-1 mediates DNA polymerase alpha gene expression. *J Biol Chem , 280*, 7702–7711.

Evdokimova, V., Ruzanov, P., Anglesio, M., Sorokin, A., Ovchinnikov, L., Buckley, J., et al. (2006). Akt-mediated YB-1 phosphorylation activates translation of silent mRNA species. *Mol Cell Biol , 26*, 277-292.

Farkas, A., Kilgore, T., & Lotze, M. (2007). Detecting DNA: Getting and begetting cancer. *Curr. Opin. Invest. Drugs , 8*, 981-986.

Fierro-Monti, I., & Mathews, M. (2000). Proteins binding to duplexed RNA: one motif, multiple functions. *TIBS , 25*, 241-246.

Fischer, & Luhrmann. (1990). An essential signaling role for the m3G cap in the transport of U1 snRNP to the nucleus. *Science , 249*, 786–790.

Fischer, U., Sumpter, V., Sekine, M., Satoh, T., & Luhrmann, R. (1993). Nucleo-cytoplasmic transport of U snRNPs: definition of a nuclear location signal in the Sm core domain that binds a transport receptor independently of the m3G cap. *The EMBO journal , 12*, 573–583.

Friedman, R., Farh, K. K., Burge, C. B., & Bartel, D. (2009). Most mammalian mRNAs are conserved targets of microRNAs. *Genome Res , 19*, 92–105.

Gabrilovich, D., Cheng, P., Fan, Y., Yu, B., Nikitina, E., Sirotkin, A., et al. (2002). H1˚ histone and differentiation of dendritic cells. A molecular target for tumor-derived factors. *J Leukoc Biol , 72*, 285-296.

Gallo, J., Jin, P., Thornton, C., Lin, H., Robertson, J., D'Souza, I., et al. (2005). The role of RNA and RNA processing in neurodegeneration. *J Neurosci. , 25*, 10372–10375.

Giuditta, A., Dettbarn, W., & Brzin, M. (1968). Protein synthesis in the isolated giant axon of the squid. *Proc. Natl. Acad. Sci. USA , 59*, 1284–1287.

Gjerset, R., Gorka, C., Hasthorpe, S., Lawrence, J., & Eisen, H. (1982). Developmental and hormonal regulation of protein H1˚ in rodents. *Proc Natl Acad Sci USA , 79*, 2333-2337.

Glisovic, T., Bachorik, J., Yong, J., & Dreyfuss, G. (2008). RNA-binding proteins and post-transcriptional gene regulation. *FEBS Lett , 582*, 1977–1986.

Goldberg, A., Banaszynski, L., Noh, K., Lewis, P., Elsaesser, S., Stadler, S., et al. (2010). Distinct factors control histone variant H3.3 localization at specific genomic regions. *Cell , 140*, 678–691.

Gonsalvez, G., & Long, R. (2012). Spatial regulation of translation through RNA localization. *F1000 Biology Reports , 4*, 16.

Good, P., Rebbert, M., & Dawid, I. (1993). Three new members of the RNP protein family in Xenopus. *Nucleic acids research , 21*, 999-1006.

Goodall, E., Heath, P., Bandmann, O., Kirby, J., & Shaw, P. (2013). Shaw Neuronal dark matter: the emerging role of microRNAs in neurodegeneration. *Front Cell Neurosci , 7*, 178.

Graumann, P., & Marahiel, M. (1998). A superfamily of proteins that contain the cold-shock domain. *Trends Biochem Sci , 23*, 286-290.

Gubitz, A., Feng, W., & Dreyfuss, G. (2004). The SMN complex. *Exp Cell Res , 296*, 51–56.

Gumy, L. F., Yeo, G. S., Tung, Y. C., Zivraj, K. H., Willis, D., Coppola, G., et al. (2011). Transcriptome analysis of embryonic and adult sensory axons reveals changes in mRNA repertoire localization. *RNA , 17*, 85–98.

Hall, K. (2002). RNA-protein interactions. *Curr Opin Struct Biol , 12*, 283-288.

Hamm, J., Darzynkiewicz, E., & Tahara, S. M. (1990). The trimethylguanosine cap structure of U1 snRNA is a component of a bipartite nuclear targeting signal. *Cell , 62*, 569–577.

Hanson, K., Kim, S., & Tibbetts, R. (2012). RNA-Binding Proteins in Neurodegenerative Disease:TDP-43 and Beyond. *RNA , 3*, 265–285.

Hanson, K., Kim, S., & Wiley, R. (2012). RNA-Binding Proteins in Neurodegenerative Disease: TDP-43 and Beyond. *Interdiscip Rev RNA , 3*, 265–285.

Hanus, C., & Schuman, E. (2013). Proteostasis in complex dendrites. *Nature Reviews Neuroscience , 14*, 638–648.

Hastings, M., Berniac, J., Liu, Y., Abato, P., Jodelka, F., Barthel, L., et al. (2009). Tetracyclines that promote SMN2 exon 7 splicing as therapeutics for spinal muscular atrophy. *Sci Transl Med , 1*, 5-12.

Henikoff, S. (2008). Nucleosome destabilization in the epigenetic regulation of gene expression. *Nat Rev Genet , 9*, 15–26.

Henikoff, S., & Ahmad, K. (2005). Assembly of variant histones into chromatin. *Annu Rev Cell Dev Biol , 21*, 133–153.

Hentze, M. (1995). Translational regulation: versatile mechanisms for metabolic and developmental control. *Curr Opin Cell Biol , 7*, 393-398.

Heulens, I., & Kooy, F. (2011). Fragile X syndrome: from gene discovery to therapy. *Front Biosci , 16*, 1211–1232.

Higashi, K., Inagaki, Y., Suzuki, N., Mitsui, S., Mauviel, A., Kaneko, H., et al. (2003). Y-box-binding protein YB-1 mediates transcriptional repression of human alpha 2(I) collagen gene expression by interferon-gamma. *J Biol Chem , 11*, 5156–5162.

Homer, C., Knight, D., Hananeia, L., Sheard, P., Risk, J., Lasham, A., et al. (2005). Y-box factor YB1 controls p53 apoptotic function. *Oncogene , 11*, 8314–8325.

Hörnberg, H., Wollerton-van Horck, D., Maurus, M., Zwart, H., Svoboda, W., & Harris, C. H. (2013). RNA-binding protein Hermes/RBPMS inversely affects synapse density and axon arbor formation in retinal ganglion cells in vivo. *J. Neurosci , 33*, 10384–1039.

Jambhekar, A., & Derisi, J. (2007). Cis-acting determinants of asymmetric, cytoplasmic RNA transport. *RNA , 13*, 625-42.

Jin, P., Duan, R., Qurashi, A., Qin, Y., Tian, D., Rosser, T., et al. (2007). Pur alpha binds to rCGG repeats and modulates repeat-mediated neurodegeneration in a Drosophila model of fragile X tremor/ataxia syndrome. *Neuron , 55*, 556–564.

Jones, P., VanBogelen, R., & Neidhardt, F. (1987). Induction of proteins in response to low temperature in Escherichia coli. *J Bacteriol , 169*, 2092–2095.

Jurchott, K., Bergmann, S., Stein, U., Walther, W., Janz, M., Manni, I., et al. (2003). YB-1 as a cell cycle-regulated transcription factor facilitating cyclin A and cyclin B1 gene expression. *J Biol Chem , 11*, 27988–27996.

Kalous, A., Stake, J., Yisraeli, J., & Holt, C. (2013). RNA binding protein Vg1RBP regulates terminal arbor formation but not long-range axon navigation in the developing visual system. *Dev. Neurobiol* , in press.

Kambach, C., Walke, S., & Nagai, K. (1999). Structure and assembly of the spliceosomal small nuclear ribonucleoprotein particles. *Current opinion in structural biology , 9*, 222–230.

Keene, J., & Tenenbaum, S. (2002). Eukaryotic mRNPs may represent posttranscriptional operons. *Mol Cell , 9*, 1161–1167.

Kislauskis, E., & Singer, R. (1992). Determinants of mRNA localization. *Curr. Opin. Cell Biol. , 4*, 975–978.

Ko, Y., Park, H., & Kim, S. (2002). Novel regulatory interactions and activities of mammalian tRNA synthetases. *Proteomics , 2*, 1304–1310.

Koenig, E. (1967). Synthetic mechanisms in the axon. IV. In vitro incorporation of[3H]precursors into axonal protein and RNA. *J. Neurochem , 14*, 437–446.

Kolb, Battle, & Dreyfuss. (2007). Molecular Functions of the SMN Complex. *Journal of child neurology , 22*, 990–994.

Kolb, S., Sutton, S., & Schoenberg, D. (2010). RNA Processing Defects Associated with Diseases of the Motor Neuron. *Muscle Nerve , 41*, 5–17.

Komar, A., & Hatzoglou, M. (2011). Cellular IRES-mediated translation: The war of ITAFs in pathophysiological states. *Cell Cycle , 10*, 229–240.

Lee, S., & Lykke-Andersen, J. (2013). Emerging roles for ribonucleoprotein modification and remodelling in controlling RNA fate. *Trends Cell Biol* , in press.

Leung, K. M., van Horck, F. P., Lin, A. C., Allison, R., Standart, N., & Holt, C. E. (2006). Asymmetrical beta-actin mRNA translation in growth cones mediates attractive turning to netrin-1. *Nat. Neurosci , 9*, 1247–1256.

Li, E. (2002). Chromatin modification and epigenetic reprogramming in mammalian development. *Nat Rev Genet , 3*, 662–673.

Li, L., & Bonini, N. (2010). Roles of trinucleotide-repeat RNA in neurological disease and degeneration. *Trends Neurosci , 33*, 292–298.

Licatalosi, D., & Darnell, R. (2006). Splicing regulation in neurologic disease. *Neuron , 53*, 93–101.

Lithgow, T., & Cuezva, J. (1997). Highways for protein delivery to the mitochondria. *Trends in Biochemical Sciences , 22*, 110-113.

Liu, Y., & Szaro, B. (2011). HnRNP K post-transcriptionally co-regulates multiple cytoskeletal genes needed for axonogenesis. *Development , 138*, 3079-3090.

Liu-Yesucevitz1, L., Bassell, G., Gitler, A., Hart, A., & Klann. (2011). Local RNA Translation at the Synapse and in Disease. *J Neurosci , 31*, 16086–16093.

Liwak, U., Faye, M., & Holcik, M. (2012). Translation control in apoptosis. *Exp. Oncol , 34*, 218–230.

Lotze, M. (2009). Label-Free, Real-Time Detection System for Molecular Interaction Analysis. *U.S. Patent* , 20,090,147,264,.

Loyola, A., & Almouzni, G. (2007). Marking histone H3 variants: how, when and why? *Trends Biochem , 32*, 425–433.

Lu, Z., Books, J., & Ley, T. (2005). YB-1 is important for late-stage embryonic development, optimal cellular stress responses, and the prevention of premature senescence. *Molecular and cell. Biology , 25*, 4625-463.

Luger, K., Mader, A., & Richmond, R. (1997). Crystal structure of the nucleosome core particle at 2.8 A resolution. *Nature , 389*, 251–60.

Luhrmann, R., Kastner, B., & Bach, M. (1990). Structure of spliceosomal snRNPs and their role in pre-mRNA splicing. *Biochimica et biophysica acta , 1087*, 265–292.

Lukong, K., Chang, K., Khandjian, E., & Richard, S. (2008). RNA-binding proteins in human genetic disease. *Trends Genet , 24*, 416–425.

Lunde, B., Moore, C., & Varani, G. (2007). RNA-binding proteins: Modular design for efficient function. *Nat. Rev. Mol. Cell Biol. , 8*, 479–490.

Lyles, V., Zhao, Y., & Martin, K. (2006). Synapse formation and mRNA localization in cultured Aplysia neurons. *Neuron , 49*, 349-356.

Maher-Laporte, M., Berthiaume, F., Moreau, M., Julien, L., Lapointe, G., Mourez, M., et al. (2010). Molecular composition of staufen2-containing ribonucleoproteins in embryonic rat brain. *PLoS One , 5*, 11350.

Makeyev, A., & Liebhaber, S. (2002). The poly(C)-binding proteins: A multiplicity of functions and a search for mechanisms. *RNA , 8*, 265–278.

Mansfield, K., & Keene, J. (2009). The ribonome: a dominant force in co-ordinating gene expression. *Biol Cel , 101*, 169–181.

Marusich, M., Furneaux, H., Henion, P., & Weston, J. (1994). Hu neuronal proteins are expressed in proliferating neurogenic cells. *J Neurobiol , 25*, 143-55.

Matsui, H., Asou, H., & Inaba, T. (2007). Cytokines direct the regulation of Bim mRNA stability by heat-shock cognate protein 70. *Molecular Cell , 25*, 99-112.

Mattaj. (1986). Cap trimethylation of U snRNA is cytoplasmic and dependent on U snRNP protein binding. *Cell , 46*, 905–911.

Mattaj, I., Boelens, W., Izaurralde, E., Jarmolowski, A., & Kambach, C. (1993). Nucleocytoplasmic transport and snRNP assembly. *Mol Biol Rep , 18*, 79–83.

Matthew, W. M., Mieyoung, C., & Gideon, D. (1995). A nuclear export signal in hnRNP A1: A signal-mediated, temperature-dependent nuclear protein export pathway. *Cell , 83*, 415–422.

McClung, C., & Nestler, E. (2008). Neuroplasticity mediated by altered gene expression. *Neuropsychopharmacology , 33*, 3–17.

Medioni, C., Mowry, K., & Besse, F. (2012). Principles and roles of mRNA localization in animal development. *Development , 139*, 3263–3276.

Meister, G., Buhler, D., Pillai, R., Lottspeich, F., & Fischer, U. (2001). A multiprotein complex mediates the ATP- dependent assembly of spliceosomal U snRNPs. *Nature cell biology , 3*, 945–949.

Merianda, T., Lin, A., Lam, J., Vuppalanchi, D., Willis, D., Karin, N., et al. (2009). A functional equivalent of endoplasmic reticulum and Golgi in axons for secretion of locally synthesized proteins. *Mol. Cell. Neurosci. , 40*, 128–142.

Michalova, E., Vojtesek, B., & Hrstka, R. (2013). Impaired Pre-mRNA Processing and Altered Architecture of 3' Untranslated Regions Contribute to the Development of Human Disorders. *Int. J. Mol. Sci. , 14*, 15681-15694.

Mikula, M., Dzwonek, A., Karczmarski, J., Rubel, T., Dadlez, M., Wyrwicz, L., et al. (2006). Landscape of the hnRNP K protein-protein interactome. *Proteomics , 6*, 2395-2406.

Moore, M. (2005). From birth to death: the complex lives of eukaryotic mRNAs. *Science , 309*, 1514–1518.

Mowry, K. (1996). Complex formation between stage-specific oocyte factors and a Xenopus mRNA localization element. . *Proc. Natl. Acad. Sci. , 93*, 14608–14613.

Muller-McNicoll, M., & Neugebauer, K. (2013). How cells get the message: Dynamic assembly and function of mRNA-protein complexes. *Nat. Rev. Genet. , 14*, 275–287.

Nastasi, D., & Scaturro, M. (1999). PIPPin is a brain-specific protein that contains a cold-shock domain and binds specifically to H1 degrees and H3.3 mRNAs. *J Biol Chem , 274*, 24087-24093.

Nastasi, T., Muzi, P., Beccari, S., Dolo, V., Bologna, M., Cestelli, A., et al. (2000). Specific neurons of brain cortex and cerebellum are PIPPin positive. *NeuroReport , 11*, 2233-2236.

Nicchitta, C. (2002). A platform for compartmentalized protein synthesis: Protein translation and translocation in the ER. *Curr. Opin. Cell Biol , 14*, 412–416.

Park, S., Ewalt, K., & Kim, S. (2005). Functional expansion of aminoacyl-tRNA synthetases and their interacting factors: new perspectives on housekeepers. *Trends in biochemical sciences , 30*, 569–574.

Park, Schimmel, & Kim. (2008). Aminoacyl tRNA synthetases and their connections to disease. *Proceedings of the National Academy of Sciences of the United States of America , 105*, 11043–11049.

Pascale, A., Amadio, M., & Quattrone, A. (2008). Defining a neuron: neuronal ELAV proteins. *Cellular and Molecular Life Sciences , 65*, 128-140.

Pellizzoni, L., Yong, J., & Dreyfuss, G. (2002). Essential role for the SMN complex in the specificity of snRNP assembly. *Science , 298*, 1775–1779.

Pina, B., & Suau, P. (1987). Changes in histones H2A and H3 variant composition in differentiating and mature rat brain cortical neurons. *Dev Biol , 123*, 51-58.

Ponte, I., Martinez, P., Ramirez, A., Jorcano, J., Monzó, M., & Suau, P. (1994). Transcriptional activation of histone H1 zero during neuronal terminal differentiation. *Brain Res Dev Brain Res , 80*, 35-44.

Quattrone, A., Pascale, A., Nogues, X., Zhao, W., Gusev, P., Pacini, A., et al. (2001). Posttranscriptional regulation of gene expression in learning by the neuronal ELAV-like mRNA-stabilizing proteins. *Proc Natl Acad Sci U S A , 98*, 11668–11673.

Raimondi, L., D'Asaro, M., Proia, P., Nastasi, T., & Di Liegro, I. (2003). RNA-binding ability of PIPPin requires the entire protein. *J Cell Mol Med , 7*, 35-42.

Rando, O., & Ahmad, K. (2007). Rules and regulation in the primary structure of chromatin. *Curr Opin Cell Biol , 19*, 250–256.

Ratti, A., Fallini, C., Colombrita, C., Pascale, A., Laforenza, U., Quattrone, A., et al. (2008). Post-transcriptional regulation of neuro-oncological ventral antigen 1 by the neuronal RNA-binding proteins ELAV. *J Biol Chem. , 283*, 7531-7541.

Ratti, A., Fallini, C., Cova, L., Fantozzi, R., Calzarossa, C., & Zennaro, E. (2006). A role for the ELAV RNA-binding proteins in neural stem cells: stabilization of Msi1 mRNA. *J Cell Sci , 119*, 1442-52.

Ravasi, T., Huber, T., Zavolan, M., Forrest, A., Gaasterland, T., & Grimmond, S. (2003). Systematic Characterization of the Zinc-Finger-Containing Proteinsin the Mouse Transcriptome. *Genome Research , 13*, 1430–1442.

Roeyen, C., Scurt, F., Brandt, S., Kuhl, V., Martinkus, S., Djudjaj, S., et al. (2013). Cold shock Y-box protein-1 proteolysis autoregulates its transcriptional activities. *Cell Commun Signal , 10*, 1186/1478-811X-11-63.

Rogakou, E., & Sekeri-Pataryas, K. (1999). Histone variants of H2A and H3 families are regulated during in vitro aging in the same manner as during differentiation. *Exp Gerontol , 34*, 741-754.

Rosen, D., Siddique, T., Patterson, D., Figlewicz, D., Sapp, P., Hentati, A., et al. (1993). Mutations in Cu/Zn superoxide dismutase gene are associated with familial amyotrophic lateral sclerosis. *Nature , 362*, 59–62.

Sala, A., Scaturro, M., Proia, P., Schiera, G., Balistreri, E., Aflalo-Rattenbach, R., et al. (2007). Cloning of a rat-specific long PCP4/PEP19 isoform. *Int J Mol Med , 19*, 501-509.

Saladino, P., Di Liegro, C., Proia, P., Sala, A., Schiera, G., Lo Cicero, A., et al. (2012). RNA-binding activity of the rat calmodulin-binding PEP-19 protein and of the long PEP-19 isoform. *Int J Mol Med , 29*, 141-145.

Salas, E. M., Lozano, G., Chamorro, J. F., Velilla, R., Galan, A., & Diaz, R. (2013). RNA-Binding Proteins Impacting on Internal Initiation of Translation. *Int. J. Mol. Science , 14*, 21705-21726.

Scaturro, M., Cestelli, A., Castiglia, D., Nastasi, T., & Di Liegro, I. (1995). Post- transcriptional regulation ofH1˚ and H3.3 histone genes in differ- entiating rat cortical neurons. *Neurochem Res , 20*, 969-976.

Scaturro, M., Nastasi, T., Raimondi, L., Bellafiore, M., Cestelli, A., & Di Liegro, I. (1998). H1˚ RNA-binding proteins specifically expressed in the rat brain. *J Biol Chem , 273*, 22788-22791.

Scaturro, M., Sala, A., Cutrona, G., Raimondi, L., Cannino, G., Fontana, S., et al. (2003). Purification by affinity chromatography of H1o RNA-binding proteins from rat brain. *Int J Mol Med. , 11*, 509-13.

Schiera, G., Sala, S., Gallo, A., Raffa, M., Pitarresi, G., Savettieri, G., et al. (2005). Permeability properties of a three-cell type in vitro model of blood-brain barrier. *Journal of Cellular and Molecular Medicine , 9*, 373–379.

Sellier, C., Rau, F., Liu, Y., Tassone, F., Hukema, R., Gattoni, R., et al. (2010). Sam68 sequestration and partial loss of function are associated with splicing alterations in FXTAS patients. *EMBO J , 29*, 1248–1261.

Serano, T., & Cohen, R. (1995). A small predicted stem–loop structure mediates oocyte localization of Drosophila K10 mRNA. *Development , 121*, 3809–3818.

Shigeoka, T., Lu, B., & Holt, C. (2013). RNA-based mechanisms underlying axon guidance. *JCB , 202*, 991-999.

Siomi, H., & Dreyfuss, G. (1997). RNA-binding proteins as regulators of gene expression. *Curr Opin Genet , 7*, 345-353.

Slemmon, J., Morgan, J., Fullerton, S., Danho, W., Hilbush, B., & Wengenack, T. (1996). Camstatins are peptide antagonists of calmodulin based upon a conserved structural motif in PEP-19, neurogranin, and neuromoduli. *J Biol Chem , 271*, 15911-15917.

Sofola, O., Jin, P., Qin, Y., Duan, R., Liu, H., de Haro, M., et al. (2007). RNA-binding proteins hnRNP A2/B1 and CUGBP1 suppress fragile X CGG premutation repeat-induced neurodegeneration in a Drosophila model of FXTAS. *Neuron , 55*, 565–576.

Spriggs, K., Bushell, M., & Willis, A. (2010). Translational regulation of gene expression during conditions of cell stress. *Mol. Cell , 40*, 228–232.

St Johnston, D. (2005). Review Moving messages: the intracellular localization of mRNAs. *Nat Rev Mol Cell Biol , 6*, 363-75.

Stark, H., Dube, P., Luhrmann, R., & Kastner, B. (2001). Arrangement of RNA and proteins in the spliceosomal U1 small nuclear ribonucleoprotein particle. *Nature , 409*, 539–542.

Stewart, M. (2007). Ratcheting mRNA out of the nucleus. *Molecular cell , 25*, 327–330.

Strah, B., & Allis, C. (2000). The language of covalent histone modifications. *Nature , 403*, 41–45.

Stratford, A., Fry, C., Desilets, C., Davies, A., Cho, Y., Li, Y., et al. (2008). Y-box binding protein-1 serine 102 is a downstream target of p90 ribosomal S6 kinase in basal-like breast cancer cells. *Breast Cancer Res , 10*, R99.

Tagami, H., Ray-Gallet, D., Almouzni, G., & Nakatani, Y. (2004). H1° and H3.3 complex mediate nucleosome assemly pathways dependent or independent of DNA synthesis. *Cell , 6*, 51-61.

Tassone, F., Hagerman, R., Taylor, A., Gane, L., Godfrey, T., & Hagerman, P. (2000). Elevated levels of FMR1 mRNA in carrier males: a new mechanism of involvement in the fragile-X syndrome. *Am J Hum Genet , 66*, 6–15.

Tennyson, V. (1970). The fine structure of the axon and growth cone of the dorsal root neuroblast of the rabbit embryo. *J. Cell Biol , 44*, 62–79.

Thapar, R., & Denmon, A. (2013). Signaling pathways that control mRNA turnover. *Cell Signal , 25*, 1699-1710.

Varani, G; Nagai, K. (1998). RNA recognition by RNP by RNP proteins during RNA processing. *Annu Rev Biophys Biomol Struct , 27*, 407-445.

Walsh, D., & Mohr, I. (2011). Viral subversion of the host protein synthesis machinery. *Nat. Rev. Microbiol. , 9*, 860–875.

Wei, P., Blundon, J., Rong, Y., Zakharenko, S., & Morgan, J. (2011). Impaired locomotor learning and altered cerebellar synaptic plasticity in pep-19/pcp4-null mice. *Mol Cell Biol , 31*, 2838- 2844.

Wellman, S., Casano, P., Pilch, D., Marzluff, W., & Sittman, D. (1987). Characterization of mouse H3.3-like histone genes. *Gene , 59*, 29-39.

Welshhans, K., & Bassell, G. J. (2011). Netrin-1-induced local beta-actin synthesis and growth cone guidance requires zipcode binding protein. *J. Neurosci , 31*, 9800–9813.

Wiedemann, S. M., Mildner, S. N., BönischC, Israel, L., Maiser, A., Matheisl, S., et al. (2010). Identification and characterization of two novel primate-specific histone H3 variants, H3.X and H3.Y. *JCB , 190*, 777-791.

Will, C., & Luhrmann, R. (2001). Spliceosomal UsnRNP biogenesis, structure and function. *Current opinion in cell biology , 13*, 290–301.

Willers, I., & Cuezva, J. (2011). Post-transcriptional regulation of the mitochondrial H(+)-ATP synthase: a key regulator of the metabolic phenotype in cancer. *Biochim Biophys Acta , 1807*, 543-51.

Wolffe, A. (1994). Structural and functional properties of the evolutionarily ancient Y-box family of nucleic acid binding proteins. *Bioessays , 16*, 245–251.

Yao, J., Sasak, i. Y., Wen, Z., Bassell, G. J., & Zheng, J. Q. (2006). An essential role for beta-actin mRNA localization and translation in Ca2+-dependent growth cone guidance. *Nat. Neurosci , 9*, 1265–1273.

Yong, J., Wan, L., & Dreyfuss, G. (2004). Why do cells need an assembly machine for RNA-protein complexes? *Trends Cell Biol , 14*, 226–232.

York, J., Odom, A., Murphy, R., Ives, E., & Wente, S. (1999). A phospholipase C-dependent inositol polyphosphate kinase pathway required for efficient messenger RNA export. *Science , 285*, 96–100.

Yuan, G., & Zhu, B. (2012). Histone variants and epigenetic inheritance. *Biochimica et Biophysica Acta , 1819*, 222–229.

Zelená, J. (1970). Ribosome-like particles in myelinated axons of the rat. *Brain Res , 24*, 359–363.

Zivraj, K. H., Tung, Y. C., Piper, M., Gumy, L., Fawcett, J. W., Yeo, G. S., et al. (2010). Subcellular profiling reveals distinct and developmentally regulated repertoire of growth cone mRNAs. *J. Neurosci.* , *30*, 15464–15478.

Zlatanova, J., & Doenecke, D. (1994). Histone H1 zero: a major player in cell differentiation. *FASEB J* , *8*, 1260-1268.

Summary